DIPLOMARBEIT

Titel der Diplomarbeit

„Biochemical and physiological investigations on the energy metabolism of ammonia oxidizing archaea"

Verfasserin

Christine Elisabeth Bauer

angestrebter akademischer Grad

Magistra der Naturwissenschaften (Mag.rer.nat.)

Wien, April 2012

Die vorliegende Diplomarbeit wurde am Department für Ökogenetik des Fachbereichs Biologie der Universität Wien unter der Leitung von Frau Univ.-Prof. Dipl.-Biol. Dr. Christa Schleper mittels der Betreuung von Herrn Dipl.-Biol. Dr. Tim Urich im Zeitraum von Juli 2011 bis April 2012 angefertigt.

Eidesstattliche Erklärung

Ich erkläre hiermit an Eides statt, dass ich den materiellen Inhalt vorliegender Arbeit ohne Hilfe Dritter und ohne Benutzung anderer als der angegebenen Hilfsmittel und Quellen angefertigt habe. Die aus fremden Quellen direkt oder indirekt übernommenen Gedanken und Fakten, sofern sie nicht wissenschaftliches Allgemeingut sind, wurden als solche kenntlich gemacht.

Die Arbeit wurde bisher in gleicher oder ähnlicher Form keiner anderen Prüfungbehörde vorgelegt und auch noch nicht veröffentlicht.

Wien, April 2012

Christine Elisabeth Bauer

Danksagung

Table of Contents

1 Abstract

Since the discovery of ammonia oxidizing archaea (AOA) in 2005, their contribution to the global nitrogen cycle is discussed. For better characterization, further understanding of their still largely unknown energy and carbon metabolism is required. In this study, the archaeal ammonia oxidation was investigated, focusing on an enzyme which is potentially involved in the second step as well as possible intermediates. In ammonia oxidizing bacteria (AOB), ammonia oxidation is divided into two steps: first, ammonia (NH_3) is oxidized to hydroxylamine (NH_2OH, short HA) by the enzyme ammonia monooxigenase (AMO). In the second step, NH_2OH is further oxidized to nitrite (NO_2^-) via the hydroxylamine oxidoreductase (HAO). Although AMO homologs are found in archaea, neither the intermediate, nor the enzyme(s) which catalyze the second step are known.

The enzyme studied is a multicopper protein of the AOA, which shows homology to nitrite reductases (NirKs). Due to its high transcription under aerobic conditions and the fact that enzymes can often catalyze their reaction in both directions, it was hypothesized that this enzyme could oxidize an intermediate of ammonia oxidation (probably NO) to NO_2^-. Apart from biochemical experiments with this protein, also studies with cell extracts and cultures of *Ca.* Nitrososphaera viennensis (*Ca.* N. viennensis) were performed to obtain information about possible activities and intermediates in the archaeal ammonia oxidation.

The NirK, which was heterologously expressed in *Escherichia coli* (*E. coli*), showed no nitrite reductase activity. In the presence of an artificial electron acceptor, it oxidized NH_2OH. However, none of the conditions tested yielded detectable amounts of nitrite (partial HAO activity). The results concerning other types of produced nitrogen species (NO, N_2O) were inconclusive. The calculated K_M value for the reaction, ranging approximately between 0.5 and 1.3 mM, did not show high enzymatic affinity for NH_2OH. Since the reduction of the electron acceptor also occurred with copper(II) chloride dihydrate solutions, the enzyme specificity of this reaction could neither be confirmed nor excluded. There was no indication that the NirK is able to oxidize other nitrogen substrates (NO, HNO, NH_4^+).

As the examined enzyme was from a metagenomic library (contig 54d9), it would be beneficial if the NirK of *Ca.* N. viennensis was available for further studies as well. Therefore, the expression of its NirK in *E. coli* was attempted. The gene was ligated into the expression vector pET28a but after sequencing of the clones it turned out that

the amplified DNA was obtained from EN123, a sister strain of *Ca.* N. viennensis which was also available in the laboratory.

In addition, detection of the NirK in various protein fractions of *Ca.* N. viennensis was attempted to determine whether its expression as observed in transcriptomic studies can be reproduced in the proteome. However, none of the peptides could be assigned to the respective nitrite reductase.

Due to the slow growth and low cell density of *Ca.* N. viennensis, it became necessary to increase the yield of cells by upscaling the culture to several liters to be able to perform biochemical experiments with crude cell extracts. Ammonium oxidation activity could not be demonstrated in the crude cell extract. HAO activity was only determined indirectly by the reduction of the electron acceptor but again without the formation of nitrite. Further, no evidence for NO activity was found.

Interestingly, nitrite reductase activity was detected in the cell extract as well as in the soluble and insoluble fraction of the cell extract. This is an indication of the relevance of this reaction in the organism. Whether this activity is due to the NirK remains unclear.

Another experiment to obtain evidence for NO as a possible intermediate in the archaeal ammonia oxidation was the cultivation of *Ca.* N. viennensis in the presence of a specific NO-scavenger (PTIO, short for 2-phenyl-4,4,5,5-tetramethylimidazolineoxyl-1-oxyl-3-oxide). Cultures of *Nitrosospira multiformis* (AOB) and *E. coli* served as controls. At comparable concentrations, the growth of *Ca.* N. viennensis was inhibited most by PTIO. Thus, NO could be an important intermediate of ammonia oxidation. Further, these results give indication for a different ammonium oxidation mechanism, or at least for a different enzymatic machinery of AOA compared to AOB.

In this study, the physiologically relevant activity of the NirK homolog could not be clearly determined. However, nitrite reductase activity was detected in cell extracts. As a possible intermediate for ammonia oxidation, only evidence for NO was obtained. Due to the complexity of the process, it seems not easy to track the ammonium oxidation *in vitro.* Complex electron transfer processes, a variety of enzymes involved and reactive N-species complicate its elucidation. Other biochemical methods must be consulted to further resolve this mechanism.

2 Introduction

2.1 The global nitrogen cycle

Nitrogen is a key element for life on Earth since it is a component of amino acids and the basis of nucleic acids. All its chemical forms are summed up in the global nitrogen cycle (Fig. 2-1) which consists of a multitude of oxidation and reduction reactions of nitrogen (N_2), resulting in compounds with N-oxidation states ranging between +5 (NO_3^-) and -3 (NH_3). The outcome of the reactions occurring in the cycle is capable of positively and negatively influencing the human environment at a large scale. Benefits vary from the removal of fixed nitrogen pollutants in wastewater treatment plants to increased crop yield because of nitrogen based fertilizers. However, the disadvantages can cause eutrophication and the production of strong greenhouse gases (N_2O). Since anthropogenic influences changed the nitrogen flux dramatically since the development of the Haber-Bosch process (Klotz and Stein, 2008), a more detailed understanding of the microorganisms involved, their contribution, their underlying metabolisms and the environmental parameters which affect their activity has become increasingly important.
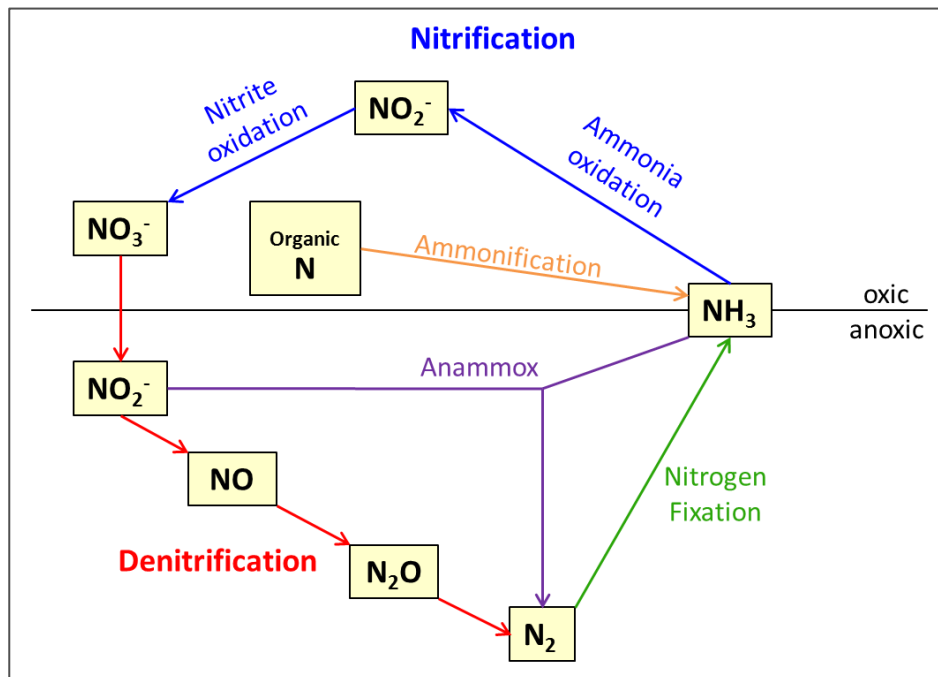
Figure 2-1: Scheme of the global nitrogen cycle.

Elemental nitrogen is a diatomic gas (N_2) accounting for ~78% of the Earth´s atmosphere. The ability of organisms to incorporate nitrogen gas is called nitrogen fixation. This process is only known to occur in prokaryotes via the enzyme complex nitrogenase (which is inactivated by oxygen) by which N_2 is reduced to ammonia (NH_3). In a process called nitrification, NH_3 is oxidized aerobically to nitrite (NO_2^-) and further to nitrate (NO_3^-) (Klotz and Stein, 2008). As far as the process is established in bacteria, it consists of two consecutive reactions: oxidation of ammonia to nitrite (Fig. 2-2), which is a two-step reaction (Arp et al., 2002) and oxidation of nitrite to nitrate. First, NH_3 is oxidized to hydroxylamine (NH_2OH, short HA), catalyzed by the enzyme ammonia monooxygenase (AMO), investing two electrons. Afterwards, hydroxylamine is further oxidized to nitrite via the enzyme hydroxylamine oxidoreductase (HAO), generating four electrons. Two of the electrons supply the AMO reaction, the other two are used to yield energy. The second step of nitrification, the oxidation of nitrite to nitrate, is accomplished by the enzyme nitrite oxidoreductase. Bacteria gaining energy with the first reaction step are called ammonia oxidizing bacteria (AOB), those which perform the second step are nitrite oxidizing bacteria (NOB). No organism has been discovered so far which is able to carry out the complete oxidation of NH_3 to NO_3^- (Kowalchuk and Stephen, 2001).

Reaction I

$$NH_3 + O_2 + 2H^+ + 2e^- \xrightarrow{\substack{\textbf{AMO} \\ \text{(ammonia monooxygenase)}}} NH_2OH + H_2O$$

Reaction II

$$NH_2OH + H_2O \xrightarrow{\substack{\textbf{HAO} \\ \text{(hydroxylamine oxidoreductase)}}} HNO_2 + 4H^+ + 4e^-$$
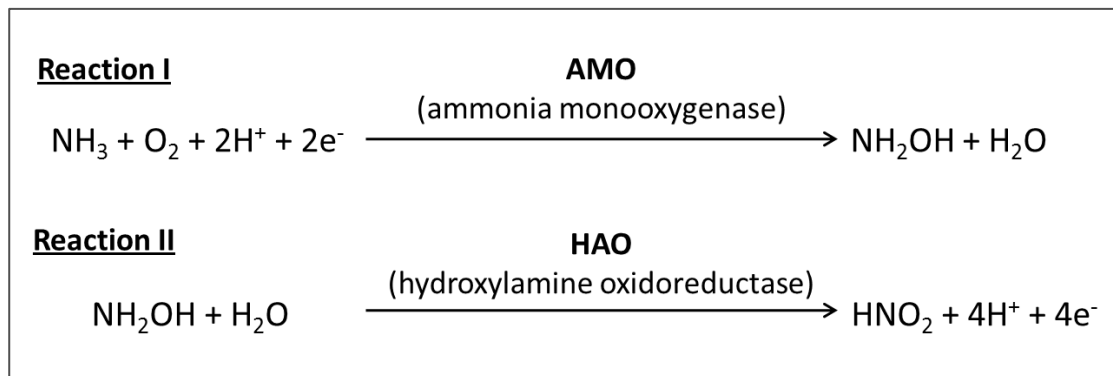
Figure 2-2: Formulas for bacterial ammonia oxidation (AOB).

During denitrification, nitrate is reduced by complex multisite metalloenzymes to dinitrogen (N_2) which is released back to the atmosphere completing the cycle. First, nitrate is reduced to nitrite via the nitrate reductase (Nar). Enzymes of the nitrite reductase (Nir) family reduce nitrite further to nitric oxide (NO). There are two classes of Nirs, CuNir and cd$_1$Nir, having either copper or heme as a cofactor. The encoding genes are called *nirK* if the cofactor of the enzyme is copper and *nirS* if it is heme. The nitric oxide reductase (Nor) reduces nitric oxide to nitrous oxide (N_2O). Finally, N_2 is formed by the nitrous oxide reductase (Nos). Not all prokaryotes are able to accomplish

the whole denitrification process, some stop at one of the intermediates which leads to the emission of greenhouse gases (like N_2O). In the 1990s, a new pathway in the cycle was discovered in which ammonia is oxidized with nitrite to dinitrogen gas. This pathway is called anoxic ammonia oxidation (ANAMMOX) (Jetten et al., 2005).

2.2 Archaea and their participation in the global nitrogen cycle

The use of the small ribosomal subunit RNA (16S rRNA) as a phylogenetic marker enabled Carl Woese in the 1970s to discover a new fundamental lineage of life, the Archaea (Woese and Fox, 1977). Because of his findings, the common eukaryote-prokaryote dichotomy of that time emerged to a new classification concept of the three domains of life (Fig. 2-3) consisting of Bacteria, Archaea and Eukaryotes (Woese et al., 1990).
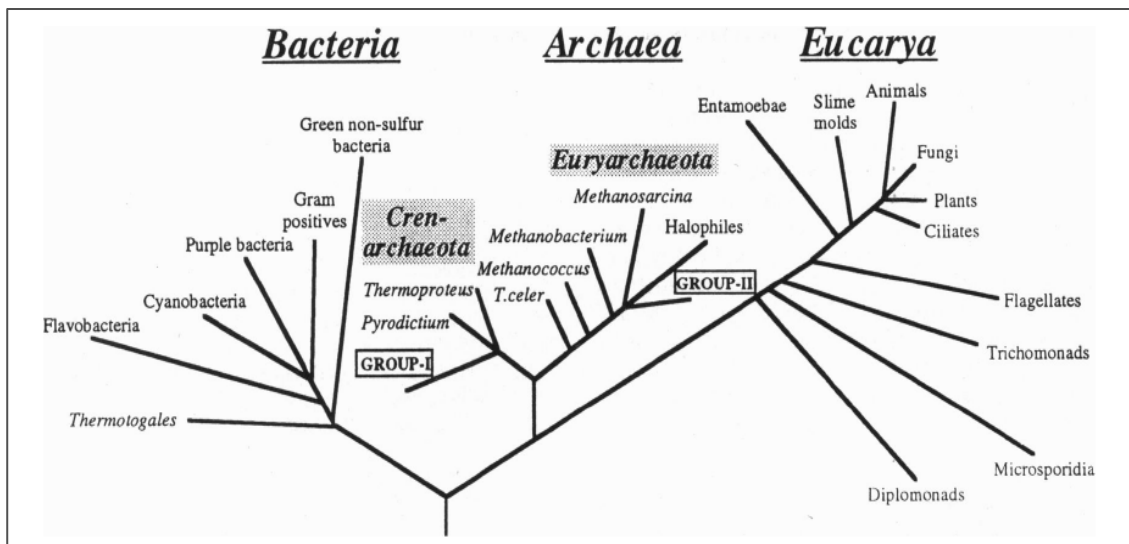
Figure 2-3: Rooted phylogenetic tree based on 16S rRNA sequences showing the three domains of life. Taken from Stein and Simon, 1996.

Based on the 16S rRNA, Woese also discovered two major phyla within the archaea, the Crenarchaeota and Euryarchaeota (Fig. 2-4). Nearly all described species of archaea belong to these two phyla (Schleper et al., 2005) but three additional phyla were later identified, the Korarchaeota in 1996 (Barns et al., 1996), the Nanoarchaeota in 2002 (Huber et al., 2002) which are still discussed (Brochier-Armanet et al., 2011) and the Thaumarchaeota (Brochier-Armanet et al., 2008). The latter contain archaeal ammonia oxidizers. A fifth phylum, the Aigarchaeota, was proposed recently (Nunoura et al., 2011).

Figure 2-4: Phylogenetic tree of all currently discussed archaeal phyla based on an aligned dataset of 26 universally conserved proteins. The tree was rooted with bacteria (not shown). For each branch, PP (posterior probability) support values are indicated. An asterisk (*) denotes those species for which the genome sequence is incomplete. Taken from Guy and Ettema, 2011.

After their first discovery, archaea were thought to be mostly extremophiles, because besides the group of methanogens, all representatives which could be cultivated were adapted to a few specific niches, coping with different inhospitable conditions (Schleper et al., 2005). A great majority of microorganisms does not grow under laboratory conditions, a phenomenon known as the "great plate count anomaly" (Staley and Konopka, 1985). This has been the reason for dramatically underestimating the distribution and diversification of archaea and also bacteria in the environment. However, the development of culture-independent techniques in the 1980s enabled the determination of the global distribution of archaea. PCR-based amplification of 16S rRNA genes revealed their occurrence in significant numbers in the ocean´s plankton (DeLong, 1992), freshwater lakes (Schleper et al., 1997), sediments (Boetius et al., 2000) and soils (Bintrim et al., 1997). Many of the detected sequences represented new phylotypes of non-thermophilic members of the archaeal kingdom Crenarchaeota, of which until then cultivated relatives were exclusively (hyper)-thermophiles. Furthermore, up to 34% of the prokaryotic biomass in coastal Antarctic surface waters

could be assigned to the Crenarchaeota, indicating that they represent one of the most abundant groups of prokaryotes in the ocean (DeLong et al., 1994).

Because of the difficulties in cultivation, their physiology and metabolic capabilities could not be fully investigated until the metagenomic approach was developed. Genes obtained from the environment enable culture-independent characterization by detecting metabolic marker genes additionally to the 16S rRNA (Schleper et al., 2005). Since the sequencing (McTavish et al., 1993) of the genes *amoA*, *amoB* and *amoC*, which encode for the key enzyme of ammonia oxidation (AMO), they are used as such molecular markers. The discovery of a unique *amoA* gene potentially encoding for a subunit of the AMO on an archaeal-associated scaffold distantly related to its bacterial counterpart obtained from a marine water sample (Venter et al., 2004) was the first hint for archaea to be involved in ammonia oxidation. Also the finding of two proteins related to subunits of ammonia monooxygenases (AmoAB) as well as a CuNir homologue on an archaeal fosmid from soil (Treusch et al., 2005), indicated that Crenarchaea might be involved in the global nitrogen cycle. In 2005, the isolation of the first autotrophic ammonia-oxidizing marine archaeon obtained from a seawater-aquarium, *Ca.* Nitrosopumilus maritimus, which as well encodes an *amoA* was published (Könneke et al., 2005). This organism provided the first experimental evidence for the postulated ammonia oxidation pathway. Just recently in 2011, Tourna et al. published the first pure culture of an ammonia oxidizing archaeon obtained from soil, *Ca.* Nitrososphaera viennensis. Besides the two pure isolates, several enrichment cultures of ammonia oxidizing archaea are now present in various laboratories.

The occurrence of AOA in terrestrial and marine ecosystems initiated an ongoing discussion on their participation in the global nitrogen cycle. Studies in the North Sea showed that the abundance of archaeal *amoA* genes is one- to two-fold higher than bacterial *amoA* genes in the ocean (Wuchter et al., 2006). Furthermore, the abundance of the archaeal *amoA* is correlated with a decline in ammonium concentrations (Wuchter et al., 2006). There is also evidence for high abundance and activity of AOA in terrestrial habitats (Leininger et al., 2006). These data suggest a major role of archaea in nitrification processes.

2.3   The unknown mechanism of archaeal ammonia oxidation

Despite intense research, the archaeal pathway of ammonia oxidation remains mainly uncharacterized (Fig. 2-5). The cultivated representatives *Ca.* N. maritimus and *Ca.* N. viennensis show the stoichiometric consumption of ammonium and formation of nitrite

during growth but apart from the AMO, enzymes as well as intermediates are unknown. Neither a counterpart of the bacterial HAO was found to be encoded in archaeal genome datasets so far, nor is there evidence for hydroxylamine as the intermediate (Walker et al., 2010).
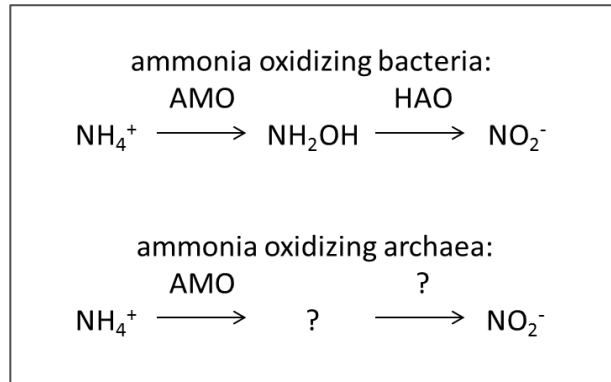
Figure 2-5: Schematic overview of ammonia oxidation in bacteria and archaea. The only similarities of bacterial and archaeal ammonia oxidation currently known are consumption of ammonium, production of nitrite and homologs of the AMO.

Under the assumption that the AMO is involved, two main competing hypotheses are debated for the process of ammonia oxidation in archaea (Walker et al., 2010): either the archaeal AMO produces hydroxylamine which is further oxidized by an enzyme (or several enzymes) without HAO homology, or the archaeal AMO produces another intermediate than hydroxylamine.

The lack of genes encoding a recognizable AOB-like HAO complex and pertinent cytochrome c proteins but the appearance of numerous copper-containing proteins, including multicopper oxidases and small blue copper-containing proteins (MCOs), suggest an alternative electron transfer mechanism (Walker et al., 2010). If a unique biochemistry exists, hydroxylamine oxidation may occur via one of the putatively periplasmic MCOs (CuHAO). Given the lack of cytochrome c proteins, the four electrons would then be transferred to a quinone reductase (QRED) via small blue copper-containing plastocyanin-like electron carriers. This apparent reliance on copper for redox reactions would be a major divergence from the iron-based electron transfer system of AOB (Walker et al., 2010).

The fact that the sequences of archaeal genes annotated as *amoA*, *amoB*, and *amoC* are not more similar to bacterial *amo* genes than they are to genes encoding bacterial particulate methane monooxygenases (pMMO) (Nicol and Schleper, 2006) could

indicate for functional differences between the archaeal and bacterial versions of the AMO enzyme. Besides hydroxylamine, NO and nitroxyl (HNO) are mostly considered as possible intermediates in the process, N_2O is probably a side product (Santoro et al., 2011). Walker et al. (2010) developed a hypothetical scenario for ammonia oxidation where the archaeal AMO does not produce NH_2OH but the reactive intermediate HNO. During archaeal ammonia oxidation, HNO might be formed by a unique monooxygenase function of archaeal AMO. Alternatively, the archaeal AMO may act as a dioxygenase and insert two oxygen atoms into NH_3, producing HNO from the spontaneous decay of HNOHOH.

2.4 The unknown function of NirK homologues in ammonia-oxidizing archaea and bacteria

During denitrification, nitrite is stepwise reduced to dinitrogen, involving a series of metalloenzymes. One of these enzymes is the so-called nitrite reductase (NirK), a multicopper protein (MCP) which is able to reduce nitrite to NO. Although associated with the denitrification process, all of the studied ammonia-oxidizing bacteria (Cantera and Stein, 2007) as well as most of the archaea have homologous genes encoding for this copper-containing NirK, with a still unknown function.

It is thought that the enzyme is involved in a process called nitrifier denitrification, the reduction of nitrite and the release of N_2O at oxic and anoxic interfaces. Studies of the NirK in the AOB model organism *Nitrosomonas europaea* (*N. europaea*) revealed the expression and activity under aerobic conditions and showed that the enzyme is dependent on nitrite rather than oxygen concentrations (Beaumont et al., 2004). In an experiment comparing a wild-type and a *nirK* deficient mutant of *N. europaea*, it was shown that the mutant grew more slowly with lower rates in substrate consumption and product formation and produced significantly more N_2O under high oxygen concentrations (Cantera and Stein, 2007). Under low oxygen, it also grew more slowly but the oxidation and formation rates were not as different. Also the oxidation of NH_2OH occurred at slower rates. This indicates that NirK has a supporting role in the ammonia-oxidizing metabolism, suggesting that its absence has some inhibitory effect on the AMO as well as the HAO. However, it is not required for nitrite reduction.

An evidence especially indicating the involvement of the NirK in the ammonia oxidation process of AOA are various metatranscriptomic studies in different ecosystems which revealed high abundance of *nirK* transcripts under aerobic conditions in soil group 1.1b

as well as marine group 1.1a archaea, comparable to the abundance of *amo* transcripts (Hollibaugh et al., 2011; Radax et al., 2012; Urich et al., 2008).

2.5   The archaeal copper containing nitrite reductase (NirK) homologue

The first archaeal gene encoding a potential NirK homologue was discovered on the soil contig 54d9 (Fig. 2-6) from a metagenomic fosmid library, representing a 43.3 kb insert which could be assigned to group 1.1b of the Crenarchaeota and contained 43 putative protein encoding genes (Treusch et al., 2005). Due to the presence of putative *amo* genes, this contig was the first hint for AOA in soils.
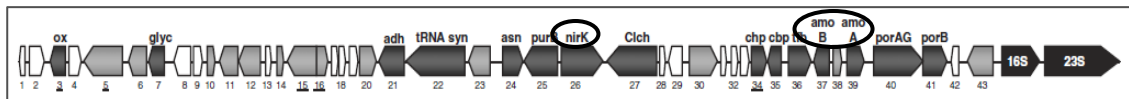
Figure 2-6: Schematic representation of the crenarchaeal fosmid clone 54d9. 15 of the protein encoding genes could be assigned to a biological function and 13 were conserved hypothetical proteins. Different shadings indicate ribosomal RNA genes (black), genes with assigned function (dark grey), conserved hypotheticals (grey), hypotheticals (white). Taken from Treusch et al., 2005. ORF 26: *nirK*, ORF 37: *amoB*, ORF 39: *amoA*.

ORF 26 showed significant similarities to protein sequences of copper-containing nitrite reductases (Treusch et al., 2005), the highest to putative homologues from the Sargasso Sea shotgun sequencing project and to homologues from *N. europaea*, halophilic archaea and *Neisseria* (30–32%). Furthermore, an amino acid alignment of various NirKs and multicopper oxidases (MCOs) revealed a conserved copper coordination (Bartossek et al., 2010) (Fig. 2-7) and more variants of this novel *nirK* within the group of Thaumarchaeota could be found in various habitats.
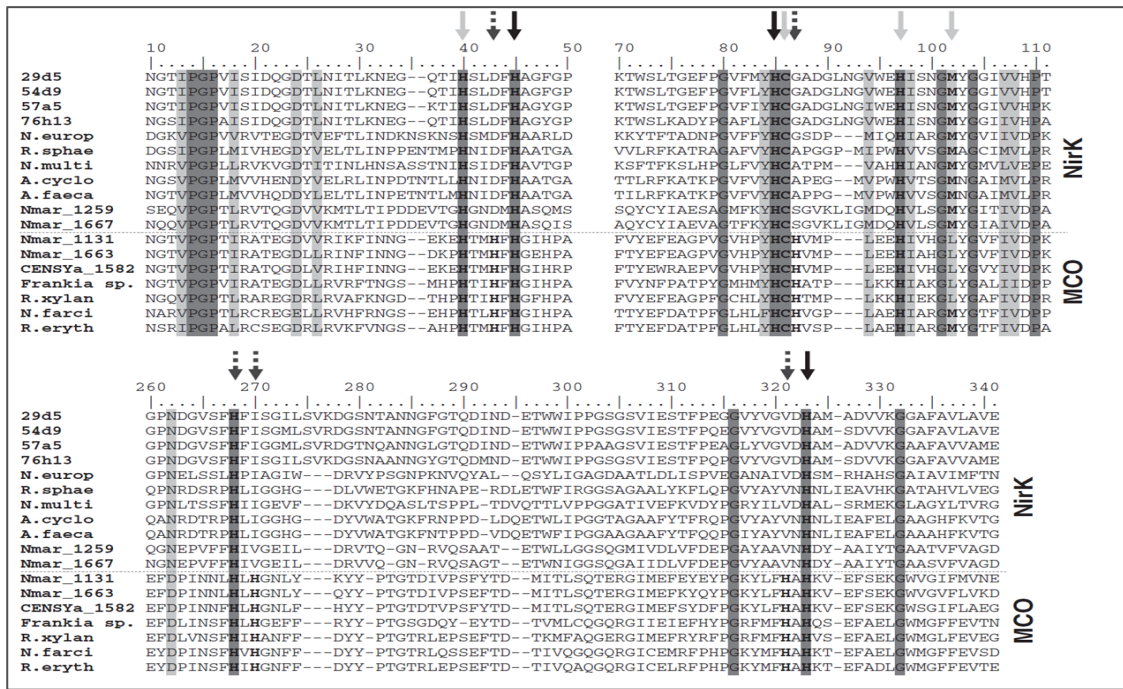
Figure 2-7: Alignment of amino acid sequences of NirKs and MCOs from a selection of archaea and bacteria with copper center type 1, 2 and 3 coordinating amino acid residues. Dark grey background shading: identical residues in all compared sequences; light grey background shading: similar residues in all compared sequences. Copper coordinating residues are highlighted in bold with solid grey, solid black and striped grey arrows indicating copper centre type 1, copper centre type 2 and putative trinuclear type 2/type 3 copper centre, respectively. Nitrite reductases are from soil fosmids 54d9, 57a5, 29d5, 76h13, *Nitrosomonas europaea* (*N. europ*), *Rhodobacter sphaeroides* (*R. sphae*), *Nitrosospira multiformis* (*N. multi*), *Achromobacter cycloclastes* (*A. cyclo*), *Alcaligenes faecalis* (*A. faeca*) and *Nitrosopumilus maritimus* (Nmar_1259 and Nmar_1667). Multicopper oxidases are from *N. maritimus* (Nmar_1131 and Nmar_1663), *Cenarchaeum symbiosum* (CENSYa_1582), a *Frankia* species, *Rubrobacter xylanophilus* (*R. xylan*), *Nocardia farcinica* (*N. farci*) and *Rhodococcus erythropolis* (*R. eryth*). Taken from Bartossek et al., 2010.

At the N-terminus, a putative transmembrane domain (amino acids 5–27) probably constitutes a signal peptide (Treusch et al., 2005). A distinctive feature is an extension of approximately 180 amino acids to the NirK domain at the C-terminus, coding for an amicyanin domain (Fig. 2-8).
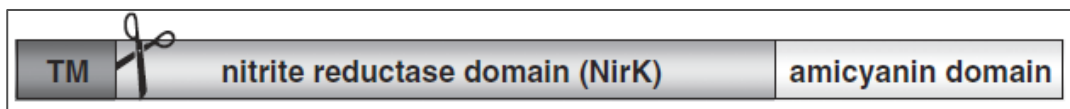
Figure 2-8: Schematic representation of the putative copper-dependent nitrite reductase encoded by ORF 26, with a signal peptide (cleavage indicated by scissors), NirK domain and amicyanin domain. TM: putative transmembrane domain. Taken from Treusch et al., 2005.

During the first heterologous expression in *E. coli*, the NirK protein could not be properly refolded (Treusch, 2004). An improved refolding protocol resulted in soluble protein (G. Sawers, Halle, Germany, pers. comm.). However, NirK activity could not convincingly be shown. Therefore, a second attempt was made to achieve the expression (Schweichhart and Urich, pers. comm.). After isolation from inclusion bodies and stepwise refolding under the presence of copper, the protein was biochemically characterized. The actual NIR activity, precisely the reduction of nitrite to NO could not be determined but the enzyme showed ability to reduce the electron acceptor potassium ferricyanide ($K_3Fe(CN)_6$) under the presence of NH_2OH (partial HAO activity) without any nitrite formation, though (Schweichhart and Urich, pers. comm.).

2.6 *Ca.* Nitrososphaera viennensis – a new archaeal model organism

To investigate the metabolism of AOA, cultivated representatives are essential. In this study the opportunity was given to work with *Ca.* Nitrososphaera viennensis. In 2011, Tourna et al. accomplished the purification of an enrichment of AOA from a garden soil in Vienna after two years of transferring the culture in media treated with antibiotics. The organism was named *Ca.* Nitrososphaera viennensis, affiliated with group 1.1b of the Thaumarchaeota (Fig. 2-9), growing chemolithoautotrophically on ammonium (Fig. 2-10A).
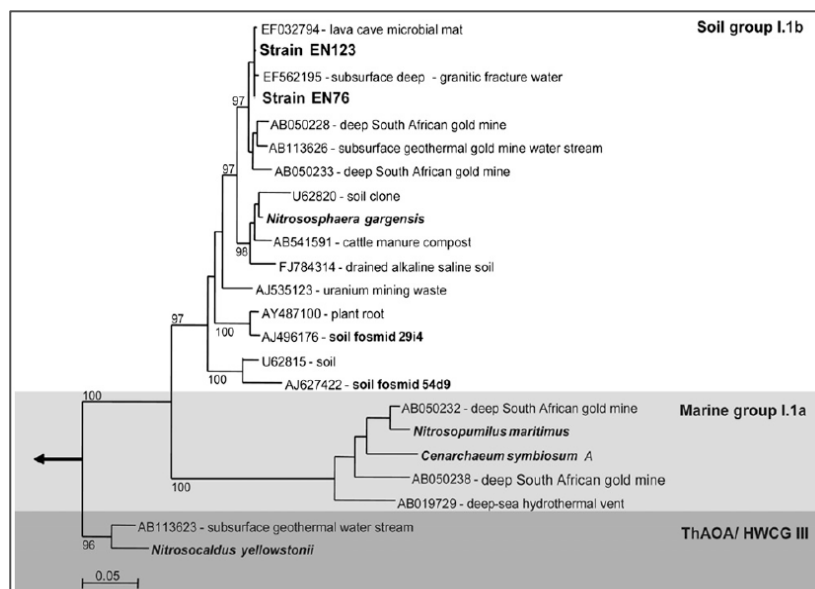
Figure 2-9: Phylogenetic relationships between archaeal 16S rRNA gene sequences of strains EN76 (*Ca.* N. viennensis), EN123 and all described AOA isolates or cultures, as well as relevant environmental clone sequences. Both EN76 and EN123 belong to the group 1.1b of Thaumarchaeota (formerly Crenarchaeota). Taken from Tourna et al., 2011.
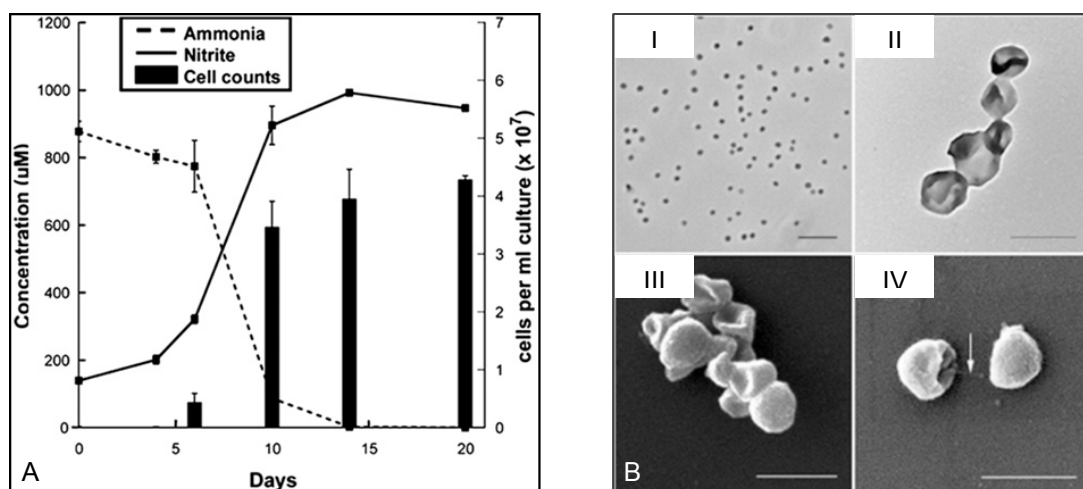
Figure 2-10: A) Correlation between cell density (solid bars), ammonia consumption (dotted line), and nitrite production (solid line) during growth of *Ca.* N. viennensis in medium with 1 mM NH_4^+, supplemented with 1 mM pyruvate. Plotted data represents means of triplicate incubations. Error bars represent SEs. **B)** Microscopy pictures of *Ca.* N. viennensis in pure culture. (I) Phase contrast-light micrograph (scale bar: 5 µm). (II) Transmission electron microscope image of negative stained cells (scale bar: 1 µm). (III and IV) Scanning electron microscope images of cells (scale bar: 1 µm). The arrow in D points to a cell appendage. Taken from Tourna et al., 2011.

2.7   Aim of the study

In this study, different physiological as well as biochemical approaches were used in order to obtain insight into the unknown pathway of archaeal ammonia oxidation. The focus was on the second step of this process which leads to nitrite formation, studying an enzyme which may be involved and different nitrogen species which could be possible intermediates.

The enzyme studied is the NirK homologue found on the previously mentioned archaeal soil fosmid, seeking evidence if this enzyme has the possibility to replace the bacterial HAO in archaea or at least if it has a functional part in the archaeal ammonia oxidation process. The hypothesis of its participation in ammonia oxidation is based on several aspects: bacterial ammonia oxidizers also contain these enzymes and data suggest a supporting role in the ammonia-oxidizing metabolism. The archaeal NirK homologue is found to be highly expressed in metatranscriptomic data, also under aerobic conditions. Usually, the NirK reduces nitrite to NO as part of the denitrification. It is well known that enzymes often can catalyze the reverse reaction as well, in this case the oxidation of NO to nitrite. Due to all these findings, a theory of the archaeal NirK homologue catalyzing nitrite production from NO or NH_2OH, which may be produced in the first step by AMO, was generated. Former studies had already shown that the NirK from fosmid 54d9 has no actual nitrite reductase activity but the ability to

reduce $K_3Fe(CN)_6$ under the presence of NH_2OH without nitrite formation. Under this aspect, the enzyme activity was characterized further. Several other nitrogen species apart from NH2OH which could be possible candidates for interacting with the enzyme as well as other possible generated products were examined. Also some external influences were tested if they would have an impact on the incomplete HAO activity. Concerning the fact that the NirK enzyme of the soil contig has an additional amicyanin domain, intent of this study was also to clone, express and isolate the homologous gene of *Ca.* N. viennensis, which does not contain this domain.

Single enzyme assays may miss out on something essential needed but which is available in a cell protein fraction. Therefore, experiments supplementing the investigation on the metabolism were performed with an available culture of *Ca.* N. viennensis. Crude cell extracts as well as cell extract fractions were analyzed for HAO or NIR activity to be able to compare the results with those of the heterologously expressed NirK homologue.

A physiological study should give information about the effect of a specific NO-scavenger on the growth of *Ca.* N. viennensis, indicating if NO is an intermediate in the AOA metabolism.

A proteomic study of *Ca.* N. viennensis whole cell extracts was done for subsequent MALDI-TOF analysis in order to detect the NirK enzyme in the proteome.

3 Materials and Methods

3.1 Materials

3.1.1 Chemicals

Chemical list

α-Naphtylethylendiamindihydrochloride	Sigma
Acetonitrile	Sigma-Aldrich
Agarose (LE)	Biozym
Ammonium chloride	Sigma-Aldrich
BSA	Fluka
Copper(II) chloride dihydrate	Roth
Dichloroisocyanuric acid sodium salt dehydrate	Fluka
Dipotassium phosphate	Roth
Dithionite	Sigma-Aldrich
DMSO	Fermentas
dNTPs	Fermentas
Ethidium bromide	AppliChem
Glycerol	Applichem
Hydrogen chloride	Roth
Hydroxylaminhydrochloride	Sigma-Aldrich
Methyl Viologen Dichloride Hydrate	Sigma-Aldrich
Monopotassium phosphate	Roth
Nitroprusside dehydrate	Fluka
NuPage® 4-12% Bis-Tris Gel 1,5mm x 10 wells	Invitrogen
NuPage® LDS Sample Buffer (4x)	Invitrogen
NuPage® MOPS SDS Running Buffer (20x)	Invitrogen
Orange G loading dye	Sigma-Aldrich
Ortho phosphoric acid	Roth
Pefabloc® SC-Protease Inhibitor	Roth
Proteinase K	AppliChem
PTIO	Sigma-Aldrich
Pyruvate	Roth
Rotiphorese® 50x TAE Buffer	Roth

Sodium chloride	AppliChem
Sodium hydroxide	Roth
Sodium nitrite	Roth
Sodium salicylate	Sigma-Aldrich
Sulfanilamide	Sigma-Aldrich
Sybr Green	Sigma-Aldrich

Antibiotics

Carbenicillin	Roth
Kanamycin	AppliChem
Streptomycin	Sigma-Aldrich

Electron acceptors

Cytochrome c from horse heart	Sigma-Aldrich
Potassium ferricyanide (III) powder ($K_3Fe(CN)_6$)	Sigma-Aldrich

NO-donors

Diethylamine (DEA) NONOate	Cayman Chemical
Diethylenetriamine (DETA) NONOate	Cayman Chemical

HNO-donor

N-Acetoxy-N-acetyl-4-chlorbenzensulfonamid	Sigma-Aldrich

3.1.2 Media

Fresh Water Medium (per liter)

Salts:		
	NaCl	1.0 g
	$MgCl_2$ $6H_2O$	0.4 g
	$CaCl_2$ $2H_2O$	0.1 g
	KH_2PO_4	0.2 g
	KCl	0.5 g

The salts were solubilized in 1 L of MilliQ water and the solution was autoclaved. Following solutions were added additionally under sterile conditions:

Modified trace elements	1.0 ml
FeNaEDTA solution	1.0 ml
Vitamin solution	1.0 ml

Sodium bicarbonate (1 M)	2.0 ml
Streptomycin (50 mg/ml)	1.0 ml
NH_4Cl (1 M)	x ml
Nitrite (0.1 M $NaNO_2$)	1.0 ml

Skinner and Walker Medium (per liter)

KH_2PO_4	0.2 g
$CaCl_2$ $2H_2O$	0.04 g
$MgSO_4$ $7H_2O$	0.04 g

The substrates were solubilized in 1 L of MilliQ water. Following solutions were added:

| FeSO4/NaEDTA | 1 ml |
| Phenol Red | 1 ml |

After autoclaving, the pH was adjusted to 7.5 by adding 5% Na_2CO_3 until the color changed from yellow to pink. Finally, ammonium chloride was added as requested.

| NH_4Cl (1 M) | x ml |

Luria Bertani (LB) Medium (per liter)

Trypton	10 g
Yeast extract	5 g
NaCl	10 g

The chemicals were solubilized in 1 L of MilliQ water and autoclaved.

For plates, additionally 15 g of Agar were added.

SOB-Medium

2% Bacto Trypton

0.5% Yeast extract

10 mM NaCl

2.5 mM KCl

SOC-Medium

SOB-Medium

20 mM Glucose

20 mM Mg_2^+

3.1.3 Solutions

Modified non-chelated trace element mixture

Distilled H_2O	987 ml	
HCl (conc. ~12.5 M)	8 ml	(100 mM)
H_3BO_3	30 mg	(0.5 mM)
$MnCl_2\ 4H_2O$	100 mg	(0.5 mM)
$CoCl_2\ 6H_2O$	190 mg	(0.8 mM)
$NiCl_2\ 6H_2O$	24 mg	(0.1 mM)
$CuCl_2\ 2H_2O$	2 mg	(0.01 mM)
$ZnSO_4\ 7H_2O$	144 mg	(0.5 mM)
$Na_2MoO_4\ 2H_2O$	36 mg	(0.15 mM)

The solution was sterilized by autoclaving.

FeNaEDTA solution (per liter, 7.5 mM)

FeNaEDTA	2753 mg
MilliQ water	filled up to 1000 ml

The solution was sterilized by autoclaving or filtration.

Vitamin solution (per liter)

Biotin	0.02 g
Folic acid	0.02 g
Pyridoxine HCl	0.10 g
Thiamine HCl	0.05 g
Riboflavin	0.05 g
Nicotinic acid	0.05 g
DL Pantothenic acid	0.05 g
P Aminobenzoic acid	0.05 g
Choline chloride	2.00 g
Vitamine B12	0.01 g

The pH of the solution was adjusted to pH 7 by adding KOH and sterilized by filtration.

Sodium bicarbonate solution (1 M)

100 ml MilliQ water were poured into a 150 ml serum flask. The solution was purged with CO_2 gas for 15 min while it was stirred with a stir bar. 8.4 g of $NaHCO_3$ were added and the vial was tightly sealed immediately with a rubber stopper. The solution was sterilized by autoclaving.

HEPES Buffer stock solution (per 500 ml, 1 M HEPES, 0.6 M NaOH)

NaOH	12.0 g
HEPES (free acid)	119.2 g

The chemicals were dissolved in 100 ml MilliQ water and the solution was sterilized by autoclaving or filtration.

$FeSO_4$/NaEDTA solution (per 100 ml)

$FeSO_4$	0.05 g
NaEDTA	0.05 g

The chemicals were dissolved in 100 ml MilliQ water and autoclaved.

Phenol Red solution (per 100 ml)

Phenol Red	0.05 g

The chemical was dissolved in 100 ml MilliQ water and autoclaved.

5% Na_2CO_3 solution (per 100 ml)

Na_2CO_3	5 g

The chemical was dissolved in 100 ml MilliQ water and autoclaved.

Bradford-Reagent

Coomassie Brilliant Blue G 2500	0.01% (w/v)
Ethanol	4.75% (v/v)
Phosphoric acid	8.5% (v/v)

0.3 M NaOH solution

785 µl of 50% sodium hydroxide were diluted in 50 ml MilliQ water.

Sodium salicylat solution

8.5 g sodium salicylat and 63.9 mg sodium nitroprusside dihydrate were dissolved in 50 ml MilliQ water. The solution had to be prepared freshly every day.

Oxidation solution

0.1 g dichloroisocyanuric acid sodium salt dihydrate was dissolved in 100 ml MilliQ water. The solution had to be prepared freshly every day.

Color reagent

0.3 M NaOH solution, sodium salicylat solution and MilliQ water were mixed at the ratio of 1:1:1. The solution had to be prepared immediately before use.

Sulfanilamide/NED reagent

150 ml orthophosphoric acid were added to 700 ml H_2O. Then 10 g of sulfanilamide were added, while the solution was stirred and warmed up a little. Afterwards, 0.5 g α-naphtylethylendiamindihydrochloride were added, the solution was filled up to 1 L and stored at 4°C in the dark.

3.1.4   Buffers

Phosphate buffer (KPi, pH 7.0, 1 M, per 100 ml)

K_2HPO_4 1 M	61.5 ml
KH_2PO_4 1 M	38.5 ml

10x MOPS-buffer

0.2 M MOPS (pH 7.0)

20 mM sodium acetate

10 mM EDTA

41.8 g MOPS were dissolved in 700 ml DEPC-treated H_2O. The pH was adjusted to 7.0 with 2N NaOH. 20 ml of DEPC-treated 1 M sodium acetate and 20 ml of DEPC-treated 0.5 M EDTA (pH 8.0) were added. The volume of the solution was adjusted to 1000 ml with DEPC-treated H_2O and filtered through a 0.45 μm Millipore filter.

3.1.5   Microorganisms

Ca. Nitrososphaera viennensis	Schleper lab, Vienna, A
Nitrosospira multiformis	Prosser lab, Aberdeen, UK
Escherichia coli TOP10	Invitrogen

3.1.6   Vectors

pET-28a(+) (5369bp)	Novagen

3.1.7 Enzymes

Polymerases

GoTaq® Flexi DNA Polymerase	Promega
Phusion® DNA Polymerase	Finnzymes

Restriction enzymes

*Ase*I	New England Biolabs
*Nco*I	New England Biolabs
*Xho*I	Fermentas

CIAP	Fermentas
T4-DNA-Ligase	Fermentas
NirK from soil contig 54d9	(Treusch et al., 2005)

3.1.8 Primers (5´– 3´)

AOA amoA gene

Cren amoA 104F (1d)	unpublished

GCAGGAGACTACATMTTCTA

Cren amoA 616R	(Tourna et al., 2008)

AOB amoA gene

amoA 1F	(Rotthauwe et al., 1997)
amoA 2R	(Rotthauwe et al., 1997)

Bacteria 16S rRNA gene

P2	(Muyzer et al., 1993)
P3	(Muyzer et al., 1993)

Primers for NirK expression

NK1 fwd.	Thermo Scientific

CTTCCATGGTCAGTCCACTTTTCAACGGATT

NK2 nat. rev.   Thermo Scientific

CATCTCGAGCAGTTAACCAGAGGTGGTGTTGC

NK3 his rev.   Thermo Scientific

CATCTCGAGCAGCTGACCAGAGGTGGTGTTGCC

NK4 thromb. rev.   Thermo Scientific

CATCTCGAGGCTGCCGCGCGGTACCAGACCAGAGGTCGTGTTGCCA

pET28 Seq. Fwd.   Eurofins

TTCAGCAAAAAACCCCTC

pET28 Seq. Rev.   Eurofins

TCTTCCCCATCGGTGATGT

pET28 + NirK Seq. F   Eurofins

AGCAGCCTGACCTCATCCT

pET28 + NirK Seq. R   Eurofins

AGGATGAGGTCAGGCTGCT

3.1.9 Kits

NucleoSpin® Extract II   Macherey-Nagel
Plasmid Mini Kit II D6945-02   OMEGA bio-tek

3.1.10 DNA and Protein Standards

GeneRuler™ 1kb DNA Ladder SM0311   Fermentas
GeneRuler™ 1kb Plus DNA Ladder SM1331   Fermentas
GeneRuler™ 100 bp DNA Ladder SM0241   Fermentas
GeneRuler™ 100 bp Plus DNA Ladder SM0321   Fermentas
SeeBlue®Plus2 Prestained Standard   Invitrogen

3.2 Methods

3.2.1 Hydoxylamine oxidoreductase (HAO) activity determination

Standard hydroxylamine oxidoreductase assay

The assay mixture consisted of the following components:

- 250 µl $K_3Fe(CN)_6$
- 250 µl KPi-buffer (100 mM, pH 7.0)
- 250 µl enzyme NirK or KPi-buffer (50 mM, pH 7.0) as a negative control
- 250 µl NH_2OH/NO-/HNO-sources

With this mixture, a final concentration of 50 mM KPi-buffer and 7.5 µg/ml NirK was achieved in the assay solution. Different concentrations of hydroxylamine were used, therefore the ferricyanide concentrations were equally adapted until a maximum of 2.5 mM, which reached the saturation range of the spectrophotometer. For some experiments the volume of the assay was scaled down to either 200 µl or 50 µl per component to gain a setup of 800 µl or 200 µl in total. Depending on the volume, the assay was performed in 1.5 ml or 840 µl plastic cuvettes.

Variations of the HAO assay composition

Based on the standard assay composition, various alterations of the used electron acceptor, the investigated enzyme and substrates as well as their concentrations and assay conditions were tested.

Alterations of the electron acceptor:

- Different concentrations varying from 500 µM to 2.5 mM.
- Cytochrome c from horse heart used as an alternative for ferricyanide.

Alterations of the investigated NirK enzyme:

- Different concentrations of NirK varying from 7.5 µg/ml to 75 µg/ml.
- NirK prereduced with methylviologen.

  The setup consisted of a 10 mM methylviologen solution in an anaerobic sealed vessel. Reduction of this electron carrier is required for activation, which is achieved by carefully drop wise addition of a 100 mM dithionite solution via a syringe until the substrate changed its color from translucent to dark blue. This change indicated the reduced condition. Drops of the reduced methylviologen were mixed with the enzyme. The therefore reduced NirK was put into the assay mix to start the reaction.

- NirK treated with protease to abolish activity.

  An aliquot with a concentration of 30 µg/µl enzyme was treated with 40 µg/µl Proteinase K at 37°C on a heating block. After one hour of incubation, the enzyme was used in a standard assay of 2.5 mM hydroxylamine and 2.5 mM electron acceptor.

- NirK exposed to different temperatures.

  Aliquots of 50 µl enzyme were incubated on a heating block at 40°C, 60°C and 80°C, additionally one was kept on room temperature. The duration of the experiment was six hours, an aliquot of enzyme which was kept on ice for the same time was used as a positive control. After one hour and six hours of incubation, the activities of the differentially treated enzymes were compared in an assay consisting of 2.5 mM NH_2OH and 2.5 mM $K_3Fe(CN)_6$.

- NirK replaced with copper solutions.

  A copper(II) chloride dihydrate solution replaced the NirK enzyme in the basic assay composition with concentrations of 25 nM, 50 nM, 100 nM, 500 nM and 1 µM copper. The theoretical copper incorporation of the recombinant enzyme was calculated to achieve comparable concentration ranges. A negative control consistent of KPi-buffer and a positive control with the NirK enzyme were performed as well. Hydroxylamine concentrations in this experimental setup were either 2.5 mM or 25 mM. Additionally, the 50 nM, 100 nM and 500 nM solutions were also treated with 40 µg/ml Proteinase K at 37°C.

Alterations of the substrates:

- Different concentrations of hydroxylamine varying from 50 µM to 25 mM.

- Hydroxylamine replaced with nitric oxide-donors.

  In this experiment, two common NO-Donors were used instead of hydroxylamine, DEA NONOate (Diethylamine NONOate diethylammonium salt) and DETA NONOate (Diethylenetriamine NONOate). The two components differ in their half-life, DEA releasing half of the possible NO in 60 minutes, DETA in 56 hours. The faster agent DEA was used in the majority of experiments. The NO-donor substrates were dissolved in a 10 mM NaOH solution which was outgassed and purged with N_2, in tightly sealed anaerobic vessels. This way the solutions were stable for at least 24 hours. In some cases the substrates were also weighed in in an anaerobic chamber to be sure to obtain the anaerobic status. Since the fine scale balance would not fit in the anaerobic chamber, the substrate was weighed in approximately, resulting in concentrations of the solutions around 10 mM. For the assays concentrations of ~2.5 mM were used, all other concentrations remained standard.

- Hydroxylamine replaced with a nitroxyl-donor.

  N-Acetoxy-N-acetyl-4-chlorobenzenesulfonamide (NANa) at a concentration of 4.3 mM in the assay was used as a HNO-donor. Because of its water insolubility, it was dissolved in 40 µl acetonitrile first and 2 ml 50 mM KPi-buffer afterwards, achieving a 17.2 mM stock solution. The concentrations of the remaining substrates are the same as described before, an additional enzyme concentration of 30 µg/µl was tested as well.

- Mix of hydroxylamine and DEA.

  This approach consisted of the standard assay composition but instead of 2.5 mM hydroxylamine, a mixture of hydroxylamine and DEA in equimolar amounts (1.25 mM final concentration each) was added.

- Hydroxylamine replaced with ammonium chloride (NH_4Cl).

  Instead of hydroxylamine, an ammonium chloride solution with a final concentration of 2.5 mM was put in the standard assay composition.

- Hydroxylamine/DEA mixed with small amounts of nitrite.

  Additionally to the hydroxylamine and DEA solutions, small amounts of nitrite were added at the start of the reaction. The final nitrite concentration was tenfold smaller as the main investigated substrate concentrations, 2.5 mM hydroxylamine or DEA with 250 µM nitrite, respectively. All other assay conditions remained the same.

Variation of external influences:

- HAO assay aerated.

  Several setups including shaking, vortexing and the introduction of gas via syringes or plastic tubes of the standard HAO assay composition were investigated. Samples were taken after defined time points (every 10 minutes or every hour) and the production of nitrite was measured via the Grieß-reaction (described later).

- HAO assay under anaerobic conditions.

  For this experiment, the usual plastic cuvettes were replaced with glass cuvettes which could be tightly sealed with a screw cap provided with a septum. Two different approaches were taken to achieve anaerobic assay conditions. The first was to aliquot all needed substrates and transfer them into an anaerobic chamber, where they were pipetted into the cuvettes. The second consisted of adding all solutions in sealed vessels which were purged with N_2 and vacuum exhaust in turn for three times. Afterwards, the solutions were pipetted in a sealed cuvette and the anaerobic treatment was repeated. These procedures were carried out with every substrate except hydroxylamine which

was anaerobicized for every approach separately in a vessel. The cuvettes were put in the photometer and shortly after the measurement started, the anaerobic hydroxylamine was added in the cuvettes with a syringe to start the reaction. Otherwise time points of the reaction would be missed. The assay conditions were 2.5 mM or 25 mM NH_2OH, 2.5 mM $K_3Fe(CN)_6$ and 7.5 µg/µl or 30 µg/µl NirK enzyme. The assay with same conditions was also repeated in plastic cuvettes which could be sealed with a rubber stopper. Possible leakage was prevented via silicone which was put on the transitions and the needle entries. After one week in an anaerobic chamber where the oxygen could outgas of the plastic, the anaerobic treatment of the solutions was done as described in the first approach above.

Calculation of activity parameters for the HAO activity of NirK

Two dilution series of hydroxylamine with consistent NirK concentrations of 7.5 µg/ml and 2.5 mM $K_3Fe(CN)_6$ were carried out to calculate the specific activity of the enzyme in u/mg. Hydroxylamine concentrations ranged between 50 µM and 5 mM or between 125 µM and 10 mM alternatively.

3.2.2   HAO assay with cell extract of *Ca.* N. viennensis

To investigate whether the *Ca.* N. viennensis cell extract possessed a hydroxylamine oxidoreductase activity, it was used instead of the NirK enzyme in the standard HAO assay composition (preparation of cells is described later). Whole crude cell extract, pellet and soluble fraction had final protein concentrations of 250 µg/ml for each fraction, hydroxylamine was given either at 2.5 mM or 25 mM and the electron acceptor $K_3Fe(CN)_6$ always had a concentration of 2.5 mM. For the cell extract experiments further substrates like 2.5 mM DEA were tested. 2.5 mM NH_4Cl was also examined with colorimetric detection of ammonium consumption or nitrite production. The sample setup for this experiment consistent of KPi-buffer, ammonium chloride, cell extract fractions and the electron acceptor ferricyanide as well as the electron donor methylviologen or a mixture of both, because it is unclear what the cell extract might need for this reaction. After one hour, small amounts of NO_2^- and NH_2OH were added additionally. After one and two hours, samples of every assay were taken and the concentration of ammonia and nitrite was determined. An equal mixture of hydroxylamine and DEA (both 2.5 mM) as well as hydroxylamine or DEA (each 2.5 mM) with the addition of small amounts of nitrite (250 µM) were investigated as

well. Nitrite and N_2O were considered as candidates for products or at least intermediates. Nitrite was determined via the Grieß-reaction, N_2O indirectly via addition of 2.5 µM PTIO to the assay containing 2.5 mM hydroxylamine and 2.5 mM ferricyanide.

3.2.3 Nitrite reductase (NIR) activity determination of the NirK enzyme and cell extracts of *Ca.* N. viennensis

Nitrite reductase activity was assessed with a modified assay from Treusch, 2004. The assay consisted of 250 µl 100 mM KPi-buffer, 340 µl 1 mM $NaNO_2$ and 80 µl of 50 mM methylviologen which were mixed in a sealed flask and treated as described before to obtain anaerobic conditions. The methylviologen was subsequently reduced by addition of 200 µl 100 mM sodium dithionite, which resulted in a blue color formation. The reaction started with the addition of 200 µl of NirK protein (final concentration 7.5 µg/ml or 30 µg/ml) or cell extract solution (final concentration 100 µg/ml or 600 µg/ml). After defined time points between 0 and 60min, samples were taken and the reaction was stopped via aeration. The remaining nitrite was determined via the colorimetric reaction with Sulfanilamide/NED. A crude cell extract of *Alcaligenes xylosoxidans* (15 µg/ml), a gram-negative aerobic Bacterium capable of denitrification acted as a positive control.

3.2.4 Nitrite measurement

Nitrite was measured via the so called Grieß-reaction, a colorimetric assay based on the chemical reaction of sulfanilamide/NED with nitrite which results in a pink color formation. For each sample 780 µl corresponding medium or buffer, 20 µl sample and 200 µl sulfanilamide/NED were added in an Eppendorf tube. For calibration, standard curve samples varying from 0 to 1 mM were made from a 1 mM $NaNO_2$ solution. After shaking, the tubes were incubated for at least 10 min at room temperature in the dark. Then, 200 µl of the mixture were transferred into a microtiter plate and the absorbance was photometrically measured at 545 nm.

3.2.5 Ammonia measurement

The assay for the detection of ammonium is based on its oxidation to chloroamine by sodium dichloroisocyansure acid which results in a green indophenol in presence of phenolic compounds in an alkaline media. For the reaction, 0.3 M NaOH solution,

sodium salicylat solution and oxidation solution were prepared. The color reagent was obtained by mixing of 0.3 M NaOH solution, sodium salicylat solution and MilliQ water at the ratio of 1:1:1. For each sample, 400 µl of media or buffer and 200 µl sample were mixed in an Eppendorf tube. To calculate the values, 8 standards ranging from 0.5 mM to 0 were prepared with a 0.85 mM NH_4Cl solution. 300 µl of color reagent and 120 µl oxidation solution were added to 600 µl of standards or sample and the tubes were put on a horizontal shaker at 300 rpm for half an hour. Afterwards, 200 µl of the mixture were transferred into a microtiter plate and the absorbance was measured with a photometer at 660 nm.

3.2.6 Nitrous oxide detection

For the measurement of N_2O, the HAO assay took place in a sealed, anaerobic vessel, containing final concentrations of 1 mM $K_3Fe(CN)_6$, 1 mM NH_2OH and 7.5 µg/ml NirK enzyme. Additionally, two controls were verified as well, one containing enzyme but no hydroxylamine, the other containing hydroxylamine but no enzyme. After 25 minutes, 12 ml gas phase were taken out via a syringe and transferred into another sealed tube. The concentration of N_2O was determined by Isotopic Ratio Mass Spectrometry (IRMS) at the Department of Terrestrial Ecosystem Research, Vienna, Austria.

3.2.7 Nitric oxide detection

As a direct measurement was not available, the possibility of NO being an intermediate or product was determined indirectly with PTIO, a specific NO-scavenger. The reagent was added directly in different amounts varying from 10 µM to 1 mM to growing cultures and to assays with NirK as well as cell extracts of *Ca.* N. viennensis, always with a final concentration of 2.5 mM. The investigated assays contained either 25 mM or 2.5 mM hydroxylamine and 2.5 mM $K_3Fe(CN)_6$. Because PTIO is barely soluble in aqueous solutions (> 0.03%), a stock solution of 1 mM was used for all experiments. The solution of the intact substrate has a dark violet appearance, which changes to translucent if it is reacting. Before using it as an NO-indicator, cross reactions with hydroxylamine were tested and also an absorbance spectrum of the solution was done.

3.2.8 Cultivation methods

Ca. N. viennensis

For growing *Ca.* N. viennensis, 250 ml Schott bottles were used, rinsed three times with MilliQ water and autoclaved to minimize contaminations. Under sterile conditions, 90 ml Fresh Water Medium was filled in. Additionally, NH_4Cl with a final concentration of 1 mM was added separately. 10 ml of an already grown culture shortly before reaching stationary phase were used as inoculum. The prepared culture was incubated at 37°C, growing up to stationary phase between 6 and 10 days. The growth was monitored via nitrite and ammonia measurements, supplemented with microscopic cell counting.

Upscaling *Ca.* N. viennensis cultivation

Instead of 250 ml screw bottles, a fermenter with a capacity of 10 L was used for cultivation, where 4 L to 8 L of culture could be cultivated in standard Fresh Water Media supplemented with 3 mM ammonia at once. The growth conditions remained similar (37°C), despite of gently shaking (100 rpm) the fermenter. The growth was monitored with nitrite and ammonia measurements, supplemented with cell counting.

N. multiformis

For cultivation of *N. multiformis*, 250 ml, 500 ml or 1 L autoclaved Schott bottles were used. Under sterile conditions, 90 ml, 180 ml or 360 ml Skinner and Walker Medium was added. The pH was adjusted with Na_2CO_3 until the media changed its color from yellow (acidic pH) to pink (alkaline pH). Afterwards, NH_4Cl with a final concentration of 3 mM was added and the culture was inoculated with 10 ml, 20 ml or 40 ml of an already grown culture. The culture was incubated at 28°C, growing up to stationary phase between 6 and 8 days. During growth, the pH had to be monitored via change of color and adapted with Na_2CO_3 if necessary. The growth was monitored every day with nitrite and ammonia measurements, supplemented with cell counting.

E. coli Top10

E. coli cells were grown in either LB-Media or on LB-Plates at 32°C or 37°C overnight, shaking with 200 rpm.

Cultivation of different microorganisms to detect nitric oxide

Three different organisms representing either AOA, AOB or heterotrophic growing Bacteria were grown with different concentrations of PTIO to study the occurrence of

nitric oxide during growth. For comparison, the cell concentration of each culture had to be adjusted to similar amounts, which was achieved by cell counting and diluting. Every inoculum contained about 4.6×10^7 cells/ml.

- *Ca.* N. viennensis

  The experiment contained four 20 ml cultures of *Ca.* N. viennensis, grown in 30 ml plastic tubes. One culture served as a control while to the others increasing concentrations of PTIO (10 µM, 50 µM or 250 µM) were added either during inoculation or during exponential phase. To determine growth, samples for nitrite and ammonia measurement were taken every day.

- *N. multiformis*

  N. multiformis was grown in 20 ml cultures. One culture remained as a control, while 50 µM or 250 µM PTIO were added in two separate cultures. In this setup, PTIO was added just during inoculation because growth rates and therefore cell amounts of the organisms are not comparable. Every day, samples were taken for nitrite and ammonia measurement to calculate growth.

- *E. coli* Top10

  E. coli was grown in 10 ml cultures in 50 ml Greiner tubes. PTIO in concentrations of 50 µM, 250 µM, 500 µM or 1 mM was added during inoculation of four different cultures, while a fifth one served as a control culture. Since *E. coli* is a fast growing organism, samples were taken at defined time points between 30 min and 20 h and the growth could be measured via optical density at 600 nm with the spectrophotometer.

3.2.9 Preparation of cells

Cell counting

To check the purity or the appearance of a cell culture, 2 µl of culture were pipetted on a glass slide. For growth determination, 10 µl of the culture was examined, counting appearing cells in at least 10 visual fields. With the average of cells the amount of cells per ml culture is calculable, therefore the value was multiplied with 2.5×10^6.

Cell harvesting

To harvest the cells, the culture was either transferred to a falcon or to a special centrifuge tube, depending on which centrifuge was used. *Ca.* N. viennensis was centrifuged at 9000 rpm for 40 min in the GS-3 rotor of the SORVALL® Evolution™ RC Superspeed Centrifuge. *N. multiformis* cells were also spun down in the same

centrifuge, using the SS-34 rotor at 20500 rpm for 40 min. *E. coli* was harvested with the Hettich Universal 320R at 4500 rpm for 10 min in the rotor numbered 1324. Every centrifugation was carried out at 4°C. Afterwards, the supernatant was discharged and the pellet was stored at -20°C or resuspended in KPi- or Tris-buffer.

Cell disruption

The harvested cells were resuspended in KPi-buffer (50 mM, pH 7) and lysed with an ultrasonic homogenizer from BANDELIN electronic, type SONOPULS UW 2070, 10 times for 1 min at 60% power, while embedded in ice. The disruption could be observed via the microscope: while intact cells had a dark, round shaped appearance, the sonicated ones looked rather see-through and disrupted. The cell extract was stored at -20°C.

Fractionation

A part of the resulting cell extract was fractionated into an insoluble and a soluble fraction via centrifugation in the Hettich Universal 320R, using the 1420a rotor at 15000 rpm for 1 h. The insoluble fraction was resuspended in KPi-buffer according to the amount of the soluble fraction. Both were stored at -20°C.

Protein quantification

To quantify the resulting protein amount after the cell disruption, a Bradford assay was performed. For calculating the protein concentrations, a standard curve ranging from 0 µg to 9 µg BSA was prepared. 20 µl of the standard solutions or the samples were put into a 1 ml plastic cuvette and gently mixed with 980 µl Bradford reagent. After incubation for 5 minutes at room temperature in the dark, the absorbance at 595 nm was measured. Since the used Bradford reagent did not seem to be accurate, a UV spectrophotometric measurement at 280 nm with the Nanodrop was used as an alternative.

3.2.10 SDS-polyacrylamide gel-electrophoresis

Ca. N. viennensis cells, a whole crude cell extract and an insoluble as well as a soluble fraction were loaded on a NuPage® 4-12% Bis-Tris Gel from Invitrogen, run in 1x NuPage® MOPS SDS Running Buffer. The cells or protein solutions were mixed with 1x NuPage® LDS Sample Buffer and 5% mercaptoethanol. After vortexing, the samples were heated up to 95°C for five minutes to denaturate the proteins and

centrifuged for 5 minutes to get rid of membrane components. The resulting supernatants were loaded in two different amounts: either 30 µl of the soluble fraction and 10 µl of *Ca.* N. viennensis cells, whole crude cell extract and insoluble fraction or 15 µl and 5 µl. The gel was run at 200 V for 45 min. 5 µl of SeeBlue®Plus2 Prestained Standard Protein Ladder were run alongside the samples to enable protein size determination.

3.2.11 Preparation of proteins for MALDI-TOF analysis

Digestion of gel-pieces

Two bands and one region of the crude cell extract lane were cut out of the gel and placed into a 1.5 ml Eppendorf tube.

- Washing

  The gel pieces were washed with 200 µl water, vortexed for 15 min and the liquid was removed. The washing step was repeated with 200 µl of 100 mM NH_4HCO_3 and 200 µl acetonitrile (ACN). Dark pieces were washed again with 50% ACN and 50 mM NH_4HCO_3. Finally, all residual liquid was removed and the gel-pieces were dried in a speed vacuum centrifuge for 5 min.

- Digestion with trypsin

  First, a digestion buffer was made containing 25 mM NH_4HCO_3, 10% acetonitrile and 5 mM $CaCl_2$. A trypsin-vial was dissolved in 50 µl 1 mM HCl and kept on ice. 600 µl of the buffer were mixed with 15 µl trypsin which resulted in a concentration of 12.5 ng trypsin per µl, as well kept on ice. This trypsin-buffer was added to the dried gel-pieces, 15 µl each. After 20 minutes, all samples were checked if the trypsin was soaked up and 10 µl were additionally added if necessary. After 45 min, the gel-pieces were washed with 100 µl digestion buffer. Finally, one droplet of buffer was added again to cover the pieces, the rack with the tubes was covered with aluminum foil and incubated at 37°C overnight.

- Extraction

  The extraction of the proteins was achieved with the addition of different concentrations of formic acid and ACN:

  – 20 µl 5% formic acid added, vortexed for 5 min, liquid removed into a fresh siliconised tube

  – 20 µl 1% formic acid, 5% ACN added, vortexed for 45 min, liquid removed into the same tube

- 20 µl 1% formic acid, 50% ACN added, vortexed for 45 min, liquid removed into the same tube
- 20 µl 1% formic acid, 90% ACN added, vortexed for 45 min, liquid removed into the same tube

After this procedure, the samples were dried in a speed vacuum centrifuge until all liquid was completely removed.

Digestion of the soluble fraction of *Ca.* N. viennensis cell extract

200 µl trypsinbuffer (10% ACN, 0.5 mM CaCl, 25 mM NH_4HCO_3 and 1 mM PMSF) was added to 100 µg of soluble proteins and incubated for 30 min at 37°C. 10 µl trypsin-beads were added and the digestion was incubated at 37°C, shaking overnight. Afterwards, the supernatant was carefully removed from the beads, transferred into another siliconised Eppendorf tube and dried in a speed vacuum centrifuge until the liquid was completely removed.

Digestion of the pellet fraction of *Ca.* N. viennensis cell extract

The pellet was solubilized in 1 mM Tris-buffer containing 8 M urea. In the first digestion step, the proteins were incubated with 5 µl of 0.1 µg/ml endoproteinase Lys-C overnight at 37°C in the dark. Afterwards, the sample was diluted to a concentration of 2 M urea with 100 mM NH_4HCO_3 and 10% ACN, pH 8.5. Also, $CaCl_2$ was added to a final concentration of 1 mM. The second digestion step was achieved by adding 10 µl trypsin-beads, the reaction was shaking overnight at 37°C. Afterwards, the supernatant was carefully removed from the beads, transferred into another siliconised Eppendorf tube and dried in a speed vacuum centrifuge until the liquid was completely removed.

3.2.12 Polymerase chain reaction

For the amplification of DNA-fragments, the polymerase chain reaction (Mullis et al., 1986) was applied. Primers were either used under their already described optimal conditions or for newly designed ones the optimal conditions were established. Every run contained a negative control without any template as well as a positive control with the gene we wanted to amplify of another organism. Dependent on whether a proofreading activity was necessary or not, a Phusion® or a GoTaq® Flexi DNA Polymerase protocol was applied.

Phusion® DNA Polymerase approach (50 µl):

H_2O	30.75 µl
5x Buffer BC	10 µl
dNTPs (10 mM)	1 µl
Primer fwd. (10 µM)	2.5 µl
Primer rev. (10 µM)	2.5 µl
BSA (20 mg/ml)	0.5 µl
DMSO	1.5 µl
Phusion Taq	0.25 µl
DNA	1 µl

GoTaq® DNA Polymerase approach (25 µl):

H_2O	15.85 µl
5x GoTaq-Buffer	5 µl
dNTPs (10 mM)	0.5 µl
Primer fwd. (10 µM)	0.5 µl
Primer rev. (10 µM)	0.5 µl
MgCl	1.5 µl
Go Taq	0.15 µl
DNA	1 µl

Basic PCR running program

Denaturation:	94°C	03:00
Amplification (35 cycles):	94°C	00:30
	54°C	00:45
	72°C	02:00
Elongation:	72°C	10:00

The steps of this basic program were modified according to specific primer annealing temperatures, the length of the amplified molecule. For colony-PCR, the denaturation temperature was increased to achieve a better lysis of the cells.

Amplification of DNA-fragments

- *nirK*

  Specific primers were designed to amplify the *nirK* of *Ca.* N. viennensis. Reverse primers were designed to amplify either the native sequence or to attach an additional His-tag or a His-tag plus a thrombine cutting site.

- *amoA*

  To detect or distinguish between ammonia oxidizing bacteria and ammonia oxidizing archaea, primers designed for the *amoA* gene were used. The used primer pairs were: the Cren amoA 104F (1d) & Cren amoA 616 pair for the *amoA* of archaea and the amoA 1F & amoA 2R primer pair for bacteria.

- genes encoding the bacterial 16S rRNA

  To identify bacteria, their small ribosomal subunit was amplified with already the established primers P2 and P3.

- pET28a sequences

  Specifically designed primers were used to amplify the sequence of the cloning vector near the multiple cloning site.

- pEt28a + *nirK* sequence parts

  To discover if the vector was carrying the specific *nirK* insert, specific primers with a combination of the vector and the *nirK* sequences were used.

"Colony"-PCR

For the identification of *E. coli* transformants which are carrying the recombinant plasmids, a colony-PCR with vector-specific primers which are flanking the multiple cloning site was used. Grown colonies were picked with a sterile toothpick or tip and the cells were directly added to the PCR reaction. In parallel, they were also stroked out on an agar-masterplate containing 50 µg/ml kanamycin. The PCR setup was similar to the GoTaq® DNA Polymerase approach.

3.2.13 Agarose-gelelectrophoresis for separation of DNA-fragments

To visualize and separate DNA-fragments, 1% or 2% agarose gels were used, depending on their size. The agarose was added to 1x TAE-Buffer (Rotiphorese®) and heated in the microwave until it was completely solubilized. When the solution cooled down, drops of ethidium bromide were added and the mixture was poured into a gel chamber. After solidification, the gel was immersed in a running buffer (0.5 x TAE) loaded with DNA and voltage (90-110 V) was applied for fragment separation. The containing ethidium bromide intercalates DNA bases and can be visualized by UV-light.

3.2.14 Purification of PCR products from agarose gels

To purify PCR products, the protocol of the NucleoSpin® Extract II Kit from Macherey-Nagel was used. The DNA was eluted two times in 20 µl Buffer NE, measured on the Nanodrop to determine its concentration and stored at -20°C.

3.2.15 Vector preparation

- Retransformation

  To propagate the vector pET28a (obtained from Alexander Treusch), it was retransformed in competent *E. coli* TOP10 cells. Five colonies were picked and sub cultured overnight.

- Glycerin stocks

  Out of these 5 ml subcultures, 1:1 100% glycerol stocks were made and stored at -80°C. The remaining 4 ml were centrifuged at 4000 rpm for 10 min at 4°C, the supernatant was discarded and the pellets were stored at -20°C.

- Extraction

  The vector was extracted using the Plasmid Mini Kit II D6945-02 protocol from OMEGA.

- Restriction map of pET28a

  To confirm the vector integrity during the retransformation process, a restriction map with the enzyme *Ase*I was produced which should give a certain pattern of five different bands. The restriction ran for 1 hour at 37°C, afterwards the approach was loaded on an agarose gel to determine the fragment size.

3.2.16 Cloning of the *nirK* gene from *Ca.* N. viennensis into the vector pET28a

3.2.16.1 Restriction of vector and purified PCR product

To clone the *nirK* gene into the vector pET28a (Fig. 3-1A), both had to be cut with the restriction enzymes *Nco*I and *Xho*I to receive compatible ends. The restriction sites were either flanking the gene or were located in the MCS (Fig. 3-1B) of the vector. The reactions were incubated at 37°C for 90 min. For both enzymes, the restriction was stopped via heat inactivation for 20 min at 65°C. (Treusch, 2004)
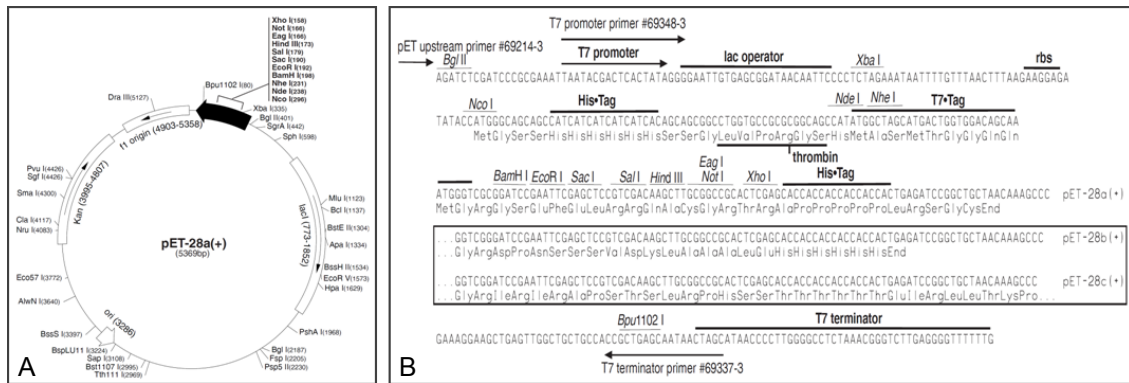
Figure 3-1: A) Schematic model of vector pET-28a. **B)** pET-28a cloning/expression region. Taken from Novagen®.

Vector reaction

Tango-Buffer (2x)	10 µl
Vector-DNA (ng/µl)	x µl
dH$_2$O	x µl
*Nco*I (10 u/µl)	1.5 µl
*Xho*I (10 u/µl)	1.5 µl
Final volume	50 µl

PCR product reaction

Tango-Buffer (2x)	10 µl
Purified PCR product	x µl
dH$_2$O	x µl
*Nco*I (10 u/µl)	1.5 µl
*Xho*I (10 u/µl)	1.5 µl
Final volume	50 µl

3.2.16.2 Vector dephosphorylation

For a successful cloning of the PCR product into pET28a, the vector was dephosphorylated according to the protocol of the alkaline phosphatase (CIAP) from Fermentas. After incubation for half an hour at 37°C, 2.5 µl buffer and 1 µl CIAP were added and the reaction was incubated for half an hour further. To confirm cleavage of the dephosphorylated vector, it was applied on an agarose-gel. The appropriate band was excised and purified.

3.2.16.3 Ligation

The cut pET28a and PCR products were ligated in a 1:3 ratio, calculated via the formula:

$$\frac{\text{conc. vector (ng)} \times \text{fragment length PCR product (nt)}}{\text{fragment length vector}}$$

The reaction was carried out by the T4 Ligase from Fermentas, overnight at 20°C.

3.2.16.4 Transformation

To transform the ligated vector, competent *E. coli* TOP10 cells were taken out of the freezer and slowly defrosted on ice. 1 µl DNA (containing between 100-150 ng) was added carefully to 25 µl competent cells and incubated for 15 min. Afterwards, they were subjected to a heat shock (42°C) for 45 seconds followed by an immediate transfer back on ice for an additional 5 min. 200 µl of SOC-media were added and the cells incubated on a shaker at 37°C, 400 rpm for at least 45 minutes. Finally, 100 µl and 50 µl were plated an LB-plates which contained 50 µg/ml kanamycin to select on the vector and incubated at 32°C overnight.

3.2.16.5 Isolation of ligated vectors from *E. coli* cultures

After transformation, grown colonies were picked and subcultured overnight. The cultures were centrifuged at 4000 rpm for 10 min at 4°C. After discharging the supernatant, the pellets were stored at -20°C. Then, the vector was extracted using the Plasmid Mini Kit II D6945-02 protocol from OMEGA.

3.2.16.6 Restriction analysis of ligated vectors

To screen for vectors containing the right insert, the isolated vector was again cut with *Nco*I and *Xho*I restriction enzymes and loaded on an agarose gel. If the vector carried an insert two bands, if not just one band would occur. The size of the second band gives evidence for the right insert size.

3.2.16.7 Sequencing

To obtain the sequences of purified DNA-products, they were mixed with the appropriate primers and sent to LGC Genomics (Munich) for sequencing.

4 Results

The metabolism of AOA was investigated from various perspectives to cover many possible aspects, concentrating on experiments analyzing the NirK homologue. Its partial HAO activity was characterized further, activity parameters were examined as well as activity under anaerobic conditions, exposure to heat and protease treatment. The experimental setup was altered to establish conditions which may lead to nitrite formation. Also possible copper side reactions were analyzed. The NIR activity assay testing the predicted activity was repeated. To study the ability of the enzyme to catalyze its reverse reaction, the substrate hydroxylamine was replaced with two NO-donors and a HNO-donor. Products other than nitrite were analyzed focusing on nitric oxide and nitrous oxide. Approaches with whole crude and fractionated cell extracts of *Ca.* N. viennensis cells were performed to overcome the possible lack of missing components or unsuitable circumstances in the more reductionist enzymatic assay approach. Further, the cell extracts were tested for various enzyme activities and possible intermediates in archaeal ammonia oxidation. To investigate NO as a possible intermediate, a physiological test observing the effect of a specific nitric oxide scavenger on the growth of a *Ca.* N. viennensis culture was performed. Another attempt was the cloning, expression and isolation of the homologous *nirK* gene from *Ca.* N. viennensis. Further, a proteomics analysis was run to detect the NirK enzyme in fractionated cell extracts of *Ca.* N. viennensis.

4.1 The archaeal NirK homologue from soil fosmid 54d9

The investigated enzyme is a putative copper containing nitrite reductase homologue with an additional C-terminal amicyanin domain whose gene was originally found on a crenarchaeal soil fosmid. The NirK-domain showed 30-32% amino acid similarity to the NirK of *N. europaea* and halophilic Archaea, with 4-5 copper ions per subunit (Treusch, 2004). It was already cloned into the expression vector pET-28a by Alexander Treusch. Afterwards, Johannes Schweichhart did a heterologous expression in *E. coli* followed by isolating and refolding of the protein from inclusion bodies, according to a protocol from G. Sawers. The purified enzyme showed no nitrite reductase activity but it has the ability to reduce the electron acceptor potassium ferricyanide ($K_3Fe(CN)_6$) in the presence of hydroxylamine (Schweichhart, pers. comm.).

To determine the ability of oxidizing hydoxylamine (HAO activity), a modified HAO assay established by Jetten, et al. 1997, modified by Johannes Schweichhart was performed in this study. $K_3Fe(CN)_6$ was used as an electron acceptor, hydroxylamine was given in equal or up to ten times higher concentrations as a substrate. The reaction was buffered with a potassium phosphate-buffer (KPi), pH 7 at a final concentration of 50 mM. If the enzyme is capable of oxidizing hydroxylamine, it transfers the electrons from the substrate to the oxidized electron acceptor which then gets reduced, resulting in a change of color from yellow (oxidized) to translucent (reduced) (Fig. 4-1A). This color change can be measured on a spectrophotometer at 418 nm to calculate the change of absorbance of $K_3Fe(CN)_6$ over time (Fig. 4-1B). For every experiment also a negative control without enzyme was done to detect possible spontaneous reactions of the compounds.
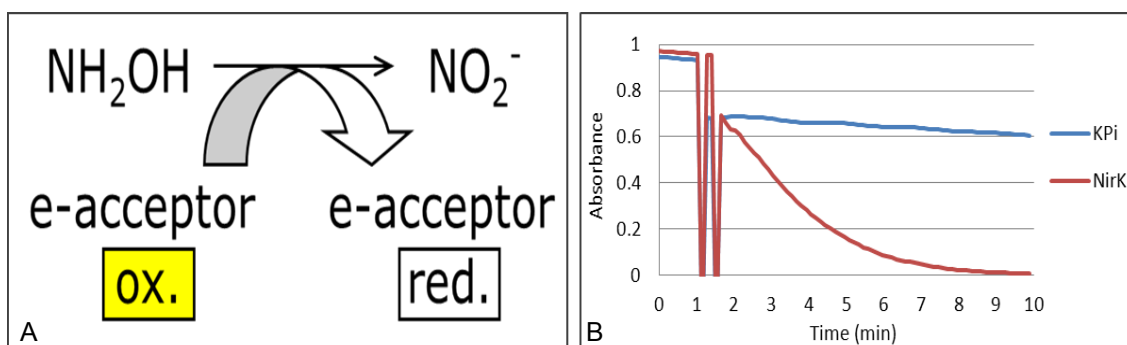
Figure 4-1: A) Scheme of the hydroxylamine oxidoreductase assay. **B)** Typical absorbance change at 418 nm over time in NirK experiment. Red curve: partial HAO activity present, blue curve: negative control.

4.1.1 HAO activity characterization

To characterize the detected hydroxylamine oxidoreductase activity of the NirK homologue further, some modifications of the enzyme were investigated. Different concentrations but also prereduced, heat incubated or protease treated enzyme was examined. Additionally, the whole assay was carried out under anaerobic conditions.

4.1.1.1 Activity parameters V_{max} & K_M

To get a first insight into the activity parameters of the NirK enzyme, two dilution series of hydroxylamine with constant NirK and $K_3Fe(CN)_6$ concentrations were performed (Fig. 4-2). Since the values of the second dilution series were not as consistent, just dilution series 1 was taken into account for calculating the parameters (Tab. 4-1),

resulting in V_{max} ~32 and K_M values ranging approximately between 0.5 and 1.3 mM (Fig. 4-2A).
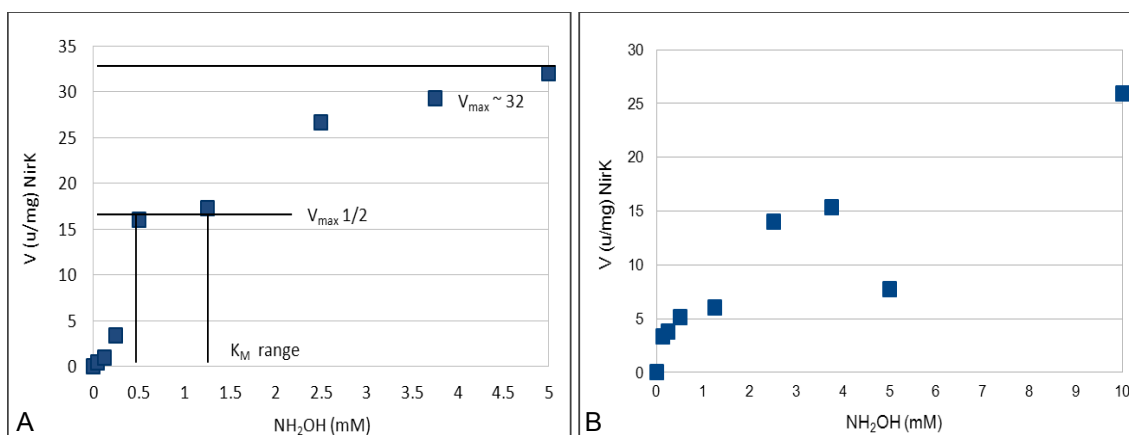
Figure 4-2: A) Dilution series 1 with NH_2OH concentrations ranging between 50 µM and 5 mM. Black lines mark the V_{max}, V_{max} ½ and the resulting K_M range values. **B)** Dilution series 2 with NH_2OH concentrations ranging between 125 µM and 10 mM.

Table 4-1: Specific enzyme activity values for different NH_2OH concentrations. Calculations based on dilution series 1.

NH_2OH [mmol/l]	Specific activity [u/mg]
0.05	0.40
0.125	0.93
0.25	3.33
0.5	16.00
1.25	17.33
2.5	26.67
3.75	29.33
5	32.00

4.1.1.2 Prereduced NirK

To investigate if the NirK enzyme Cu-centers have to be loaded with electrons to get activated, methylviologen (MV) was used as a prereducing agent. This is an electron donor with a strong negative redox-potential. The results were similar to the standard HAO assay, no differences could be observed. (Data not shown).

4.1.1.3 HAO activity under anaerobic conditions

To figure out if the NirK enzyme requires oxygen for HAO activity, the assays were carried out anaerobically. To obtain anaerobic conditions, the plastic cuvettes were

replaced with glass cuvettes which could be sealed but unfortunately the background of the reaction increased dramatically after this change. It is implausible that glass, an inert substance, reacted with some agents in the assay. Maybe some residual copper remained in the glass cuvettes although they were cleaned with detergent, ethanol and MilliQ water several times. Nevertheless, the difference of the final activity was far too big that this could be the only reason for the phenomenon. To find sealable plastic cuvettes as an alternative and to assure their anaerobic status was challenging, but after outgassing of the plastic in an anaerobic chamber and sealing the cuvette additionally with silicone, anaerobic to microaerophilic conditions should be obtained. In the plastic cuvettes the non-enzymatic activity was smaller, it showed only an eighth of the NirK enzyme activity. Also using concentrations of just 2.5 mM hydroxylamine and increasing enzyme concentrations helped to keep the background lower.

Although these difficulties occurred, a difference between enzymatic and spontaneous reaction in glass cuvettes could still be detected. The difference in absorption changes over time was about a factor of two but because of the background the specific enzyme activity could not be calculated (Fig. 4-3A). The HAO assay with equal conditions in plastic cuvettes yielded a more stable control but the background was still 4 to 5 fold higher then under aerobic conditions (control: 8.26 u/mg, NirK: 71.38 u/mg) (Fig. 4-3B). Also under anaerobic conditions hardly any nitrite was measured.
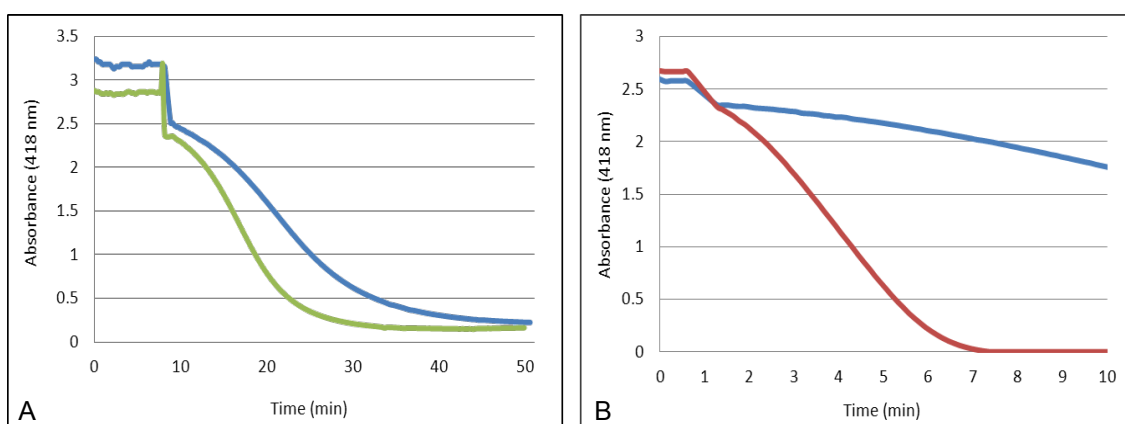
Figure 4-3: A) Anaerobic assay in glass cuvettes, 2.5 mM NH_2OH either with 7.5 µg/µl NirK (green curve) or KPi-buffer (blue curve), 2.5 mM $K_3Fe(CN)_6$ each. **B)** Anaerobic assay in plastic cuvettes, 2.5 mM NH_2OH either with 7.5 µg/µl NirK (red curve) or KPi-buffer (blue curve), 2.5 mM $K_3Fe(CN)_6$ each.

4.1.2   Alternative substrates

To investigate other substrates which may lead to nitrite formation, hydroxylamine was replaced with various nitrogen containing agents which could be possible candidates

for occurring intermediates in ammonia oxidation. Two NO- and one HNO-donor as well as ammonium or nitrite and additional mixes of these substances were investigated. Nitrite, the product of the ammonia oxidation process, was also used in small amounts in the assay as it may trigger the start of the reaction. Despite of a specific nitrite reductase assay, all other substrates were tested under basic HAO assay conditions. Ammonia and nitrite were tried to determine via colorimetric methods, alternatively.

4.1.2.1 Nitric oxide

The NO-donors diethylamine (DEA) NONOate and diethylenetriamine (DETA) NONOate were used to investigate if the enzyme is able to use NO as a substrate. There was no transfer of electrons onto the electron acceptor detectable, meaning no NirK activity with the substrates under the tested conditions. Additionally, nitrite was always produced in large amounts during the release of the NO-substrates, which made a detection of any occurring product impossible. (Data not shown).

4.1.2.2 Nitroxyl

The HNO releasing agent N-Acetoxy-N-acetyl-4-chlorobenzenesulfonamide (NANa) was used to investigate if the enzyme could use nitroxyl as a substrate. Like in the upper approach, neither change in the electron acceptor nor HNO reductase activity was reasonable under HAO assay conditions. Again, nitrite was spontaneously produced in large amounts. (Data not shown).

4.1.2.3 Mixture of hydroxylamine and diethylamine (DEA) NONOate

To study if the hypothetical intermediate may just interact with the enzyme in some mixture with another possible intermediate, we gave hydroxylamine and DEA in equimolar amounts. Again, no further activity despite hydroxylamine oxidoreductase was detectable. The electron acceptor got reduced just as much as the amount of hydroxylamine was added. (Data not shown).

4.1.2.4 Triggering nitrite production with small amounts of nitrite

To examine if the full reaction of oxidizing hydroxylamine to nitrite by the enzyme may be dependent on a certain amount of the nitrification product, small concentrations of nitrite were added in the beginning of the HAO assay, investigating hydroxylamine as well as DEA as a substrate. The nitrite addition neither changed the activity parameters

of the hydroxylamine oxidoreductase nor helped to activate nitric oxide reductase activity. (Data not shown).

4.1.2.5 Ammonium

To determine if the enzyme may be capable to interact with ammonium, thus accomplishing the first step in the nitrification pathway, hydroxylamine was replaced with ammonium in the basic assay composition. Neither reduction of the ferricyanide could be detected, nor any nitrite production or ammonia depletion via the colorimetric assay. (Data not shown).

4.1.2.6 Nitrite reductase (NIR) activity determination

To test for the activity of a nitrite reductase, a specific nitrite reductase assay was used, modified from Alexander Treusch (Treusch, 2004). Methylviologen which was prereduced with dithionite acted as an electron donor for the enzyme. If the enzyme is active it should transfer the electrons donated from methylviologen onto nitrite. A cell free extract of *Alcaligenes xylosoxidans*, a bacterium capable of denitrification, acted as a positive control. In the negative control the enzyme was replaced with KPi. The activity was analyzed using the colorimetric reaction of the remaining nitrite with sulfanilamide/NED. No nitrite reductase activity was detected (Fig. 4-4).
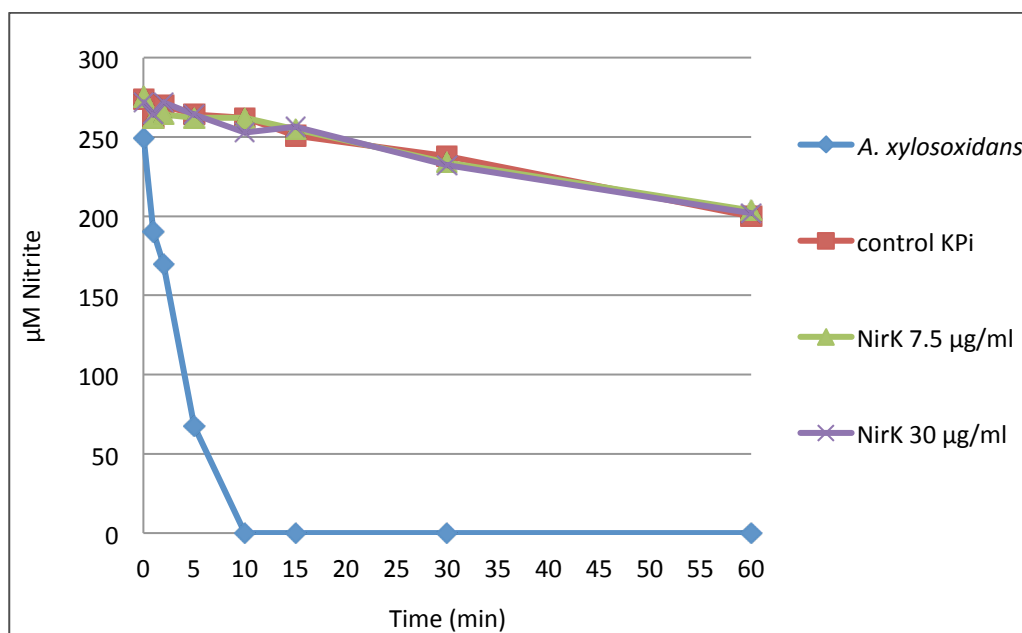
Figure 4-4: Nir assay with the NirK enzyme from soil fosmid 54d9. Positive control was a cell-free extract of *Alcaligenes xylosoxidans* (15 µg/ml). The negative control was without addition of enzyme. Two different NirK concentrations, 7.5 µg/ml and 30 µg/ml were tested.

4.1.3 Products and intermediates of HAO, HNO and NO reactions

The main focus was set on the detection of nitrite, which was expected to be the main product of the oxidation of hydroxylamine. Since nitrite formation was not seen despite the reduction of the electron acceptor, other potential products were investigated.

4.1.3.1 Nitrite

Nitrite was measured in the solutions with the Grieß-reaction, where the interaction of sulfanilamide/NED and nitrite results in a pink color formation which can be detected with a spectrophotometer. There was no evidence for the formation of nitrite in the basic assay composition, also various alterations in hydroxylamine concentrations and electron acceptor changes were not effective. For the alternative substrates DEA, DETA and NANa the quantification of nitrite was not even possible because of non-enzymatic production of nitrite during release of the substrate.

Because early experiments had suggested that the production of nitrite may be increased under increased oxygen concentrations (Falcone et al., 1963), the impact of additional aeration on the HAO assay was investigated. Again, no nitrite production could be observed. (Data not shown).

4.1.3.2 Nitrous oxide

To determine if N_2O was a product or intermediate of the HAO activity, the gas phase of the assay and two additional controls were analyzed via Isotopic Ratio Mass Spectrometry (IRMS) (Department Terrestrial Ecosystem Research, Vienna). In the samples containing hydroxylamine, 3.26 ppm and 3.23 ppm of N_2O could be measured (Fig. 4-5), although one of the assays was just hydroxylamine without enzyme added. This leads to the conclusion that the observed N_2O formation was due to a spontaneous degradation of the hydroxylamine and not based on enzyme activity.
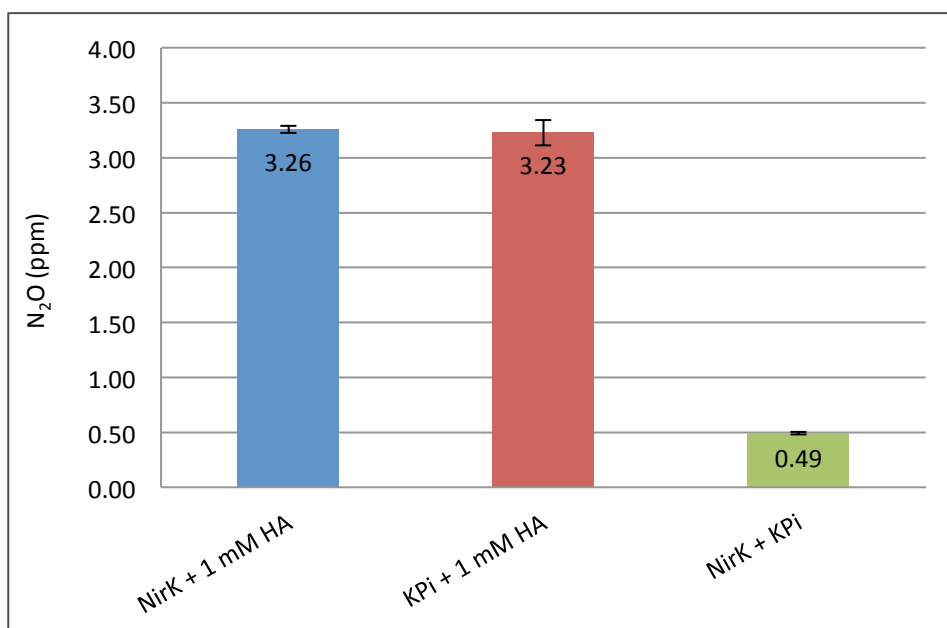
Figure 4-5: N_2O measurements of the gas phase in HAO assay as well as two controls. The setup was consistent of 1 mM $K_3Fe(CN)_6$, 1 mM HA, 7.5 µg/ml NirK. One control was without hydroxylamine addition, the other without addition of NirK.

4.1.3.3 Nitric oxide

To measure the formation of nitric oxide in the standard HAO assay, the specific NO-scavenger PTIO was used. After testing for cross reactions with hydroxylamine (Fig. 4-6A), which were negligible, an absorbance spectrum of the solution was made, which ascertained that the color change could be measured at 550 nm without interfering with the ferricyanide spectrum (Fig. 4-6B).
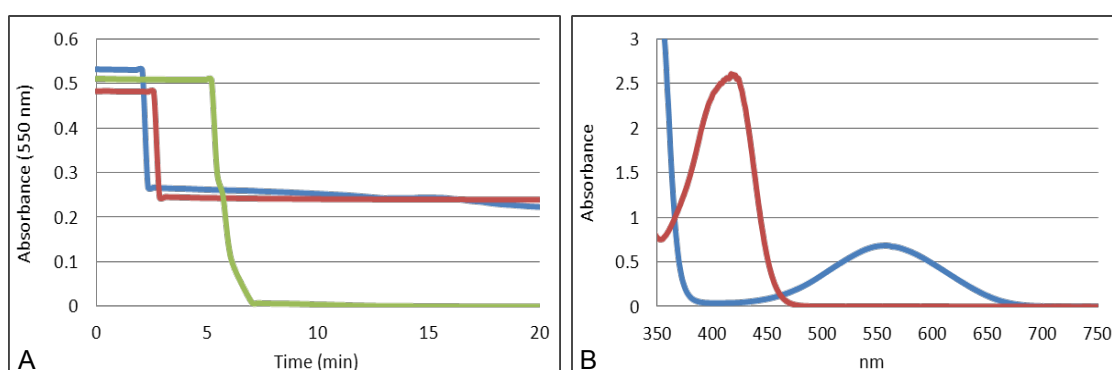
Figure 4-6: A) PTIO cross reactions with either 2.5 mM NH_2OH (red curve) or 25 mM NH_2OH (blue curve) under KPi buffered conditions. The green curve represents the interaction of PTIO with 2.5 mM DEA. **B)** Wavelength scan of PTIO and $K_3Fe(CN)_6$. Absorbance spectra do not interfere with each other.

PTIO does not interfere with the reduction of the electron acceptor, but an enzyme specific degradation of PTIO under high hydroxylamine concentrations could be

observed (Fig. 4-7A) which occurs faster with increasing NirK concentrations (Fig. 4-7B).
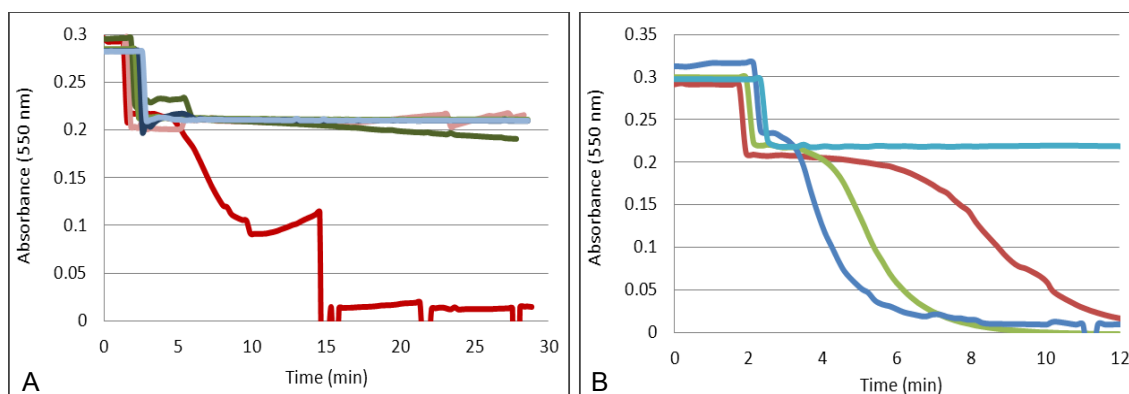
Figure 4-7: A) HAO assay with 250 µM PTIO, 2.5 mM $K_3Fe(CN)_6$ and different NH_2OH concentrations. Each NH_2OH concentration was run with 7.5 µg/ml NirK as well as KPi buffer. 25 mM NH_2OH with NirK (dark red), 25 mM NH_2OH with KPi (light red), 2.5 mM NH_2OH with NirK (dark green), 2.5 mM NH_2OH with KPi (light green), 250 µM NH_2OH with NirK (dark blue), 250 µM NH_2OH with KPi (light blue). **B)** HAO assay with 250 µM PTIO, 2.5 mM $K_3Fe(CN)_6$, 25 mM NH_2OH and different NirK enzyme concentrations: 7.5 µg/ml (red curve), 30 µg/ml (green curve), 75 µg/ml (purple curve).

4.1.4 Testing for enzymatic stability and non-enzymatic activity

To test the stability of the occurring HAO activity, the NirK was incubated at different temperatures. To assure that the observed reaction is enzyme dependent, the enzyme was treated with a protease. Additionally, it was replaced with various copper(II) chloride dihydrate solutions to investigate non enzymatic side reactions of the incorporated copper.

4.1.4.1 Heat stability
To examine the stability of the HAO activity at various temperatures, NirK was incubated at room temperature, 40°C, 60°C or 80°C. After one and six hours, the activity of the enzymes was compared. Both incubation times gave similar results, indicating that the high temperatures do not influence the enzyme activity significantly (Tab. 4-2, Fig. 4-8).

Table 4-2: Calculated specific enzyme activity values after exposure to different temperatures for six hours.

Substrates	Specific activity [u/mg]
KPi-buffer	1.23
Room temperature	18.10
40°C	19.20
60°C	17.17
80°C	18.65
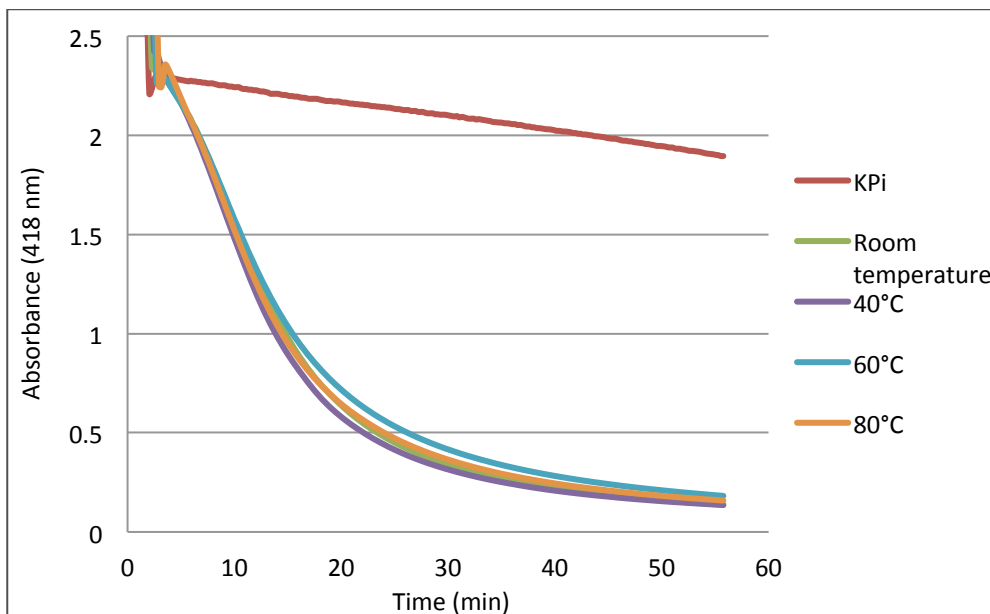
Figure 4-8: HAO assay with 2.5 mM $K_3Fe(CN)_6$, 2.5 mM NH_2OH, NirK incubated at various temperatures for six hours.

4.1.4.2 Protease treatment

To determine if the observed HAO activity in the assay is really enzyme dependent, the NirK was treated with Proteinase K. This enzyme belongs to a family which is able to hydrolyze the peptide bonds in proteins, leading to proteolysis. As expected, no enzyme activity could be detected after the treatment any longer. (Data not shown).

4.1.4.3 Copper side reaction

To analyze possible non enzymatic side reactions of the enzyme containing copper, the NirK was replaced with copper(II) chloride dihydrate solutions. The theoretical copper incorporation of the heterologously expressed enzyme was calculated to obtain comparable concentration ranges, revealing 72 nM built in copper in 7.5 µg/ml enzyme (calculations based on Schweichhart data). Some of the solutions were also treated

with Proteinase K to investigate if this treatment interferes with the occurring copper reaction as well.

4.1.4.3.1 Copper reaction

The NirK enzyme in the HAO assay was replaced with various concentrated copper solutions. Copper, although not incorporated in a catalytic center of a protein, was able to reduce the electron acceptor ferricyanide in the presence of hydroxylamine. But the entire enzyme complex seemed to have a higher activity than the calculated copper concentration itself (Fig. 4-9).
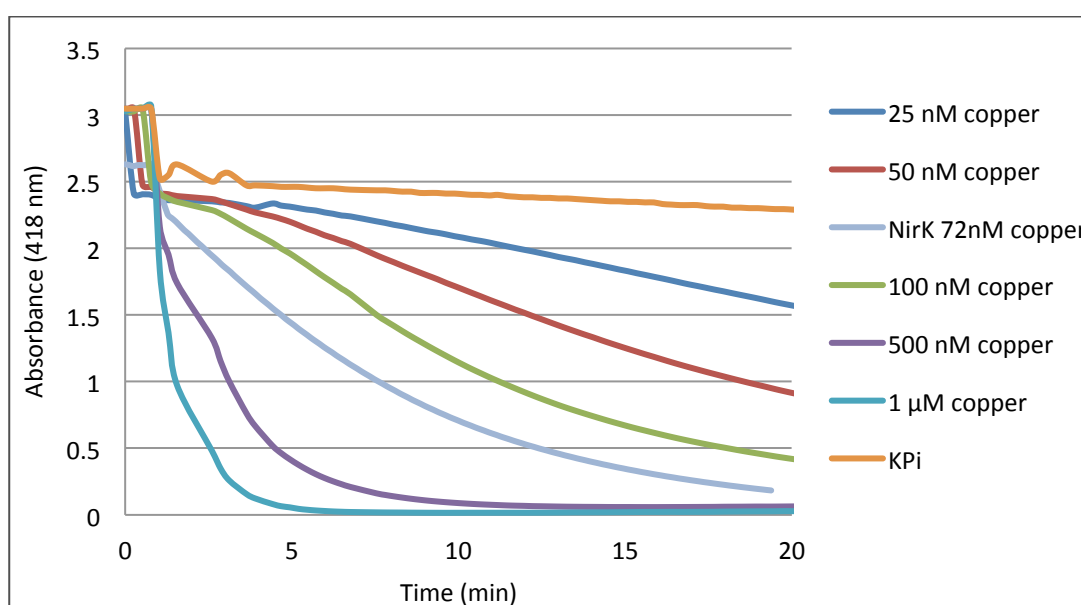
Figure 4-9: HAO assay with various copper concentrations, positive and negative control, 2.5 mM $K_3Fe(CN)_6$, 2.5 mM NH_2OH.

4.1.4.3.2 Proteinase treatment

Three solutions containing 50 nM, 100 nM and 500 nM copper respectively, were treated with Proteinase K to look for interference between these two substrates. Indeed, the activity of the 50 nM and 100 nM solutions were strongly reduced, whereas the activity of the 500 nM was only slightly reduced (Fig. 4-10).
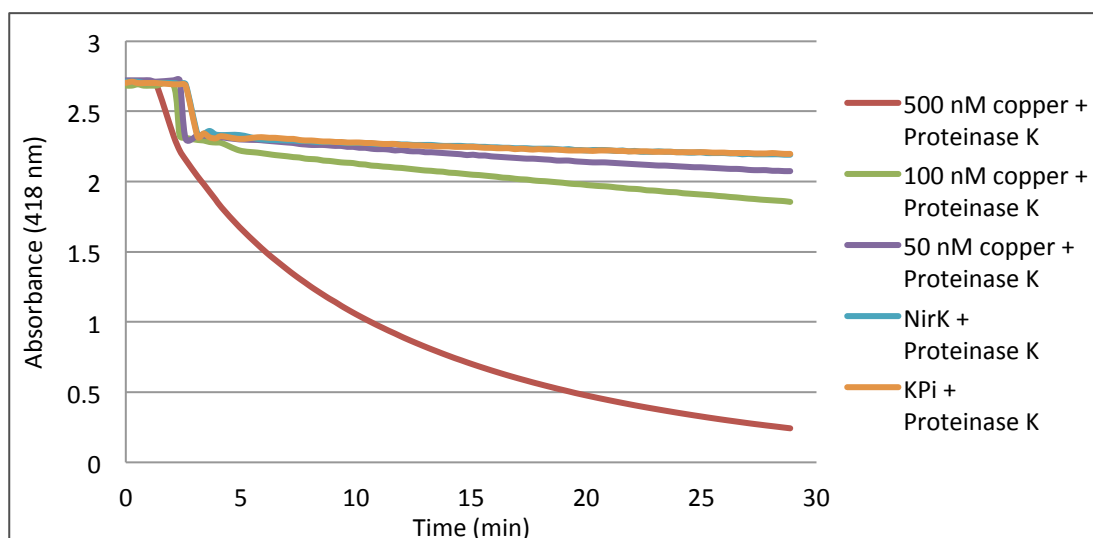
Figure 4-10: Copper assay with 40 µg/ml Proteinase K treatment, 2.5 mM $K_3Fe(CN)_6$, 2.5 mM NH2OH.

4.2 Enzymatic activities in crude cell extracts

Beside the reductionist approach of studying a single candidate enzyme, the whole protein mix of a living organism, the ammonia oxidizing archaeon *Ca.* N. viennensis, was investigated.

4.2.1 Upscaling of growth

Since the growth of *Ca.* N. viennensis is slow and does not yield high cell densities (stationary phase ~4.6×10^7 cells/ml), a new method of cultivation had to be developed to obtain enough cell mass needed for biochemical experiments. Upscaling the growth was possible but hard to accomplish without any contaminations or growth losses. The cultivation capacities were upscaled from 250 ml cultures in a 1 l bottle to 4-8 l of culture in a 10 l fermenter to gain more cells from one cultivation step (Fig. 4-11). The media and growth conditions remained similar despite shaking the fermenter which seemed to slightly increase growth. After some experimental setups, a 4 l as well as a 6 l culture was grown at once, resulting in approximately 200 mg wet weight of cells.

Figure 4-11: Fermenter setup for growth of *Ca.* N. viennensis.

4.2.2   Harvesting and lysis of cells

After six to eight days of growth, shortly before reaching stationary phase, the cells were harvested, solubilized in 2 ml KPi-buffer and disrupted by a sonicator. A small amount of cell suspension was examined under the microscope to control for successful lysis of the cells. After assuring a nearly complete cell disruption, the cell extract was fractionated. Half of the solution remained as whole crude cell extract, the other half was further divided via centrifugation into a supernatant and a pellet to characterize soluble and membrane-associated proteins. The insoluble fraction was again solubilized in the same amount of KPi-buffer as the soluble fraction. At the end the protein concentrations were quantified, resulting in 6 mg/ml crude cell extract, 2.35 mg/ml supernatant and 1.7 mg/ml insoluble fraction (Tab. 4-3). For the experiments, the concentrations were adapted to equal amounts when necessary. An additional cell extract which was used for proteome analysis was also prepared from an independent culture (Tab. 4-3, Fermenter II).

Table 4-3: Data on the amount of cells and resulting protein yield obtained from either a 4 or 6 l *Ca.* N. viennensis culture, used for cell extract (Fermenter I) and proteome (Fermenter II) analysis.

	Fermenter I	Fermenter II
Culture volume [l]	4	6
Cell wetmass [mg]	220	180
Amount total protein [mg]	~10-12	~4.5-5
Crude cell extract [mg]	6.04	4.45
Insoluble protein fraction [mg]	1.71	0.08
Soluble protein fraction [mg]	2.35	not detectable

One has to note that the protein yield compared to the cell mass was actually small. From 220 mg wetmass of cells only around 10-12 mg crude cell extract could be obtained. Lysis of the cells turned out to be difficult. It was only achieved with severe repeated treatments with an ultrasonicator. With less power or shorter exposure, the cells looked still intact under the microscope. Only after the harsh treatment fewer cells appeared and looked disintegrated. Also the color change of the pellet from fawn to a dark appearance was considered as an indication for cell lysis. Nevertheless, comparisons between wet weight of cells and obtained protein concentrations suggest that part of the proteins remained in the cells. Maybe the cell wall got disrupted while most of the cytoplasmic membrane remained intact. Other treatments to achieve cell disruption and increase protein yields like exposure to heat or use of detergents were not performed because the cellular proteins should be as less affected as possible.

4.2.3 HAO activity

All fractions of the cell extract were tested for HAO activity. Every fraction showed the ability to reduce the electron acceptor ferricyanide. Two hydroxylamine concentrations were tested, with the higher hydroxylamine concentration leading to a faster reaction (Fig. 4-12). The insoluble fraction showed the highest activity of all fractions with both hydroxylamine concentrations (Tab. 4-4). But like in the HAO assays with the NirK enzyme, no nitrite formation could be detected. Because of this reason, several other substrates and products were investigated as well.
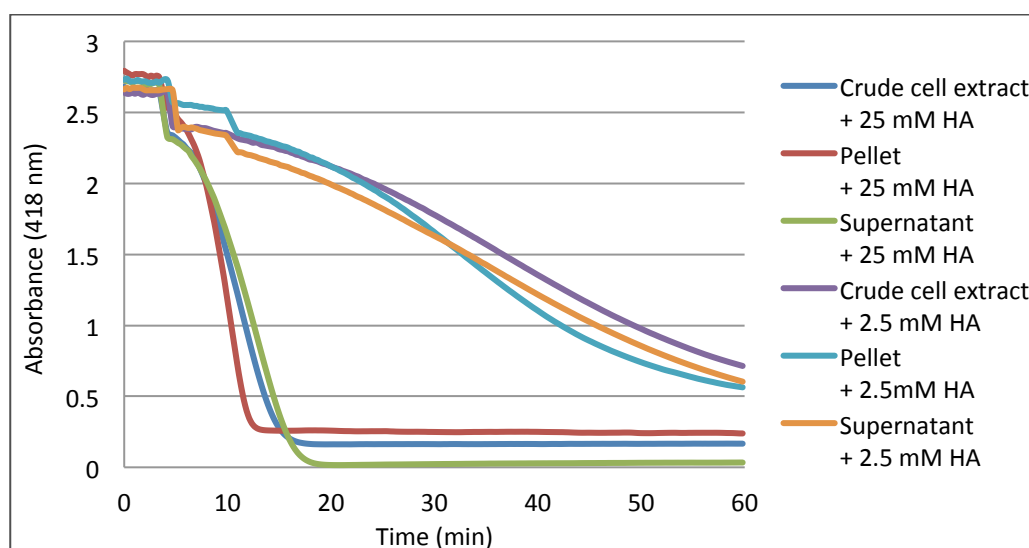
Figure 4-12: HAO assay with crude cell extract, insoluble fraction and soluble fraction. 250 µl/ml protein (all fractions), 25 mM or 2.5 mM NH_2OH (HA), 2.5 mM $K_3Fe(CN)_6$.

Table 4-4: Specific enzyme activities calculated for all cell extract fractions with 2.5 mM or 25 mM NH_2OH concentrations.

Sample	Specific activity [u/mg]
Crude cell extract + 25 mM NH_2OH	1.450
Insoluble fraction + 25 mM NH_2OH	2.284
Supernatant + 25 mM NH_2OH	1.343
Crude cell extract + 2.5 mM NH_2OH	0.205
Insoluble fraction + 2.5 mM NH_2OH	0.285
Supernatant + 2.5 mM NH_2OH	0.209

4.2.4   Other enzymatic activities with alternative substrates

To investigate other substrates, some experiments already done with the NirK enzyme were repeated with the crude cell extracts. Besides hydroxylamine, ammonia, nitrite and one of the NO-donors (DEA) was tested. Additionally, a mix of DEA and hydroxylamine as well as small amounts of nitrite with hydroxylamine or DEA was examined.

4.2.4.1   Nitric oxide

NO was used instead of NH_2OH in the standard HAO assay composition with crude cell extract but no reduction of the electron acceptor could be detected. (Data not shown).

4.2.4.2   Ammonium

To investigate the ability of the cell extract fractions to oxidize ammonium, the NH_2OH in the standard HAO assay was replaced with NH_4Cl. Because no change in the electron acceptor occurred, a colorimetric detection of ammonium consumption or nitrite production over time was attempted. Unfortunately, both experimental setups showed no activity in ammonia consumption as well as nitrite production in any cell extract fraction. (Data not shown).

4.2.4.3   Mix of hydroxylamine and nitric oxide

Also a mix of NH_2OH and NO in equal amounts was investigated as a substrate for the HAO assay, but again no reduction of the electron acceptor occurred. (Data not shown).

4.2.4.4 Mix of hydroxylamine and nitric oxide with small amounts of nitrite

Nitrite as hypothetical product was given in small amounts at the beginning of the assay with either NH_2OH or NO to trigger the reaction of nitrite formation, but no changes in the results were observed. (Data not shown).

4.2.5 Products

The main target of the product investigation was the detection of nitrite. With ammonia, hydroxylamine as well as nitric oxide as a substrate, nitrite could not be determined. Therefore, the NO-scavenger PTIO was used to investigate nitric oxide as a possible intermediate or product. PTIO did not interfere with the activity of the cell extract, insoluble and soluble fraction in the HAO assay. There was no interaction of PTIO with ammonia and a fast degradation of PTIO with DEA. When the used substrate was hydroxylamine, PTIO was degraded with a delay but before the reduction of the ferricyanide ended (Fig. 4-13).
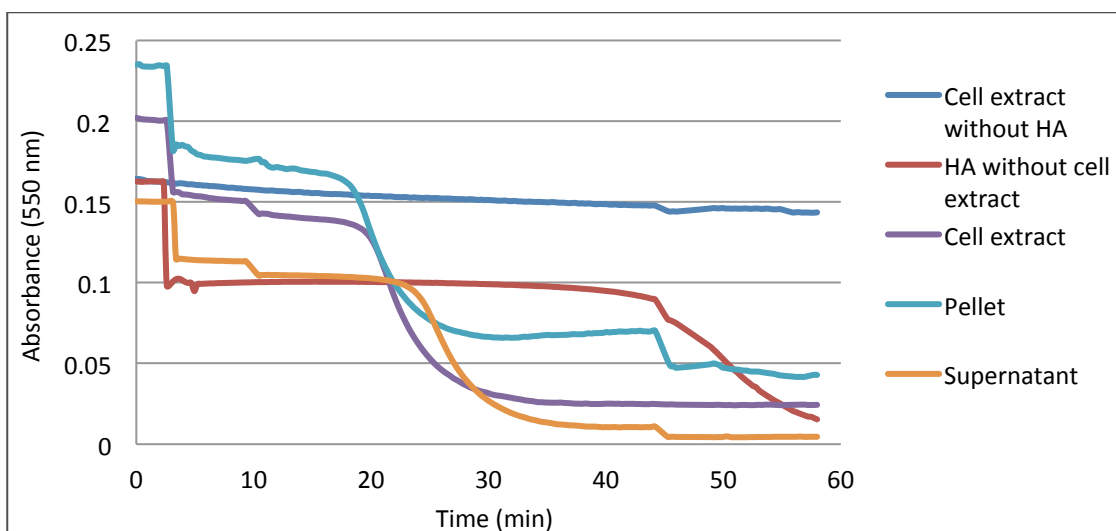
Figure 4-13: HAO assay with all fractions of the cell extract. Two controls: cell extract without addition of hydroxylamine and hydroxylamine without the addition of cell extract (always replaced by KPi-buffer). 2.5 mM $K_3Fe(CN)_6$, 2.5 mM NH_2OH, 250 µM PTIO.

4.2.6 Nitrite reductase activity

To test the crude cell extract fractions for nitrite reductase activity, the predicted but not detectable activity of the NirK homologue, the already described NIR assay was used. Prereduced methylviologen acted as an electron donor, the activity was detected via the colorimetric reaction of the remaining nitrite with sulfanilamide/NED after defined

time points. The reaction started with the addition of the different cell extract fractions. A cell free extract from *Alcaligenes xylosoxidans* acted again as the positive control. The nitrite reductase activity could be detected in all cell extract fractions, with the highest activity in the pellet fraction if all 100 µg/ml concentrations are compared. As expected, the 600 µg/ml of the whole crude cell extract showed even higher activity (Fig. 4-14).
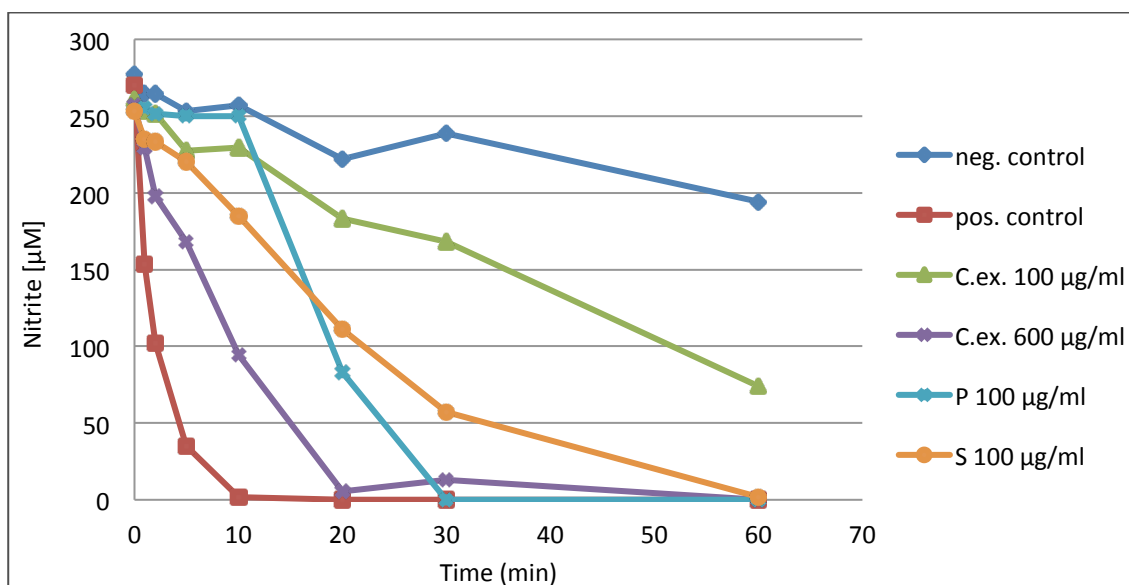
Figure 4-14: NIR assay with cell extract fractions. Two different concentrations of cell extract fraction (100 µg/ml or 600 µg/ml), pellet and soluble fraction with 100 µg/ml concentrations, positive control consistent of 15 µg/ml cell extract from *A. xylosoxidans* and negative control.

4.3 Growth experiments investigating nitric oxide as a possible intermediate in the archaeal ammonia oxidation

To investigate the production of NO in growing cultures, *Ca.* N. viennensis cells were grown in the presence of PTIO at various concentrations. This way, investigations not only on the proteomic level, either one single protein or the whole cell proteome, but also on the cellular level could be achieved. PTIO (short for 2-phenyl-4,4,5,5-tetramethylimidazolineoxyl-1-oxyl-3-oxide) is a blue compound with a solubility in water less than 0.03%. As a nitric oxide scavenger, it is able to react with NO to yield PTI (2-phenyl-4,4,5,5-tetramethyl-imidazoline-1-oxyl) and NO_2 in a stoichiometric manner (Fig. 5-2) (Maeda et al., 1994).
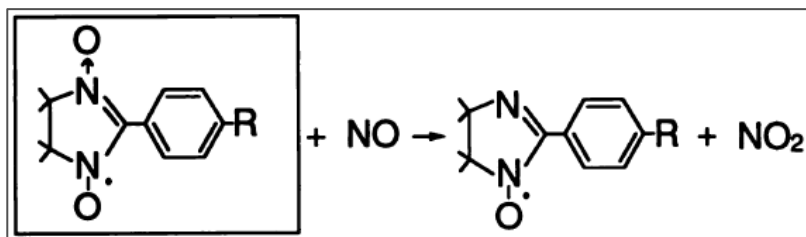
Figure 4-15: Structure of PTIO and the reaction scheme with NO (Maeda et al., 1994). R = 2-phenyl-4,4,5,5-tetramethylimidazoline-1 -oxyl-3-oxide (PTIO).

If nitric oxide is occurring during ammonia oxidation, PTIO would bind the intermediate and remove it from the reaction. Therefore, the whole process will come to a standstill which results in a stop of growth. Further, the results allow comparison between different organisms. Each microorganism in this experiment represented a different metabolism or group, *Ca.* N. viennensis for ammonia oxidizing archaea, *N. multiformis* for ammonia oxidizing bacteria and *E. coli* for a heterotrophic bacterium. The ammonia oxidizing bacteria was chosen as a control to distinguish if growth is similar or differentially inhibited, which would either indicate for an alike or a more distinct metabolism. A heterotrophically growing organism was chosen to ensure for no general concentration dependent toxic effect of PTIO. To ensure the obtained results were comparable, every inoculum had to have similar cell concentrations. Because *Ca.* N. viennensis had the lowest cell density, the concentrations of the two other organisms were adjusted via dilution to 4.6×10^7 cells/ml. For the ammonia oxidizing organisms the growth was monitored with daily measurements of ammonia and nitrite, for *E. coli* via OD measurements.

For *Ca.* N. viennenis three different PTIO concentrations were tested, 10 µM, 50 µM and 250 µM. The agent was given during inoculation or during exponential phase, respectively. As 10 µM PTIO showed nearly no effect, this concentration was omitted in the following experiments. Furthermore, the effect of the 50 µM solution was lower when added already at the start of the exponential phase, which indicated that this NO-scavenger concentration is just sufficient for lower amounts of cells and that the growth comparison was only possible as long as the growth rate was nearly similar. Therefore, PTIO was just directly added during inoculation of *N. multiformis* and *E. coli*. Because the very distinct metabolism of *E. coli* was thought to be not as easily affected and to efficiently exclude a general toxic effect, additionally two higher concentrations of PTIO were chosen.

It has to be noted that there was a possibility for an unspecific reaction of PTIO with hydroxylamine. In KPi-buffer this kind of side reaction was negligible (see 4.1.3.3) but after repeating the control with Fresh Water Medium it was revealed that PTIO is able to interact with higher concentrations of NH_2OH under this condition (Fig. 4-15). Nevertheless, the hydroxylamine concentration tested was 40 times higher than the PTIO concentration.
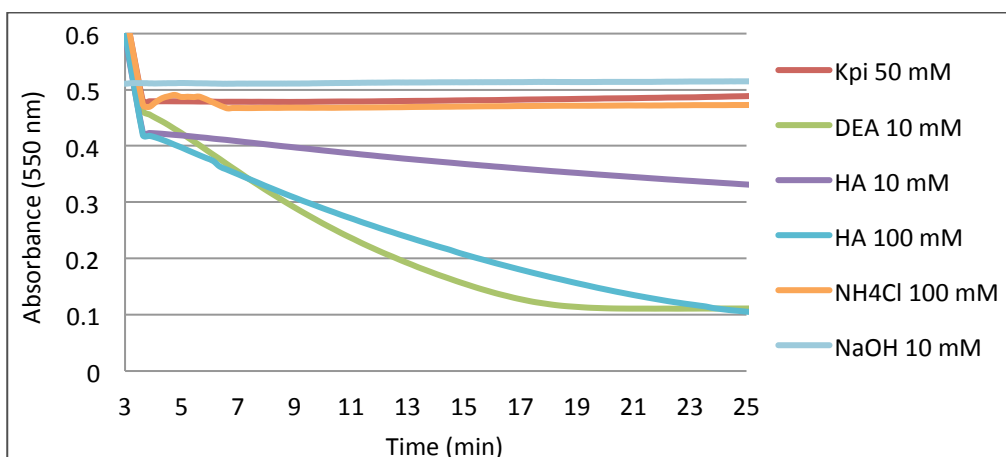
Figure 4-16: PTIO stability with different substrates in Fresh Water Medium.

4.3.1 *Ca.* N. viennensis

The growth of the *Ca.* N. viennensis culture was almost not affected by 10 μM, but completely inhibited with 50 μM and 250 μM PTIO given at the time point of inoculation (Fig. 4-16A). In the second experiment where PTIO was added at the starting of the exponential phase (day 3), the culture containing 50 μM PTIO could recover and also grow up to stationary phase, although more slowly (Fig. 4-16B).
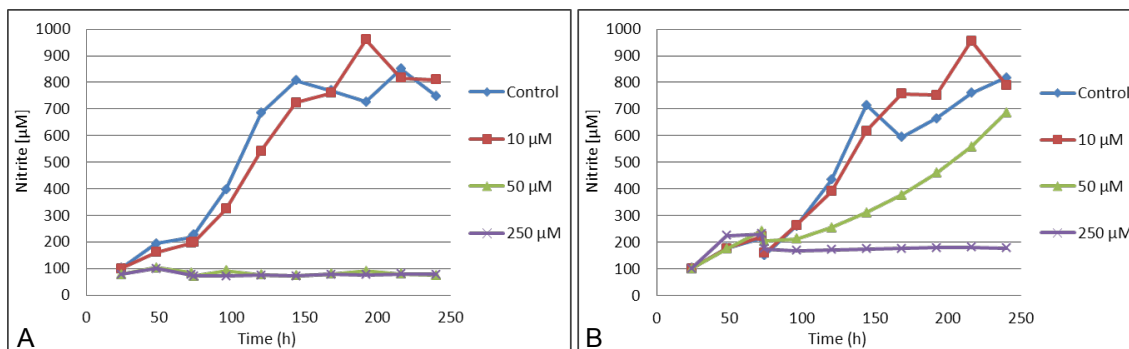
Figure 4-17: A) *Ca.* N. viennensis + PTIO from inoculation, nitrite measurement over time. **B)** *Ca.* N. viennensis + PTIO from exponential phase, nitrite measurement over time.

4.3.2 *N. multiformis*

Since 10 µM PTIO was not affecting the AOA, *N. multiformis* was only grown with concentrations of 50 µM and 250 µM PTIO. Also the agent was only given during inoculation because the growth rate of *N. multiformis* is faster than *Ca.* N. viennensis and the amount of cells in the beginning of exponential phase is not comparable. No growth inhibition with 50 µM occurred but a retarded growth with following growth stop was observed with 250 µM PTIO (Fig. 4-17).
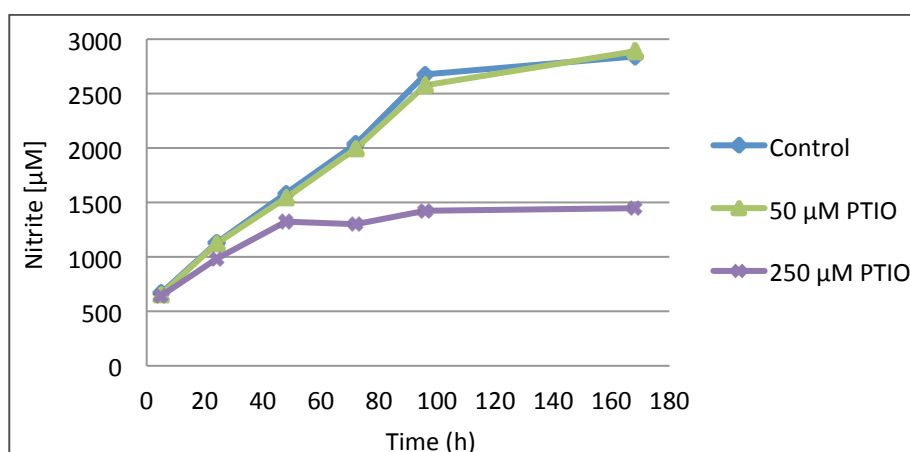
Figure 4-18: *N. multiformis* + PTIO from inoculation, nitrite measurement over time.

4.3.3 *E. coli*

E. coli was used to identify potential general toxic or at least growth inhibiting effects, not only on ammonia oxidizers but living organisms in general. Therefore, the concentration of PTIO was even increased to 500 µM and 1 mM. Since the growth rate of this organism is much faster than that of the archaeal and bacterial ammonia oxidizers, the cell density was only comparable at the beginning of growth. Therefore, only the values obtained from the first two hours were considered. At these time points and at comparable PTIO concentrations, no growth inhibition could be detected. There was a delay in growth only with 500 µM PTIO and even stronger at 1 mM, but this dosage was already 4fold higher than that used for the ammonia oxidizers (Fig. 4-18).
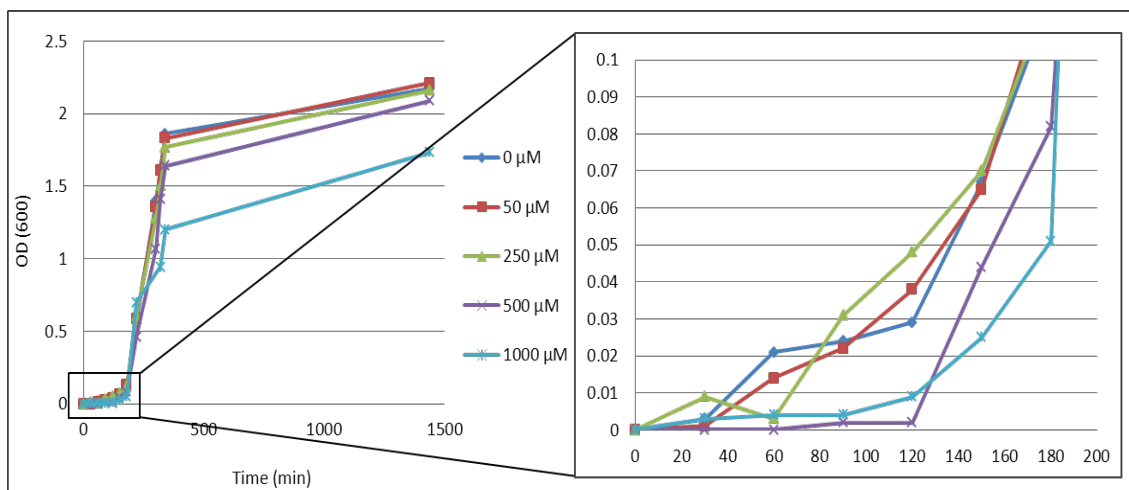
Figure 4-19: *E. coli* + PTIO from inoculation, OD 600 measurement over time. Zoom in the first 200 minutes where the cell densities of the cultures were comparable.

4.4 Proteomics

To trace the NirK enzyme in the proteome of *Ca.* N. viennensis, an SDS-gel electrophoresis with different cell extracts was performed. Either the cells were only treated with the detergent mercaptoethanol or the cells were lysed via ultrasonication and fractionated into whole crude cell extract, pellet and soluble fraction. The amount of protein loaded on the gel could not be precisely calculated because the Bradford protein quantification appeared not reliable. Therefore, two different amounts of the fractions were loaded, either 30 µl of the soluble fraction and 10 µl for all others or 15 µl and 5 µl. Both concentrations gave clear, still detectable bands (Fig. 4-19A).

The patterns of the different fractions looked very similar, there were just two exceptions. In the range of 20 kDa and 100-140 kDa, bands were much more strongly represented in the crude cell extract and pellet fraction. In the range of the predicted size of the NirK enzyme (41.9 kDa) the pattern did not differ (Fig. 4-19A). The overall similar appearance of the different fractions could be due to an incomplete separation of insoluble and soluble proteins, because the small protein solution amounts of 1 ml each could not be separated with the ultracentrifuge.
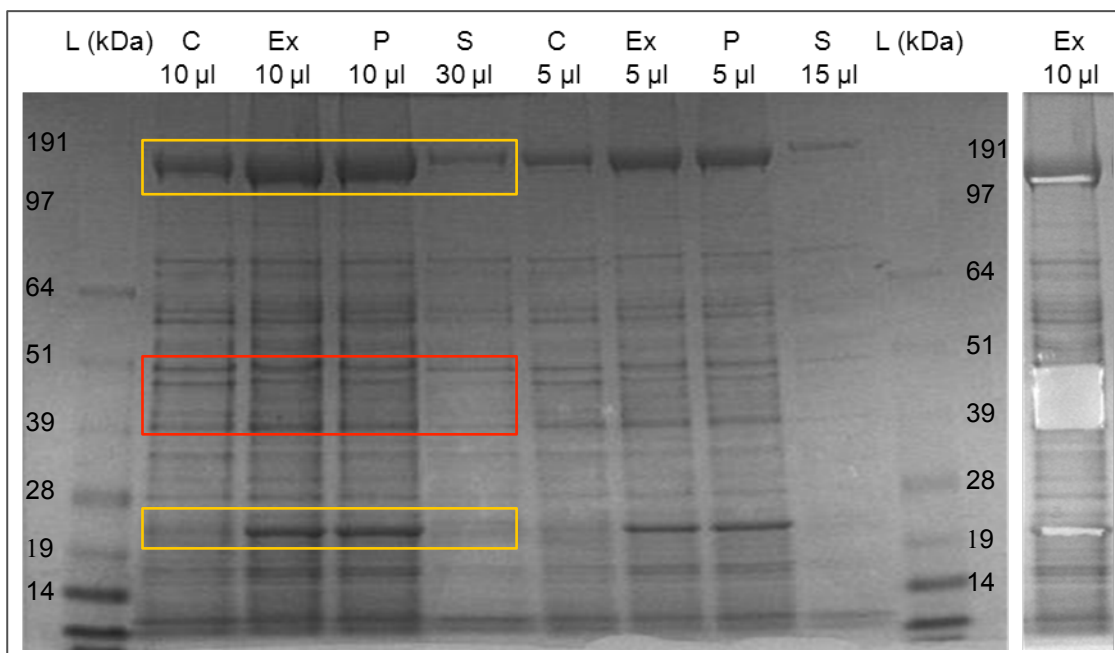
Figure 4-20: A) SDS-gel picture. L = Ladder (SeeBlue®Plus2 Prestained Standard), C = harvested cells just treated with mercaptoethanol, Ex = crude cell extract, P = insoluble fraction, S = soluble fraction. 30 µl of the soluble fraction and 10 µl (first four rows) for all others or 15 µl and 5 µl (last four rows) loaded. The red square marks the the rigion of the NirK size, the yellow squares mark two different patterns. **B)** 10 µl loaded crude cell extract lane, after cutting out the three bands.

The region of the NirK size (40-55 kDa) in the crude cell extract lane was cut out of the gel (Fig. 4-19B), washed and digested via trypsin. To get further insight into the proteome, the procedure was repeated for two other bands in other size regions (Fig. 4-19B) which differed in their pattern in the various fractions. As the proteome of *Ca.* N. viennensis was investigated for the first time, an insoluble as well as a soluble fraction was prepared for analysis as well. During the preparation of these two fractions, the suspicion of wrong concentration values was confirmed. Based on the measured total protein amount (Tab. 4-3, Fermenter I), both prepared solutions should contain 100 µg protein. However, after the digestion step and removal from the liquid a visible protein pellet occurred in both tubes which indicated at least 1 mg protein. Maybe the discrepancies as mentioned before (4.2.2) in cell mass and protein outcome were based on incorrect protein quantifications.

The proteins of the gel pieces as well as additional protein preparations of the insoluble and soluble fraction were analyzed by MALDI-TOF (Department Molecular Systems Biology, Vienna). The obtained results were compared to a FASTA-database of *Ca.* N. viennensis proteins.

The gel pattern in the range of the NirK enzyme size did not differ. Therefore, not only just a small band but a region of about 1 cm was analyzed to increase the probability of identifying the enzyme. In total, 47 proteins could be assigned to the gel piece but no NirK enzyme could be detected.

The upper band was just consistent of 3 proteins, of which one could be identified as a DNA-directed RNA polymerase and the other as a rpoB DNA-directed RNA polymerase subunit B. Because of its huge size, the third protein of unknown function might represent the archaeal S-layer protein. In the 20 kDa region, 15 different proteins could be detected but no prominent protein was revealed.

The analysis of the insoluble and soluble fractions provided 39 proteins in the insoluble and 148 proteins in the soluble fraction which could be assigned. 6 detected sequences were unique only for the insoluble, 115 just for the soluble fraction and 33 occurred in both. The detailed list for the three gel pieces as well as for the insoluble and soluble fraction proteins is listed in the Appendix.

4.5 Heterologous expression of NirK from *Ca.* N. viennensis

To be able to investigate the homologous NirK of our laboratory strain *Ca.* N. viennensis in addition to the putative NirK found on the soil fosmid 54d9 and to do comparisons between those two, cloning, expression and isolation of the enzyme was attempted. The process was based on the approach of Alexander Treusch cloning the environmental NirK homologue (Treusch, 2004). Accordingly, the same vector pET-28a as well as the same cutting sites *Nco*I and *Xho*I were used.

4.5.1 NirK constructs design

The aim was to achieve three different constructs, the native sequence as well as the native sequence with an additional hexa-histidine-tag or a hexa-histidine-tag plus a thrombin cutting site (Fig. 4-20). With these constructs, two purification strategies could be pursued. The native NirK enzyme could be purified from inclusion bodies, the NirK enzyme with the histidine-tag with affinity purification. The third construct would also allow cutting the His-tag after purification to restore the native structure.
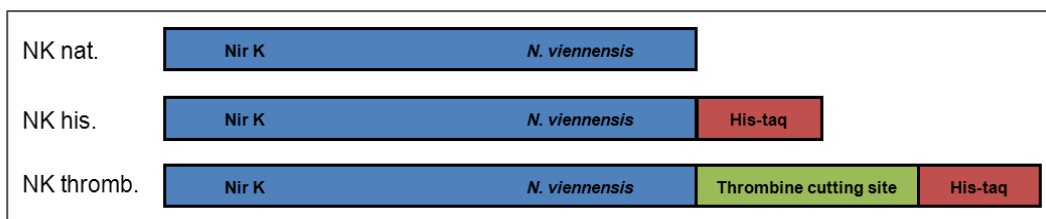
Figure 4-21: Scheme of the constructs for heterologous expression of the NirK of *Ca.* N. viennensis. NK nat.: *nirK* native sequence, NK his.: *nirK* sequence plus a hexa-histidine-tag, NK thromb.: *nirK* sequence with a hexa-histidine-tag plus a thrombine cutting site.

4.5.2 Primer verification

For the amplification of the enzyme, specific primers were designed. One forward primer and three different reverse primers were used, which either amplified the native sequence or additionally attached a His-tag or a His-tag plus a thrombine cutting site.
To determine the affinity of the reverse primers, a PCR with a temperature gradient of 52.3°C to 58°C was performed. All primers worked at the tested annealing temperatures, the reverse primer which amplified the native sequence was working best at 52.3°C and 54°C. The reverse primers with the attachments gave the highest amplification results at 54°C and 56°C. Both of them amplified various side products as well but the product of correct size was dominating (Fig. 4-21). Concerning these results, the primer binding temperature was set to 54°C which allowed amplifying all constructs in one PCR run.
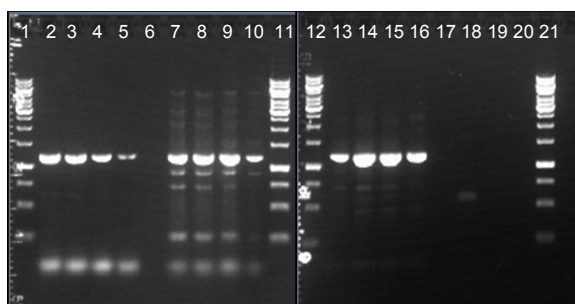
Figure 4-22: Agarose gel picture of the gradient-PCR of the primers specific for the amplification of NirK from *Ca.* N. viennensis. Slots 2-5: native reverse primer at 52.3°C, 54°C, 56°C, 58°C. Slot 7-10: reverse primer with His-tag at 52.3°C, 54°C, 56°C, 58°C. Slot 13-16: reverse primer with His-tag and thrombine cutting site at 52.3°C, 54°C, 56°C, 58°C. Slot 1, 11, 12, 21: DNA Ladder 1kb.

4.5.3 Ligation and Transformation

After preparation of the vector pET-28a and the PCR products, they were cut with the restriction enzymes *Nco*I and *Xho*I, respectively. The two molecules were ligated and the ligation approach was used to transform competent *E. coli* cells. With some of the grown clones a colony-PCR was done, revealing eleven clones with the right insert size (Fig. 4-22). Five transformants showed the correct insert size for the native *nirK* sequence, seven for the sequences with the additional His-tag. The PCR product with the His-tag as well as the thrombine cutting side could not be positively transformed in the vector. After that outcome, the focus was on the two constructs which remained. Three clones of each product were purified and sent for sequencing (Fig. 4-22).
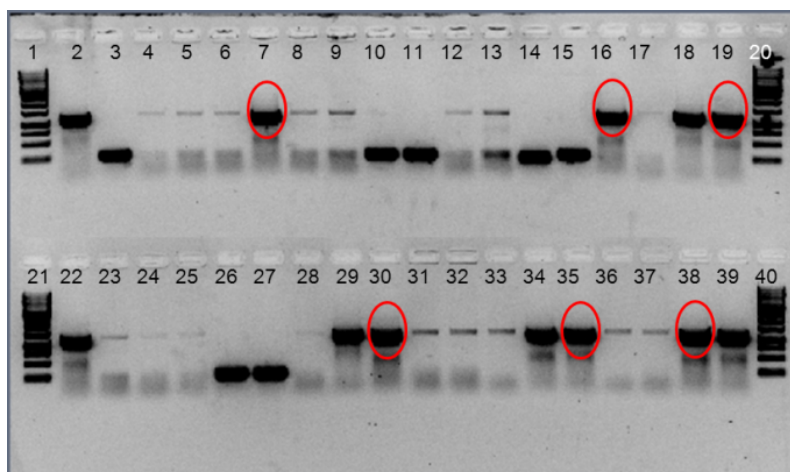
Figure 4-23: Colony-PCR of transformed clones, Slot 2-29: native *nirK* clones, Slot 30-39: *nirK* clones with additional His-tag, Slot 1, 20, 21, 40: DNA Ladder 1kb. Some transformants carrying the desired insert size, some have smaller inserts and some carry no insert. The thin line at the correct size is just background of the unligated PCR product. The red circles represent the clones which were sent for sequencing.

4.5.4 Sequences of clones

The three sequences which should represent the native *nirK* and the three representing the His-tag attached *nirK* sequences were apart from the attachment nearly identical (99-100%). But when compared to the *Ca.* N. viennensis genome sequence, the similarity was just 88% identity on the nucleotide level and 87% identity with 91% positives on the amino acid level (Fig. 4-23). This result was too consistent to be explained with an incorrect PCR or sequencing reaction and too less consistent to be from the same origin sequence. After several tests, the cloned sequence could be assigned to the *nirK* gene from a sister strain of *Ca.* N. viennensis, EN123 which is

another enriched culture in the laboratory (see Fig. 2-9). Apparently, this DNA was used for gene amplification. Final proof was given by an alignment of the *amoA* sequences of both organisms differing by 12 point mutations which all could be detected (Fig. 4-24).
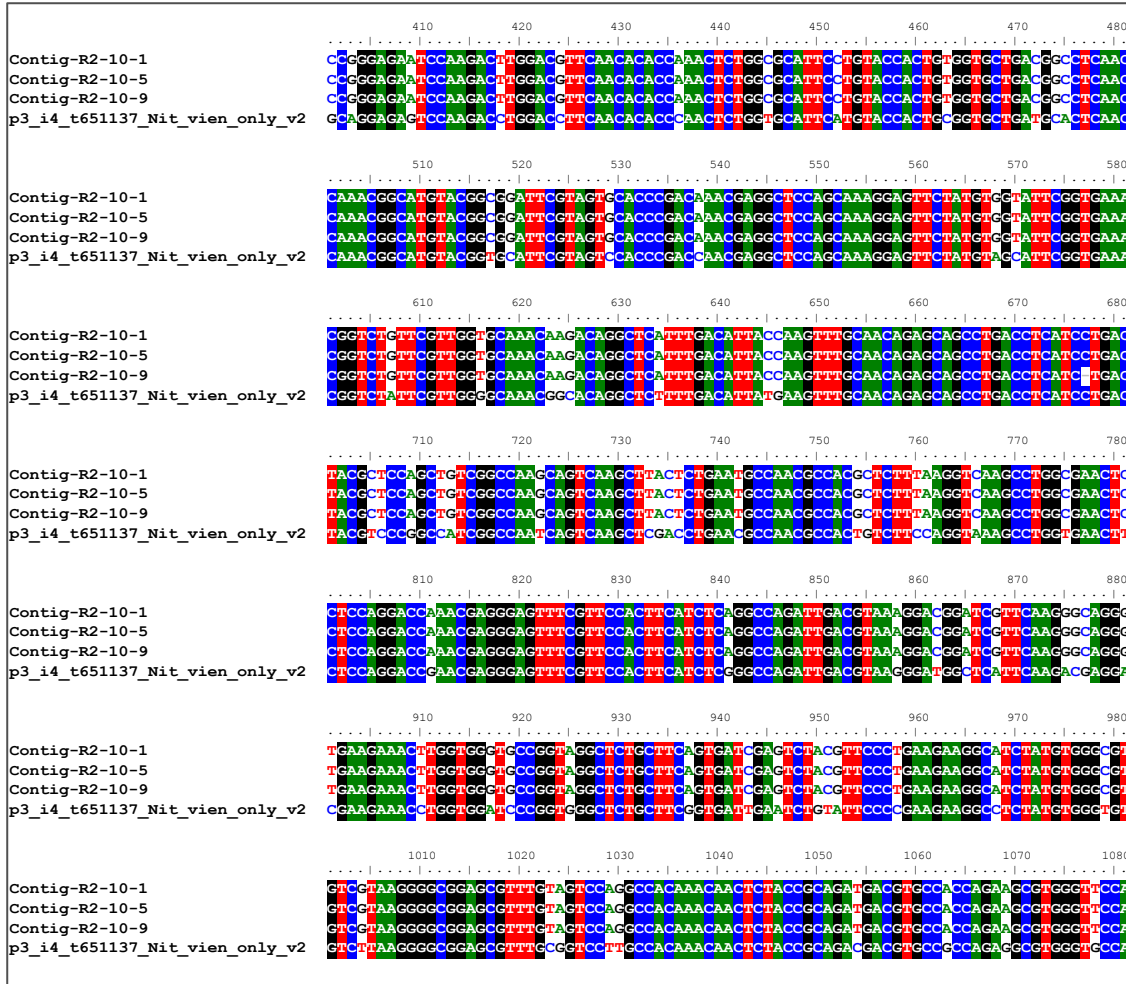
Figure 4-24: Alignment of the three sequenced clones (Contig-R2-10-1 Contig-R2-10-5 Contig-R2-10-9) which should carry the native sequence of the *nirK* from *Ca.* N. viennensis with *Ca.* N. viennensis genomic data (p3_i4_t651137_Nit_vien_omly_v2).
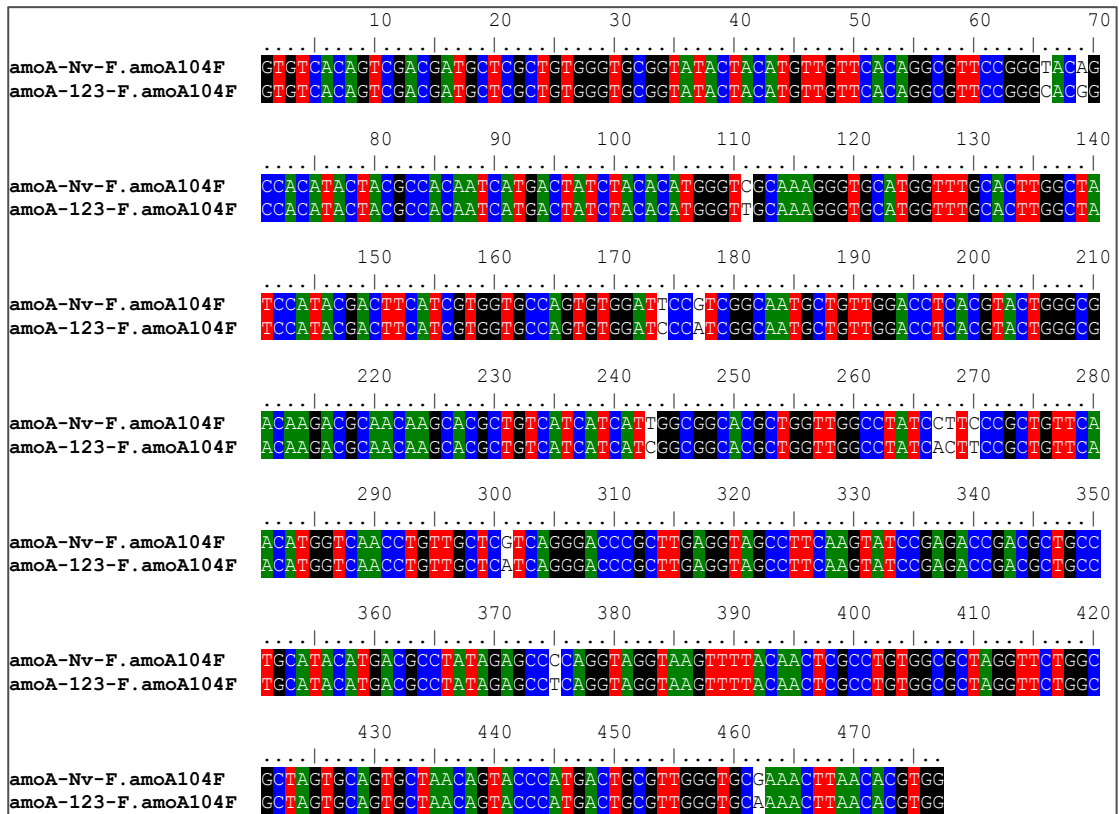
Figure 4-25: Alignment of the *amoA* sequences from *Ca.* N. viennensis (amoA-Nv-F.amoA104F) and EN 123 (amoA-123-F.amoA104F). Point mutations are labeled with a white background.

Furthermore, at the time point of primer design, the annotation of the *Ca.* N. viennensis genome had just started. After checking an updated version, it became clear that the nitrite reductase gene was annotated differently. The first time, an ATT-codon was mistaken as a start codon, later an usual ATG-codon upstream represented the start. Archaea are known to have sometimes unusual start codons, therefore it took longer to reveal the correct sequence. Concerning the construct, the reading frame remained but the first 60 nucleotides were missing (Fig. 5-5).
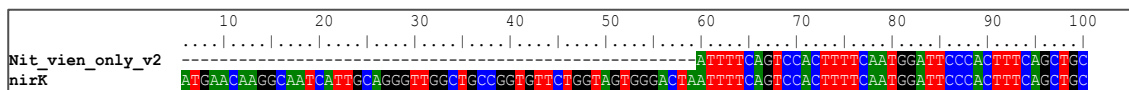
Figure 4-26: Comparison between amplified sequence (Nit vien_only_v2) and the final annotated nitrite reductase gene sequence (*nirK*).

5 Discussion

In the course of this study, the biochemistry of ammonia oxidizing archaea was investigated in order to gain insight into their unknown energy metabolism. A scheme in Fig. 5-1 gives an overview on the questions raised in this study. The heterologously expressed NirK enzyme was analyzed for its HAO and NIR activity. Also its ability to oxidize HNO, NO and NH_4^+ was examined. To determine potential intermediates, enzymatic assays with the same substances were repeated with cell extract fractions of *Ca.* N. viennensis. NO and N_2O were examined as possible side products. Additional physiological tests with the NO-scavenger PTIO were performed as well. The results and data achieved from these and further experiments as well as current hypothesis on the archaeal ammonia oxidation are discussed here.
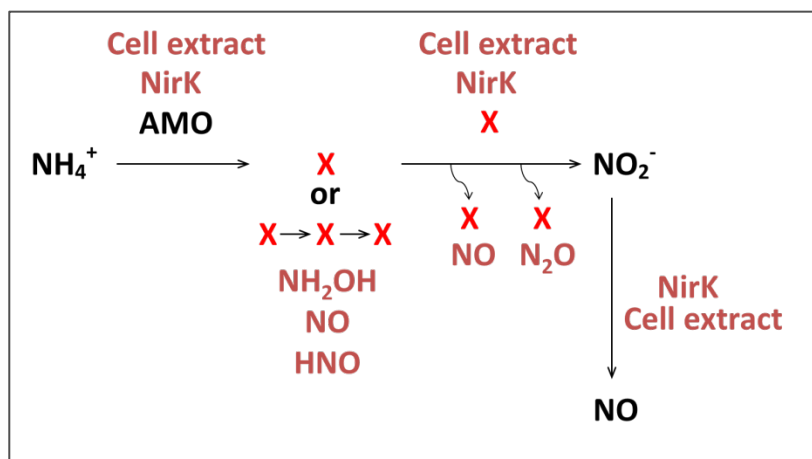
Figure 5-1: The knowns and unknowns of archaeal ammonia oxidation. If there is just one intermediate or a chain of intermediates is still unknown, as is the occurrence of side products. Cell extracts of *Ca.* N. viennensis and the NirK enzyme from soil contig 54d9 were tested for their ability to oxidize NH_2OH, NO, HNO and NH_4^+.

5.1 Biochemical studies with NirK

Although it has ~30% similarity to Sargasso Sea NirK sequences, *N. europaea* and halophilic archaea (Treusch et al., 2005) as well as conserved copper center coordination (Bartossek et al., 2010), the nitrite reductase from soil contig 54d9 showed no nitrite reductase activity, confirming former studies (Schweichhart and Urich, pers. comm.). The fact that in HAO assays the electron acceptor got reduced in the presence of hydroxylamine without any nitrite formation led to two main focuses in this work:

further characterization of the detected potential HAO activity and testing for alternative substrates which may lead to nitrite formation.

5.1.1   Characterization of partial HAO activity

The partial HAO activity increased with higher concentrations of hydroxylamine. Although the saturation was still missing with a maximum concentration of 10 mM tested, V_{max} and K_M ratios were calculated to gain a first insight into enzymatic parameters. The results were about 32 u/mg for V_{max} and around 1 mM for K_M. Compared to other V_{max} and K_M values of HAOs from different organisms, with V_{max} for the HAO of Anammox with 21 u/mg and for the HAO of *N. europea* 75 u/mg (Schalk et al., 2000), V_{max} is fitting in the range. Nevertheless, compared to K_M values around 26 µM for Anammox, 3.6 µM in *N. europea* (Schalk et al., 2000) and 1.1 µM in *Nitrosocystis* (Hooper and Nason, 1965), the calculated value for K_M seems high which suggests low affinity to the substrate hydroxylamine.

The HAO activity under anaerobic conditions could not be directly compared to that under aerobic conditions because the control was unstable. The non-enzymatic reduction of the electron acceptor occurred half as fast as the enzyme-depending reaction. Apart from the anaerobic treatment, the only difference in the setup was the exchange of plastic against glass cuvettes. The reason why the reduction of the electron acceptor happened so much faster under these circumstances could not be revealed. After finding plastic cuvettes which could be sealed with a rubber stopper, the background reaction was more stable and showed only one eighth of the enzymatic HAO activity. Under these conditions at similar hydroxylamine concentrations, the calculated enzyme activity was about four times higher than under aerobic conditions.

The results indicate that the partial HAO activity is probably not oxygen dependent. For bacterial HAOs it had been shown that under anaerobic conditions, the reduction of the electron acceptor is not affected whereas the nitrite production is inhibited: anaerobically, the HAO derived from *N. europaea* catalyzed the rapid reduction of mammalian cytochrome c by hydroxylamine without formation of nitrite but nitrous oxide (Falcone et al., 1963). Hooper and Nason (1965) did not observe a decrease in the rate of cytochrome c reduction by carrying out the enzymatic reaction anaerobically with the HAOs of *N. europaea* and *Nitrosocystis oceanus* and nitrous oxide rather than nitrite was evolved. Anaerobically, whole or crushed cells of *Nitrosomonas* were able to reduce the electron acceptor methylene blue; the disappearance of hydroxylamine did

not result in nitrite formation but nitric oxide and nitrous oxide were produced in amounts equivalent to the hydroxylamine added (Anderson, 1964). This indicates that the formation of nitrite is oxygen dependent, whereas the reduction of the electron acceptor is not. Under anaerobic conditions, the formation of gas bubbles was also observed in the NirK reaction. Aerobically, gas bubbles were sometimes observed but not as consistent as anaerobically. This could be a hint on a gaseous intermediate (see below 5.1.2). Since nitrous oxide and nitric oxide were excluded, the gas could be probably N_2.

To test for non-enzymatic reactions, the enzyme was exposed to heat and treated with protease. Additionally, side reactions caused by copper were investigated. When the enzyme was incubated at 80°C for several hours, no loss of activity could be detected, revealing high enzymatic stability to heat exposure. First, these results appeared like evidence for non-enzymatic activity but several studies on various NirKs from different organisms concluded exceptional thermal stability as well (Prudencio et al., 1999). The characterization of the wild type NirS from *Alcaligenes faecalis* indicated that the interactions between the various subunits appear to be strong enough to prevent monomer separationThe high melting temperature together with the high value of the denaturation enthalpy, confirmed Nir as a very stable protein (Stirpe et al., 2005).

The treatment with Proteinase K demonstrated the inactivation of the NirK and supported the enzyme-dependent HAO activity. However, the copper(II) chloride solutions which replaced the NirK in the reaction to test for copper side reactions showed the ability to reduce ferricyanide as well, increasing with higher concentrations. The oxidative loss of hydroxylamine in the presence of low concentrations of copper ions and air with only traces of nitrite formation was already reported in 1964 (Anderson, 1964). To compare the non-enzymatic copper-dependent with the enzymatic reaction, the amount of copper incorporated into the enzyme was calculated, resulting in ~72 nM copper in the NirK solution (calculations based on Schweichhart data, Urich, pers. comm.). If compared with the activity of a copper solution with the same concentration, the enzyme showed higher activity, ranging between the 100 nM and 500 nM copper solution activities. Nevertheless, the difference between enzymatic and non-enzymatic was not as big as expected. Also, the actual amount of copper which is incorporated into the catalytic center of the protein cannot be determined because of copper atoms which are bound unspecifically to the protein or dissolve back in the solution. Therefore, variations in the actual amount cannot be excluded. If copper is an essential part of the catalytic center of a protein, it is likely to react with the

substrate also without being incorporated but this complicates a distinction between non-enzymatic and enzymatic activity.

After these experiments, the copper solutions in the activity range of the NirK enzyme (50 nM, 100 nM and 500 nM) were additionally treated with protease to look for interactions between these two substrates. In fact, 40 µg/ml Proteinase K strongly inhibited the 50 nM and 100 nM non-enzymatic copper reactions, in contrast the 500 nM solution was not affected. The results of this experiment revealed that in the range of the incorporated copper concentrations, Proteinase K is able to interfere with the observed reduction of the electron acceptor. That means that protease treatment is not an appropriate method to assure for enzyme-dependent reactions. It is not able to discriminate between enzymatic and non-enzymatic activity and a method which allows a better distinction has to be developed. Under this aspect, enzymatic activity of the heterologously expressed NirK is still doubtful.

5.1.2 Formation of nitrite and other possible products/intermediates

Although various alterations of the HAO assay conditions were carried out, nitrite formation was not detected in any case. The reduction of the electron acceptor only occurred with hydroxylamine as a substrate and without nitrite formation. Nitric oxide, nitroxyl, ammonium, mixes of the substrates and addition of small amounts of nitrite did neither lead to reduction of the electron acceptor nor enzymatic production of nitrite. Also prereducing the enzyme based on the hypothesis of activating the Cu-centers by loading them with electrons did not show any effect, as well as running the reaction under anaerobic conditions. Since anaerobic conditions inhibited nitrite production in the HAO of ammonia oxidizing bacteria (Anderson, 1964; Falcone et al., 1963; Hooper and Nason, 1965), an additional experiment with strongly aerating the NirK reaction was performed but again nitrite formation could not be observed.

Concerning the impossibility to detect nitrite, it has to be mentioned that in the beginning of investigating the HAO in AOB, more precisely in *Nitrosomonas europaea* and *Nitrosocystis oceanus*, nitrite accounted for only 5% to 10% of the disappeared hydroxylamine (Hooper and Nason, 1965). It was also discovered that the inclusion of FeCl$_3$ in the *Nitrosocystis* reaction mixture markedly increased the quantity of nitrite produced as well as the ratio of nitrite formed to hydroxylamine oxidized (Hooper and Nason, 1965). By analogy (the *Nitrosocystis* enzyme contains iron in the catalytic center) the NirK enzyme was perhaps not loaded with enough copper to achieve the

complete reaction. It could also indicate that the assay conditions have to be further developed.

Regarding other products besides nitrite, the observation of gas bubble formation during the reaction led to the hypothesis that the reaction might stop at a gaseous intermediate. This aspect is further supported by the ongoing discussion on the appearance of other intermediates besides hydroxylamine in the bacterial ammonia oxidation process. Previous studies suggest that the metabolism of hydroxylamine is not a one- but a two-step process (Anderson, 1964): in the first step, hydroxylamine is dehydrogenated to form nitroxyl which decomposes to nitrous oxide and further to nitric oxide. Then, nitric oxide is converted into nitrite by an enzyme system requiring oxygen.

Because of this hypothesis, nitric oxide and nitrous oxide as possible intermediates or side products were investigated. Nitrous oxide was measured via Isotopic Ratio Mass Spectrometry (IRMS). The headspace of an HAO assay and two additional controls (one without enzyme, one without substrate) was sent for analysis. Nitrous oxide could be detected in similar amounts in the enzymatic reaction as well as in the control containing hydroxylamine. In contrast, the control without hydroxylamine barely showed nitrous oxide. It seemed that under aerobic conditions, nitrous oxide is always produced in small amounts by the spontaneous degradation of hydroxylamine but not because of enzymatic activity. The formation of nitric oxide was determined indirectly with PTIO, which is degraded in the presence of nitric oxide molecules. At a 100fold higher concentration of hydroxylamine PTIO was completely, if the concentration was 10fold higher only small amounts were degraded. Side reactions of PTIO with hydroxylamine were negligible. The monitoring of the PTIO degradation was challenging: because of its insolubility only small amounts of it could be used in the reaction. Degradation of PTIO under high hydroxylamine concentrations could be a hint for nitric oxide production. Experiments with different NirK concentrations predicted enzyme dependence of this reaction as well. Nevertheless, it seems like the production of nitric oxide is 100 times less than the given substrate, so it is probably formed in the reaction as a side product. In case the intermediate would be nitric oxide, it should not be neglected that this is a very reactive compound and therefore highly toxic for living cells. That would mean that the compound has to be tightly bound on the transferring or reducing molecule to not harm the cell. Therefore, only traces might be detectable.

Another hypothesis on the incomplete oxidation of hydroxylamine refers to a significant difference in the C-terminus of the NirK of the soil contig 54d9. Contrary to many other

NirKs, it has an additional amicyanin domain with a still unknown function. This additional domain might complicate the correct refolding of the protein in *E. coli*, which could be a reason for inefficient activity of the heterologously expressed enzyme. Further, amicyanin is a type I copper protein that is catalyzing reactions in the electron transfer. Maybe it plays an important role for the enzymatic activity but the conditions which are needed to obtain a functional amicyanin domain for this enzyme are not yet identified. The requirement of a correct copper incorporation for activity complicates the issue further, as this is a challenging step in the refolding process.

Because of this amicyanin domain, it would be important to obtain the enzyme from *Ca.* N. viennensis as well, in which this feature is not occurring. This could simplify the complex refolding process and allows comparison between those two related proteins. To gain the investigated enzyme of a cultivated representative would also offer further characterization methods because comparison between the isolated enzyme and protein extracts would be possible.

5.2 Enzymatic activities in *Ca.* N. viennensis cell extracts

Concerning the complexity of the ammonia oxidation metabolism, requiring an electron transport chain, a single expressed and refolded protein might be missing some external factors to work correctly *in vitro*. Having a crude cell extract of an AOA helps to achieve more natural conditions and further enables a step-wise investigation of interesting processes as well as isolation of enzymes. Activity with ammonia as a substrate would indicate the ability of the cell extract to achieve complete ammonia oxidation, formation of hydroxylamine or nitric oxide would indicate intermediates.

To perform that kind of experiments, a certain amount of cell mass is required. This is challenging, because *Ca.* N. viennensis only grows up to low cell densities, ~5×10^7 cells/ml maximum. So the cultivation method needed to be upscaled (see 4.2.1). After obtaining enough cell extract, the same enzymatic assays as with the NirK enzyme were performed to compare the results. When hydroxylamine was replaced with ammonia in the HAO assay, no reduction of the electron acceptor occurred. Therefore, a second attempt was established to detect the oxidation of ammonium via a colorimetric assay. Ammonium, cell extract and KPi-buffer were mixed together with an electron donor, an electron acceptor or both to cover occurring electron transfer processes. Also with this attempt ammonia oxidation could not be detected. Although for AOBs cell free ammonia oxidation was already observed in

1970 (Suzuki and Kwok, 1970), the process investigated did either not remain functional because of the lysis treatment or the chosen setup of the assays.

When the HAO assay was repeated, activity was detected in the crude cell extract as well as in the insoluble and soluble fraction with similar enzymatic activities, indicating an incomplete separation of insoluble and soluble proteins. No nitrite formation occurred just as in the NirK experiments. Neither replacing hydroxylamine with nitric oxide, a mixture of hydroxylamine and nitric oxide nor addition of small amounts of nitrite had any positive effect on nitrite formation. Investigations on nitric oxide as an intermediate/product in the HAO assay provided results comparable to the NirK experiments. The ability of the different cell extracts to reduce the electron acceptor was not inhibited by the addition of the NO-scavenger PTIO. About 10 min after the reduction of the electron acceptor, degradation of PTIO started and ended before the reaction was finished. The delay could be due to a certain nitric oxide threshold, which is needed to start the NO-scavenging reaction if nitric oxide is produced.

The only significant difference between the NirK enzyme and cell extract analysis was the ability of the cell extract to reduce nitrite. Whole crude cell extract, insoluble as well as soluble fraction showed nitrite reductase activity, highest in the insoluble protein fraction. It is known that AOB as well as most of the AOA have NirK homologues, which is thought to be responsible for the nitrifier denitrification, a process which describes the release of N_2O especially at the interface between aerobic and anaerobic habitats (Cantera and Stein, 2007). If *Ca.* N. viennensis cultures are able to grow anaerobically using nitrite as a substrate is still discussed. First experiments indicate that it is not capable of denitrification (Stieglmeier, pers. comm.) but more investigations to affirm this hypothesis are necessary.

Since the reduction of nitrite just requires the substrate and the appropriate enzyme, this process is less complex than ammonia oxidation, which needs a broad oxidation-reduction gradient with various involved proteins. Therefore, nitrite reduction could be more easily detected in the protein solution even if the reaction occurs only at negligible levels in the cell.

5.3 Physiological experiments investigating nitric oxide as an intermediate

A different approach was to investigate the possible intermediate nitric oxide in a growing culture, as *Ca.* N. viennensis was available for experiments. Therefore,

Ca. N. viennensis*, the AOB *N. multiformis* and *E. coli* were incubated with different concentrations of PTIO. This agent is commonly used to study reactions where NO radicals play an important role ranging from beneficial physiological functions such as blood pressure regulation and neurotransmission to negative effects like modulating inflammatory, infectious, and degenerative diseases (Goldstein et al., 2003). Further, PTIOs are considered as biochemical and physiological effectors and potential therapeutic agents. The applied concentrations in the literature vary from minimum of 0.1 nM (Gualda et al., 2011) to a maximum of 2 mM (Yoon et al., 2011), depending on the investigated question. The concentrations in this experiment were within this range to assure the non-toxicity of the substrate.

The results of these experiments suggest that AOA are more strongly affected by PTIO than AOB, which indicates that nitrous oxide may be an essential intermediate and could have an important function in their energy metabolism. However, this theory is questioned by the growth inhibition of *N. multiformis* by PTIO at higher concentrations. *N. multiformis* was not as sensitive as *Ca.* N. viennensis which was affected more severe, but still experienced negative effects on growth at concentrations of 250 µM. A hypothesis for this result could be that nitric oxide occurs as an intermediate in both processes but in AOA is less tightly bound to enzymes than in AOB, where it is an intermediate which is processed further really quickly by HAO. In this case, PTIO could have an effect on the bacterial metabolism as well but to interfere with the NO which is more difficult to access, higher concentrations would be necessary. Because PTIO is applied in a broad range of experiments with various cell types as well as the results obtained from the *E. coli* experiment, a general toxic effect of the substance to living cells could be excluded. Nevertheless, it has to be noted that side reactions with other substrates (for example hydroxylamine) could not be completely excluded.

5.4 Proteomics

Ca. N. viennensis crude cell extract as well as soluble and insoluble protein fractions were loaded on a SDS-gel to detect the NirK enzyme in the *Ca.* N. viennensis proteome. If the enzyme plays a role in archaeal ammonia oxidation, detectable amounts of NirK should be present in the cell extract. Various former metatranscriptomic studies showed high abundance of *nirK* transcripts in soil group 1.1b as well as marine group 1.1a Archaea (Hollibaugh et al., 2011; Radax et al., 2012;

Urich et al., 2008). Therefore, it was investigated if similar results could be achieved on the proteome level as well.

In total, 154 proteins could be identified but no NirK was found. This was quite surprising because metatranscriptomic studies obtain different results (mentioned above). Although it might be that the enzyme is not frequently translated, it has to be mentioned that especially membrane associated proteins are very difficult to detach. Maybe the treatment was not rigorous enough and the protein did not get into solution. Another reason could be the difficulty to ionize certain proteins because otherwise they are not detectable with the applied method. This phenomenon is also seen with AMO, which is essential for the metabolism and also highly transcribed but not detected in high abundance in the proteome. AmoB was represented with 4 peptides, AmoA and AmoC were not detected. In a further proteomic study with a different extraction protocol optimized for membrane-associated proteins, NirK was represented 1 time and the AmoA, AmoB, AmoC subunits either 1 time, 2 times and 4 times (Kerou, pers. comm.). Only these small amounts were detected in the proteome, although transcription studies of *Ca.* N. viennensis reveal high transcription of these genes (Feigl, pers. comm.).

Since the ammonia oxidation pathway requires a membrane gradient, one could assume that the involved enzymes are membrane-attached and therefore remain in the insoluble fraction, like AMO (Hyman and Wood, 1983), NAR or NOR (Zumft, 1997). Nevertheless, in denitrifying organisms NIRs are periplasmatic and not membrane attached. This was shown for several representatives of NirKs via the finding of the enzymes in the periplasm fraction of the soluble proteins and later via direct immunocytochemical location *in situ* (Zumft, 1997). Nevertheless, part of the enzyme seems to be sometimes strongly membrane associated but the mechanism is still unknown (Zumft, 1997). Up to now there are no results on the location of the NirK from *Ca.* N. viennensis. The only evidence is the N-terminal amino acid region 5 to 27 which was assigned a transmembrane domain, probably a signal peptide (Treusch, 2004) which seems to be responsible for the transport in the periplasm. If this region is cut off after the transport or further involved in membrane association is not known. Therefore, the strength of the association with the membrane is still unknown and the occurrence of the NirK could not be predicted. Also the HAO of AOBs is considered to be a periplasm-associated enzyme (Kowalchuk and Stephen, 2001).

5.5   Conclusion

A series of experiments with purified enzyme, crude cell extracts and growing cultures was performed in this study in order to investigate the second step of ammonia oxidation in archaea. Table 5-1 summarizes all investigations:

Table 5-1: Overview on investigated enzyme activities as well as intermediates. (* result from Stieglmeier et al., pers. comm.). n.d. = not determined.

Enzyme activity	NirK homologue	Crude cell extracts	*Ca.* N. viennensis culture
AMO	-	-	+
HAO	+/-	+/-	n. d.
HNO OR	-	-	n. d.
NO OR	-	-	n. d.
NIR	-	+	n. d.
Intermediates			
NO	+	+	+
N_2O	-	n. d.	+ *

The heterologously expressed NirK enzyme from archaeal fosmid 54d9 showed no nitrite reductase activity. It was able to oxidize hydroxylamine in presence of an artificial electron acceptor. Nitrite production was not detected, though. This partial HAO activity was measured indirectly via the reduction of the electron acceptor. The calculated K_M values for the substrate indicate only low hydroxylamine affinity. Its ability to oxidize nitric oxide and nitroxyl was investigated but no activity with any of the tested substrates was detected. Although several conditions were examined, stoichiometric nitrite production as well as other product formation was never observed. Discrimination between specific enzymatic activity and copper side reactions could not convincingly be shown.

Enzymatic experiments with cell extract fractions (whole crude cell extract, soluble and insoluble fraction) of *Ca.* N. viennensis showed no ammonia oxidation activity. Only partial HAO activity was detectable, in the presence of hydroxylamine the reduction of the electron acceptor was detected indicating hydroxylamine oxidation but again without any nitrite formation. Similar results were obtained for the isolated Nirk enzyme as well. In all fractions of the cell extract nitrite reductase activity was demonstrated. Therefore, this pathway is present in the organism although it has not been shown in growing cultures, so far. If this activity is caused by the NirK homologue remains unclear but likely, although the isolated enzyme did not show that activity.

The complete ammonia oxidation process could only be observed in growing *Ca.* N. viennensis cultures. Growth inhibition due to the nitric oxide scavenger PTIO suggests NO to be an important intermediate in ammonia oxidation and that the mechanism or at least the enzymatic apparatus for oxidation of ammonia in AOA and AOB is different.

The understanding of the process (or subprocesses) of ammonium oxidation in crude cell extracts seems to be challenging, probably because the involvement of complex electron transfer processes which are not easy to study. Furthermore, most of the involved proteins are membrane bound or associated. The activity of the NirK enzyme could not be clearly resolved. To fully reveal the archaeal ammonia oxidation pathway, many challenges in cultivation of representatives, heterologous expression of complex enzymes containing metal cofactors and the handling of reactive nitrogen species have to be overcome. These results suggest that other biochemical methods should be involved to investigate the mechanism of ammonium oxidation in archaea. Nevertheless, the findings of this thesis contribute to the understanding of the pathway and are a foundation for further studies.

6 References

Anderson, J. H.
>   1964   The metabolism of hydroxylamine to nitrite by Nitrosomonas. Biochem J 91(1):8-17.

Anderson, J. H.
>   1964   The Copper-catalysed Oxidation of Hydroxylamine. Analyst, 89, 357-362

Arp, D. J., L. A. Sayavedra-Soto, and N. G. Hommes
>   2002   Molecular biology and biochemistry of ammonia oxidation by Nitrosomonas europaea. Arch Microbiol 178(4):250-5.

Barns, S. M., et al.
>   1996   Perspectives on archaeal diversity, thermophily and monophyly from environmental rRNA sequences. Proc Natl Acad Sci U S A 93(17):9188-93.

Bartossek, R., et al.
>   2010   Homologues of nitrite reductases in ammonia-oxidizing archaea: diversity and genomic context. Environ Microbiol 12(4):1075-88.

Beaumont, H. J., et al.
>   2004   Expression of nitrite reductase in Nitrosomonas europaea involves NsrR, a novel nitrite-sensitive transcription repressor. Mol Microbiol 54(1):148-58.

Bintrim, S. B., et al.
>   1997   Molecular phylogeny of Archaea from soil. Proc Natl Acad Sci U S A 94(1):277-82.

Boetius, A., et al.
>   2000   A marine microbial consortium apparently mediating anaerobic oxidation of methane. Nature 407(6804):623-6.

Brochier-Armanet, C., et al.
>   2008   Mesophilic Crenarchaeota: proposal for a third archaeal phylum, the Thaumarchaeota. Nat Rev Microbiol 6(3):245-52.

Brochier-Armanet, C., P. Forterre, and S. Gribaldo
>   2011   Phylogeny and evolution of the Archaea: one hundred genomes later. Curr Opin Microbiol 14(3):274-81.

Cantera, J. J., and L. Y. Stein
>   2007   Role of nitrite reductase in the ammonia-oxidizing pathway of Nitrosomonas europaea. Arch Microbiol 188(4):349-54.

DeLong, E. F.
>   1992   Archaea in coastal marine environments. Proc Natl Acad Sci U S A 89(12):5685-9.

DeLong, E. F., et al.
>   1994   High abundance of Archaea in Antarctic marine picoplankton. Nature 371(6499):695-7.

Falcone, A. B., A. L. Shug, and D. J. Nicholas
>   1963   Some Properties of a Hydroxylamine Oxidase from Nitrosomonas Europaea. Biochim Biophys Acta 77:199-208.

Goldstein, S., A. Russo, and A. Samuni

    2003   Reactions of PTIO and carboxy-PTIO with *NO, *NO2, and O2-*. J Biol Chem 278(51):50949-55.

Gualda, L. B., et al.

    2011   5-HT1A autoreceptor modulation of locomotor activity induced by nitric oxide in the rat dorsal raphe nucleus. Braz J Med Biol Res 44(4):332-6.

Guy, L., and T. J. Ettema

    2011   The archaeal 'TACK' superphylum and the origin of eukaryotes. Trends Microbiol 19(12):580-7.

Hollibaugh, J. T., et al.

    2011   Metatranscriptomic analysis of ammonia-oxidizing organisms in an estuarine bacterioplankton assemblage. ISME J 5(5):866-78.

Hooper, A. B., and A. Nason

    1965   Characterization of hydroxylamine-cytochrome c reductase from the chemoautotrophs Nitrosomonas europaea and Nitrosocystis oceanus. J Biol Chem 240(10):4044-57.

Huber, H., et al.

    2002   A new phylum of Archaea represented by a nanosized hyperthermophilic symbiont. Nature 417(6884):63-7.

Hyman, M. R., and P. M. Wood

    1983   Methane oxidation by Nitrosomonas europaea. Biochem J 212(1):31-7.

Jetten, M. S., P. de Bruijn, and J. G. Kuenen

    1997   Hydroxylamine metabolism in Pseudomonas PB16: involvement of a novel hydroxylamine oxidoreductase. Antonie Van Leeuwenhoek 71(1-2):69-74.

Jetten, M., et al.

    2005   Anammox organisms: enrichment, cultivation, and environmental analysis. Methods Enzymol 397:34-57.

Klotz, M. G., and L. Y. Stein

    2008   Nitrifier genomics and evolution of the nitrogen cycle. FEMS Microbiol Lett 278(2): 146-56.

Konneke, M., et al.

    2005   Isolation of an autotrophic ammonia-oxidizing marine archaeon. Nature 437(7058): 543-6.

Kowalchuk, G. A., and J. R. Stephen

    2001   Ammonia-oxidizing bacteria: a model for molecular microbial ecology. Annu Rev Microbiol 55:485-529.

Leininger, S., et al.

    2006   Archaea predominate among ammonia-oxidizing prokaryotes in soils. Nature 442(7104):806-9.

Maeda, H., et al.

    1994   Multiple functions of nitric oxide in pathophysiology and microbiology: analysis by a new nitric oxide scavenger. J Leukoc Biol 56(5):588-92.

References

McTavish, H., J. A. Fuchs, and A. B. Hooper

1993   Sequence of the gene coding for ammonia monooxygenase in Nitrosomonas europaea. J Bacteriol 175(8):2436-44.

Mullis, K., et al.

1986   Specific enzymatic amplification of DNA in vitro: the polymerase chain reaction. Cold Spring Harb Symp Quant Biol 51 Pt 1:263-73.

Muyzer, G., E. C. de Waal, and A. G. Uitterlinden

1993   Profiling of complex microbial populations by denaturing gradient gel electrophoresis analysis of polymerase chain reaction-amplified genes coding for 16S rRNA. Appl Environ Microbiol 59(3):695-700.

Nicol, G. W., and C. Schleper

2006   Ammonia-oxidising Crenarchaeota: important players in the nitrogen cycle? Trends Microbiol 14(5):207-12.

Nunoura, T., et al.

2011   Insights into the evolution of Archaea and eukaryotic protein modifier systems revealed by the genome of a novel archaeal group. Nucleic Acids Res 39(8):3204-23.

Prudencio, M., R. R. Eady, and G. Sawers

1999   The blue copper-containing nitrite reductase from Alcaligenes xylosoxidans: cloning of the nirA gene and characterization of the recombinant enzyme. J Bacteriol 181(8):2323-9.

Radax, R., et al.

2012   Metatranscriptomics of the marine sponge Geodia barretti: tackling phylogeny and function of its microbial community. Environ Microbiol.

Rotthauwe, J. H., K. P. Witzel, and W. Liesack

1997   The ammonia monooxygenase structural gene amoA as a functional marker: molecular fine-scale analysis of natural ammonia-oxidizing populations. Appl Environ Microbiol 63(12): 4704-12.

Santoro, A. E., et al.

2011   Isotopic signature of N(2)O produced by marine ammonia-oxidizing archaea. Science 333(6047):1282-5.

Schalk, J., et al.

2000   Involvement of a novel hydroxylamine oxidoreductase in anaerobic ammonium oxidation. Biochemistry 39(18):5405-12.

Schleper, C., W. Holben, and H. P. Klenk

1997   Recovery of crenarchaeotal ribosomal DNA sequences from freshwater-lake sediments. Appl Environ Microbiol 63(1):321-3.

Schleper, C., G. Jurgens, and M. Jonuscheit

2005   Genomic studies of uncultivated archaea. Nat Rev Microbiol 3(6):479-88.

Staley, J. T., and A. Konopka

1985   Measurement of in situ activities of nonphotosynthetic microorganisms in aquatic and terrestrial habitats. Annu Rev Microbiol 39:321-46.

Stein, J. L., and M. I. Simon

1996   Archaeal ubiquity. Proc Natl Acad Sci U S A 93(13):6228-30.

Stirpe, A., et al.

    2005   Calorimetric and spectroscopic investigations of the thermal denaturation of wild type nitrite reductase. Biochim Biophys Acta 1752(1):47-55.

Suzuki, I., and S. C. Kwok

    1970   Cell-free ammonia oxidation by Nitrosomonas europaea extracts: effects of polyamines, Mg2+ and albumin. Biochem Biophys Res Commun 39(5):950-5.

Tourna, M., et al.

    2008   Growth, activity and temperature responses of ammonia-oxidizing archaea and bacteria in soil microcosms. Environ Microbiol 10(5):1357-64.

Tourna, M., et al.

    2011   Nitrososphaera viennensis, an ammonia oxidizing archaeon from soil. Proc Natl Acad Sci U S A 108(20):8420-5.

Treusch, A. H.

    2004 Herstellung und Charakterisierung von Umweltgenbanken aus Böden zur Aufklärung von genetischen und physiologischen Eigenschaften nicht-kultivierter Crenarchaeota. Darmstadt,Techn. Univ., Dissertation

Treusch, A. H., et al.

    2005   Novel genes for nitrite reductase and Amo-related proteins indicate a role of uncultivated mesophilic crenarchaeota in nitrogen cycling. Environ Microbiol 7(12):1985-95.

Urich, T., et al.

    2008   Simultaneous assessment of soil microbial community structure and function through analysis of the meta-transcriptome. PLoS One 3(6):e2527.

Venter, J. C., et al.

    2004   Environmental genome shotgun sequencing of the Sargasso Sea. Science 304(5667):66-74.

Walker, C. B., et al.

    2010   Nitrosopumilus maritimus genome reveals unique mechanisms for nitrification and autotrophy in globally distributed marine crenarchaea. Proc Natl Acad Sci U S A 107(19):8818-23.

Woese, C. R., and G. E. Fox

    1977   Phylogenetic structure of the prokaryotic domain: the primary kingdoms. Proc Natl Acad Sci U S A 74(11):5088-90.

Woese, C. R., O. Kandler, and M. L. Wheelis

    1990   Towards a natural system of organisms: proposal for the domains Archaea, Bacteria, and Eucarya. Proc Natl Acad Sci U S A 87(12):4576-9.

Wuchter, C., et al.

    2006   Archaeal nitrification in the ocean. Proc Natl Acad Sci U S A 103(33):12317-22.

Yoon, M. Y., et al.

    2011   Contribution of cell elongation to the biofilm formation of Pseudomonas aeruginosa during anaerobic respiration. PLoS One 6(1):e16105.

Zumft, W. G.

    1997   Cell biology and molecular basis of denitrification. Microbiol Mol Biol Rev 61(4):533-616.

7 Appendix

A. MALDI-TOF analysis of *Ca.* N. viennensis proteome

Proteins identified in the upper band

Accession	MW [kDa]	Description	Coverage	Peptides
NIVIEv2_71058	140,9	DNA-directed RNA polymerase	32,78	29
NIVIEv2_100071	122,9	exported protein of unknown function	54,87	43
NIVIEv2_71059	124.6	rpoB DNA-directed RNA polymerase subunit B	2.86	2

Proteins identified in the 40 to 55 kDa band

Accession	MW [kDa]	Description	Coverage	Peptides
NIVIEv2_70799	42,7	3-hydroxybutyryl-CoA dehydrogenase	7,33	2
NIVIEv2_100025	50,2	ansB Aspartate ammonia-lyase	10,2	3
NIVIEv2_100047	39,1	argC N-acetyl-gamma-glutamyl-phosphate/N-acetyl-gamma-aminoadipyl-phosphate reductase	35,14	11
NIVIEv2_100050	44,6	argG Argininosuccinate synthase	9,45	2
NIVIEv2_140093	36,4	ATP phosphoribosyltransferase	38,46	7
NIVIEv2_71061	28,7	Conserved exported protein of unknown function	57,93	10
NIVIEv2_120033	40,7	conserved protein of unknown function	29,38	7
NIVIEv2_71150	41,3	conserved protein of unknown function	29,14	8
NIVIEv2_100136	35,6	conserved protein of unknown function	26,2	5
NIVIEv2_71087	43,3	conserved protein of unknown function	12,9	3
NIVIEv2_71113	45,7	conserved protein of unknown function	10,84	2
NIVIEv2_140118	40,7	degT Pleiotropic regulatory protein	12,83	3
NIVIEv2_140135	41,6	dnaJ Chaperone protein dnaJ, heat shock protein (Hsp40), co-chaperone with dnaK	6,43	2
NIVIEv2_140258	45,2	eif2g Translation initiation factor 2 subunit gamma	11,19	4
NIVIEv2_70886	44,9	eno Enolase	18,47	5
NIVIEv2_100071	122,9	exported protein of unknown function	3,11	2
NIVIEv2_20092	36,8	exported protein of unknown function	34,69	8
NIVIEv2_71146	27,5	exported protein of unknown function	30,91	3
NIVIEv2_70925	40	exported protein of unknown function	25,47	4
NIVIEv2_130060	48,6	glyA Serine hydroxymethyltransferase	27,09	8
NIVIEv2_70240	43,1	Glyceraldehyde-3-phosphate dehydrogenase	8,97	2
NIVIEv2_140032	39,3	H(+)-transporting two-sector ATPase	37,39	8
NIVIEv2_20080	48,8	hemL Glutamate-1-semialdehyde 2,1-aminomutase 2	9,82	3
NIVIEv2_180235	37,4	ilvC acetohydroxy-acid isomeroreductase	55,26	13
NIVIEv2_180221	37,7	Isocitrate/isopropylmalate dehydrogenase	26,32	6
NIVIEv2_180113	38,2	mtnA Methylthioribose-1-phosphate isomerase	10,26	2
NIVIEv2_70520	36,2	Myo-inositol-1-phosphate synthase	42,06	7

NIVIEv2_70050	43,7	pgk Phosphoglycerate kinase	6,47	2
NIVIEv2_70398	46,6	Phosphoglycerate mutase	6,68	2
NIVIEv2_70382	47,4	Phosphomethylpyrimidine kinase (Hmp-phosphate kinase)	6,5	2
NIVIEv2_100147	48,7	Pre-mRNA processing ribonucleoprotein, binding domain protein	5,92	2
NIVIEv2_70494	35,3	protein of unknown function	29,19	7
NIVIEv2_71131	38,9	purP 5-formaminoimidazole-4-carboxamide-1-(beta)-D-ribofuranosyl 5'-monophosphate synthetase	7,16	2
NIVIEv2_140099	40,4	putative CBS domain pair protein	22,37	5
NIVIEv2_170008	39,1	putative CRISPR-associated regulatory protein, DevR family	8,65	2
NIVIEv2_70902	42,1	putative enzyme	10,76	3
NIVIEv2_140091	40,4	putative Histidinol-phosphate aminotransferase	10,99	2
NIVIEv2_71217	40,5	putative Luciferase-like monooxygenase	44,17	10
NIVIEv2_70869	44,4	putative Respiratory-chain NADH dehydrogenase, 49 Kd subunit	15,03	4
NIVIEv2_140176	38,3	putative zinc-binding dehydrogenase	16,19	4
NIVIEv2_100297	38,1	putative zinc-binding dehydrogenase	9,17	3
NIVIEv2_70928	45,5	rocG glutamate dehydrogenase	32,85	8
NIVIEv2_70212	36,5	rpl3p 50S ribosomal protein L3P	24,7	5
NIVIEv2_70377	39,6	sucC Succinyl-CoA ligase [ADP-forming] subunit beta	14,86	5
NIVIEv2_70951	46,7	sufS cysteine desulfurase	9,88	2
NIVIEv2_71149	47,3	tuf Elongation factor 1-alpha	66,36	22

Proteins identified in the lower band

Accession	MW [kDa]	Description	Coverage	Peptides
NIVIEv2_140114	19,7	4Fe-4S ferredoxin iron-sulfur binding domain protein	16,29	3
NIVIEv2_130054	24,8	conserved protein of unknown function	12,23	4
NIVIEv2_120018	22,8	dps DNA protection during starvation protein	21,89	5
NIVIEv2_71143	23,7	exported protein of unknown function	28,7	4
NIVIEv2_140242	17,7	Glyoxalase/bleomycin resistance protein/dioxygenase	17,5	2
NIVIEv2_180311	23	pdxT glutamine amidotransferase for pyridoxal phosphate synthesis	15,17	2
NIVIEv2_180325	20	protein of unknown function	23,94	2
NIVIEv2_20159	24,6	protein of unknown function	21,27	6
NIVIEv2_110006	20,1	protein of unknown function	21,08	3
NIVIEv2_71015	21,2	protein of unknown function	15,59	2
NIVIEv2_130131	21,4	putative adenylate kinase	12,44	2
NIVIEv2_71102	22,2	rps5p 30S ribosomal protein S5P	46,6	7
NIVIEv2_71054	22,5	rps7p 30S ribosomal protein S7P	33,83	4
NIVIEv2_180391	23,3	sodA superoxide dismutase	54,59	9
NIVIEv2_70808	20,4	Thiol-disulfide isomerase	25	2

Proteins identified in the insoluble fraction

Accession	MW [kDa]	Description	Coverage	Peptides
NIVIEv2_140114	19,7	4Fe-4S ferredoxin iron-sulfur binding domain protein	14,61	2
NIVIEv2_100113	56,4	abfD 4-hydroxybutyryl-CoA dehydratase/vinylacetyl-CoA-Delta-isomerase	6,51	2
NIVIEv2_71080	55,8	accC acetyl-CoA carboxylase subunit (biotin carboxylase subunit)	10,5	3
NIVIEv2_180214	20,3	AmoB-like protein	39,46	4
NIVIEv2_140025	66,2	atpA V-type ATP synthase alpha chain	10,83	4
NIVIEv2_140026	50,7	atpB V-type ATP synthase beta chain	18,36	5
NIVIEv2_140024	23,1	atpE V-type proton ATPase subunit E	21,63	3
NIVIEv2_140082	79,4	Cell division cycle protein 48 homolog AF_1297	8,59	3
NIVIEv2_70010	76,6	CoA-binding domain-containing protein	9,34	4
NIVIEv2_71061	28,7	conserved exported protein of unknown function	29,52	4
NIVIEv2_180108	8,9	conserved protein of unknown function	48,15	2
NIVIEv2_70013	51,9	conserved protein of unknown function	12,37	3
NIVIEv2_70066	8,7	Deoxyribonuclease/rho motif-related TRAM (fragment)	35,8	2
NIVIEv2_120018	22,8	dps DNA protection during starvation protein	12,94	2
NIVIEv2_100071	122,9	exported protein of unknown function	42,35	24
NIVIEv2_180106	41,8	exported protein of unknown function	32,39	6
NIVIEv2_71146	27,5	exported protein of unknown function	30,91	5
NIVIEv2_180227	62,2	exported protein of unknown function	18,2	5
NIVIEv2_130051	54,5	exported protein of unknown function	7,17	2
NIVIEv2_71296	80,8	fusA Elongation factor 2	7,37	3
NIVIEv2_140032	39,3	H(+)-transporting two-sector ATPase	12,46	3
NIVIEv2_71105	32,2	mdh Malate dehydrogenase	14,47	2
NIVIEv2_71084	19,8	Peroxiredoxin	25,84	3
NIVIEv2_10026	29,7	putative exosome complex exonuclease 2	13,5	2
NIVIEv2_71217	40,5	putative Luciferase-like monooxygenase	13,61	3
NIVIEv2_140176	38,3	putative zinc-binding dehydrogenase	20,74	4
NIVIEv2_100060	11,4	rpl12p 50S ribosomal protein L12P	53,15	4
NIVIEv2_71103	26	rpl18p 50S ribosomal protein L18P	22,36	2
NIVIEv2_100064	24,5	rpl1p 50S ribosomal protein L1P	16	2
NIVIEv2_70199	18,8	rpl5p 50S ribosomal protein L5P	17,75	2
NIVIEv2_71059	124,6	rpoB DNA-directed RNA polymerase subunit B	2,69	2
NIVIEv2_70159	26,3	R-protein S3ae	19,66	3
NIVIEv2_70209	15,3	rps19p 30S ribosomal protein S19P	34,07	2
NIVIEv2_71054	22,5	rps7p 30S ribosomal protein S7P	15,92	2
NIVIEv2_70691	10	SSB-like single OB-fold protein	31,58	2
NIVIEv2_70377	39,6	sucC Succinyl-CoA ligase [ADP-forming] subunit beta	10,54	2
NIVIEv2_140158	59,6	thsA Thermosome subunit alpha	24,96	8
NIVIEv2_180287	59	thsA Thermosome subunit alpha	15,88	6
NIVIEv2_71149	47,3	tuf Elongation factor 1-alpha	18,08	5

Proteins identified in the soluble fraction

Accession	MW [kDa]	Description	Coverage	Peptides
NIVIEv2_140114	19,7	4Fe-4S ferredoxin iron-sulfur binding domain protein	25,84	4
NIVIEv2_100113	56,4	abfD 4-hydroxybutyryl-CoA dehydratase/vinylacetyl-CoA-Delta-isomerase	17,16	5
NIVIEv2_71080	55,8	accC acetyl-CoA carboxylase subunit (biotin carboxylase subunit)	6,73	2
NIVIEv2_180314	83,1	aco putative aconitate hydratase, mitochondrial	4,2	2
NIVIEv2_100022	36,8	adh NAD-dependent alcohol dehydrogenase	9,43	2
NIVIEv2_70796	46,1	ahcY Adenosylhomocysteinase	20,65	5
NIVIEv2_100046	28,2	argB Acetylglutamate/acetylaminoadipate kinase	13,11	2
NIVIEv2_140168	39,4	asd Aspartate-semialdehyde dehydrogenase	21,51	4
NIVIEv2_70043	48,4	aspS Aspartyl-tRNA synthetase	10,21	3
NIVIEv2_140093	36,4	ATP phosphoribosyltransferase	21,23	4
NIVIEv2_140025	66,2	atpA V-type ATP synthase alpha chain	38,33	13
NIVIEv2_140026	50,7	atpB V-type ATP synthase beta chain	58,32	15
NIVIEv2_140024	23,1	atpE V-type proton ATPase subunit E	15,38	2
NIVIEv2_140082	79,4	Cell division cycle protein 48 homolog AF_1297	22,58	11
NIVIEv2_70010	76,6	CoA-binding domain-containing protein	26,31	13
NIVIEv2_71061	28,7	conserved exported protein of unknown function	19,56	3
NIVIEv2_180108	8,9	conserved protein of unknown function	88,89	6
NIVIEv2_70013	51,9	conserved protein of unknown function	21,17	4
NIVIEv2_10008	10	conserved protein of unknown function	39,08	2
NIVIEv2_70320	20,9	conserved protein of unknown function	17,39	2
NIVIEv2_70354	11,9	conserved protein of unknown function	76,64	4
NIVIEv2_70771	20	conserved protein of unknown function	16,76	2
NIVIEv2_71037	18,5	conserved protein of unknown function	20,59	2
NIVIEv2_100136	35,6	conserved protein of unknown function	15,34	2
NIVIEv2_120033	40,7	conserved protein of unknown function	7,22	2
NIVIEv2_130123	8,4	conserved protein of unknown function	34,25	2
NIVIEv2_130127	15,5	conserved protein of unknown function	41,13	5
NIVIEv2_140022	21,8	conserved protein of unknown function	16,42	2
NIVIEv2_140054	8,5	conserved protein of unknown function	53,42	2
NIVIEv2_140199	75,2	conserved protein of unknown function	19,97	8
NIVIEv2_180095	10,3	conserved protein of unknown function	36,26	3
NIVIEv2_180218	23,3	conserved protein of unknown function	19,23	3
NIVIEv2_70545	30,5	crt 3-hydroxybutyryl-CoA dehydratase	24,83	5
NIVIEv2_130135	50,1	cshA DEAD-box ATP-dependent RNA helicase CshA	12,12	3
NIVIEv2_170060	8,2	Deoxyribonuclease/rho motif-related TRAM	59,74	4
NIVIEv2_70066	8,7	Deoxyribonuclease/rho motif-related TRAM (fragment)	51,85	5
NIVIEv2_70060	14,3	Deoxyribonuclease/rho motif-related TRAM (modular protein)	51,82	3
NIVIEv2_71058	140,9	DNA-directed RNA polymerase	17,65	13

NIVIEv2_140134	65,7	dnaK Chaperone protein dnaK (Heat shock protein 70) (Heat shock 70 kDa protein) (HSP70)	7,19	3
NIVIEv2_70036	9,9	ef1b Elongation factor 1-beta	70,97	4
NIVIEv2_100015	14,7	eif5a Translation initiation factor 5A	42,86	2
NIVIEv2_70886	44,9	eno Enolase	10,07	2
NIVIEv2_70539	23,5	ESCRT-III 2	12,96	2
NIVIEv2_100071	122,9	exported protein of unknown function	41,09	31
NIVIEv2_130051	54,5	exported protein of unknown function	13,4	4
NIVIEv2_140211	61,3	exported protein of unknown function	11,62	3
NIVIEv2_70949	52,2	FeS assembly protein SufD	6,13	2
NIVIEv2_71296	80,8	fusA Elongation factor 2	18,28	8
NIVIEv2_100252	55,1	glnA Glutamine synthetase	6,15	2
NIVIEv2_71164	12,4	glnB Nitrogen regulatory protein P-II	22,81	3
NIVIEv2_70240	43,1	Glyceraldehyde-3-phosphate dehydrogenase	8,44	2
NIVIEv2_180230	15,5	Glyoxalase/bleomycin resistance protein/dioxygenase	22,46	2
NIVIEv2_140077	51,3	guaB Inosine-5'-monophosphate dehydrogenase (IMP dehydrogenase) (IMPDH) (IMPD)	12,37	3
NIVIEv2_140136	21,7	Heat shock protein Hsp20	32,64	4
NIVIEv2_180235	37,4	ilvC acetohydroxy-acid isomeroreductase	24,02	6
NIVIEv2_70175	59,3	ilvD Dihydroxy-acid dehydratase (DAD)	9,66	3
NIVIEv2_70566	60,5	ilvI Acetolactate synthase large subunit (AHAS) (Acetohydroxy- acid synthase large subunit) (ALS)	5,52	2
NIVIEv2_180221	37,7	Isocitrate/isopropylmalate dehydrogenase	9,65	2
NIVIEv2_10024	30,3	KH type 1 domain protein (modular protein)	17,61	4
NIVIEv2_71105	32,2	mdh Malate dehydrogenase	22,7	3
NIVIEv2_70533	61,2	Mg-chelatase subunit	11,27	4
NIVIEv2_70520	36,2	Myo-inositol-1-phosphate synthase	20,29	4
NIVIEv2_70506	32	Oxidoreductase FAD/NAD(P)-binding domain protein	25	5
NIVIEv2_180387	58	pckA Phosphoenolpyruvate carboxykinase [ATP] (PEP carboxykinase) (Phosphoenolpyruvate carboxylase) (PEPCK)	6,31	2
NIVIEv2_180311	23	pdxT glutamine amidotransferase for pyridoxal phosphate synthesis	15,17	2
NIVIEv2_71084	19,8	Peroxiredoxin	35,96	4
NIVIEv2_70398	46,6	Phosphoglycerate mutase	16,13	4
NIVIEv2_150001	20,1	ppa Inorganic pyrophosphatase	17,88	2
NIVIEv2_70233	61,6	protein of unknown function	24,68	9
NIVIEv2_70494	35,3	protein of unknown function	9,06	2
NIVIEv2_70848	14,4	protein of unknown function	52,27	5
NIVIEv2_100290	33,3	protein of unknown function	27,54	5
NIVIEv2_110073	11,2	protein of unknown function	26,8	2
NIVIEv2_120044	10	protein of unknown function	40,45	2
NIVIEv2_180033	86,6	protein of unknown function	5,62	3
NIVIEv2_70215	26,7	psmA Proteasome subunit alpha	40,41	7
NIVIEv2_180331	37	putative Aldo/keto reductase family protein	14,89	3
NIVIEv2_71081	18,2	putative biotin-requiring enzyme	18,82	2

NIVIEv2_170008	39,1	putative CRISPR-associated regulatory protein, DevR family	14,7	3
NIVIEv2_70902	42,1	putative enzyme	12,07	3
NIVIEv2_10025	27,2	putative exosome complex exonuclease 1	25,2	4
NIVIEv2_10026	29,7	putative exosome complex exonuclease 2	43,8	7
NIVIEv2_70913	28,2	putative FKBP-type peptidyl-prolyl cis-trans isomerase	28,35	6
NIVIEv2_40011	45,1	putative HMGL-like protein	8,82	2
NIVIEv2_180137	35	putative iron-containing alcohol dehydrogenase	11,71	2
NIVIEv2_71217	40,5	putative Luciferase-like monooxygenase	37,22	8
NIVIEv2_120058	47,9	putative molybdopterin biosynthesis protein	14	4
NIVIEv2_71166	12,7	putative nitrogen regulatory protein P II	17,54	2
NIVIEv2_71079	56,1	putative propionyl-CoA carboxylase beta chain	17,32	5
NIVIEv2_100144	57,5	putative Pyridoxal-phosphate dependent enzyme	6,24	2
NIVIEv2_70523	29,5	putative ribose 1,5-bisphosphate isomerase	10,99	2
NIVIEv2_70130	9,4	putative snRNP Sm-like protein	44,58	2
NIVIEv2_180125	56	putative tRNA synthetase class II core domain (G, H, P, S and T)	5,88	2
NIVIEv2_140176	38,3	putative zinc-binding dehydrogenase	49,43	11
NIVIEv2_100297	38,1	putative zinc-binding dehydrogenase	23,78	5
NIVIEv2_10022	27,1	RNA polymerase insert	20,24	2
NIVIEv2_70928	45,5	rocG glutamate dehydrogenase	26,62	5
NIVIEv2_70224	64,3	Rossmann-fold oxidoreductase	11,89	6
NIVIEv2_70052	19,2	rpl10e 50S ribosomal protein L10e	20,93	2
NIVIEv2_180292	16,3	rpl11p 50S ribosomal protein L11P	33,13	3
NIVIEv2_100060	11,4	rpl12p 50S ribosomal protein L12P	53,15	5
NIVIEv2_70202	15,7	rpl14p 50S ribosomal protein L14P	19,86	2
NIVIEv2_71100	15,9	rpl15p 50S ribosomal protein L15P	32,88	3
NIVIEv2_71103	26	rpl18p 50S ribosomal protein L18P	24,89	3
NIVIEv2_100064	24,5	rpl1p 50S ribosomal protein L1P	33,78	6
NIVIEv2_180216	11,3	rpl21e 50S ribosomal protein L21e	24,24	2
NIVIEv2_140243	26,1	rpl2p 50S ribosomal protein L2P	22,36	3
NIVIEv2_71101	17,6	rpl30p 50S ribosomal protein L30P	18,47	2
NIVIEv2_20013	15,9	rpl32e 50S ribosomal protein L32e	17,86	2
NIVIEv2_70212	36,5	rpl3p 50S ribosomal protein L3P	35,84	8
NIVIEv2_70211	29,2	rpl4p 50S ribosomal protein L4P	39,56	9
NIVIEv2_70199	18,8	rpl5p 50S ribosomal protein L5P	24,26	5
NIVIEv2_70196	19,2	rpl6p 50S ribosomal protein L6P	25,71	3
NIVIEv2_71059	124,6	rpoB DNA-directed RNA polymerase subunit B	21,31	14
NIVIEv2_70074	21,5	rpoE DNA-directed RNA polymerase subunit E'	17,5	2
NIVIEv2_71060	9,3	rpoH DNA-directed RNA polymerase subunit H	31,71	2
NIVIEv2_100063	32,3	R-protein L10p	37,5	6
NIVIEv2_20014	17,3	R-protein L19e	20,13	3
NIVIEv2_71233	14,3	R-protein S11p	21,48	2

NIVIEv2_100001	14	R-protein S24e	14,29	4
NIVIEv2_70159	26,3	R-protein S3ae	55,56	10
NIVIEv2_70535	21,8	rps13p 30S ribosomal protein S13P	32,23	4
NIVIEv2_70155	16,5	rps15p 30S ribosomal protein S15P/S13e	20,81	2
NIVIEv2_140174	16,8	rps19e 30S ribosomal protein S19e	25,17	4
NIVIEv2_70209	15,3	rps19p 30S ribosomal protein S19P	34,07	2
NIVIEv2_140162	7	rps27e 30S ribosomal protein S27e	31,82	2
NIVIEv2_70206	24,9	rps3p 30S ribosomal protein S3P	23,28	3
NIVIEv2_70536	19,6	rps4p 30S ribosomal protein S4P	30,29	4
NIVIEv2_71102	22,2	rps5p 30S ribosomal protein S5P	20,39	3
NIVIEv2_140259	14,9	rps6e 30S ribosomal protein S6e	28,87	2
NIVIEv2_71054	22,5	rps7p 30S ribosomal protein S7P	33,83	4
NIVIEv2_70404	14,2	rps8e 30S ribosomal protein S8e	26,92	4
NIVIEv2_70197	14,8	rps8p 30S ribosomal protein S8P	22,31	2
NIVIEv2_10019	17,1	rps9p 30S ribosomal protein S9P	18,59	2
NIVIEv2_180391	23,3	sodA superoxide dismutase	26,57	3
NIVIEv2_70691	10	SSB-like single OB-fold protein	50,53	3
NIVIEv2_70377	39,6	sucC Succinyl-CoA ligase [ADP-forming] subunit beta	22,16	5
NIVIEv2_70376	33	sucD succinyl-CoA synthetase, alpha subunit, NAD(P)-binding	41,8	7
NIVIEv2_100151	22,2	tbp TATA-box-binding protein	25,37	3
NIVIEv2_70808	20,4	Thiol-disulfide isomerase	25	2
NIVIEv2_10034	32,4	Thiosulfate sulfurtransferase	18,02	3
NIVIEv2_100086	72,7	thrS Threonyl-tRNA synthetase	8,06	3
NIVIEv2_140158	59,6	thsA Thermosome subunit alpha	48,47	18
NIVIEv2_180287	59	thsA Thermosome subunit alpha	47,65	21
NIVIEv2_180322	9	Transcriptional regulator, AsnC family	45,12	3
NIVIEv2_10040	44,4	trpS Tryptophanyl-tRNA synthetase	7,95	2
NIVIEv2_71149	47,3	tuf Elongation factor 1-alpha	69,79	21
NIVIEv2_70914	12,6	yutM putative chaperone involved in Fe-S cluster assembly	26,72	2

B. Zusammenfassung

Seit der Entdeckung Ammoniak oxidierender Archaea (AOA) im Jahr 2005 wird ihr Beitrag zum globalen Stickstoffkreislauf diskutiert. Zur besseren Charakterisierung müssen jedoch mehr Erkenntnisse über ihren noch weitgehend unbekannten Energie- und Kohlenstoffmetabolismus gewonnen werden. In dieser Arbeit wurde die archaeale Ammoniakoxidation untersucht, mit Fokus auf den zweiten Teilschritt und ein potenziell darin involviertes Enzym sowie mögliche (Zwischen-) Produkte. In Ammoniak oxidierenden Bakterien (AOB) wird im ersten Schritt dieses Prozesses mittels des Enzyms Ammoniummonooxigenase (AMO) Ammonium zu Hydroxylamin oxidiert und im zweiten Schritt wird dieses mittels der Hydroxylaminoxidoreduktase (HAO) weiter oxidiert zu Nitrit. In Archaea finden sich zwar AMO-Homologe, jedoch sind weder das Zwischenprodukt, noch das/die Enzym(e), die den zweiten Schritt katalysieren, bekannt.

Das hier untersuchte Enzym ist ein *Multicopperprotein* der AOA, welches Homologie zu Nitritreduktasen (NirKs) aufweist. Aufgrund seiner starken Transkription unter aeroben Bedingungen und der Tatsache, dass Enzyme oftmals ihre Reaktion in beide Richtungen katalysieren können, wurde die Hypothese aufgestellt, dass dieses Enzym ein Zwischenprodukt der Ammoniakoxidation (möglicherweise NO) zu Nitrit oxidieren könnte. Neben biochemischen Experimenten mit diesem Protein wurden auch Versuche mit Rohextrakten und Kulturen von *Ca.* Nitrososphaera viennensis durchgeführt, um Hinweise auf mögliche Aktivitäten und Zwischenprodukte in der archaealen Ammoniakoxidation zu erhalten.

Die in *Escherichia coli* heterolog exprimierte NirK zeigte keine Nitritreduktaseaktivität. In Gegenwart eines künstlichen Elektronenakzeptors wurde Hydroxylamin oxidiert, jedoch wurde unter keinen der getesteten Bedingungen nachweisbares Nitrit freigesetzt (partielle HAO-Aktivität). Die Ergebnisse bezüglich andersartiger Stickstoff-Produkte (NO, N_2O) waren nicht eindeutig. Der berechnete K_M Wert für diese Reaktion von 0,5–1,3 mM zeigte keine hohe Affinität des Enzyms für Hydroxylamin. Da die Reduktion des Elektronenakzeptors auch mit Kupfer(II)-chlorid-dihydrat Lösungen erfolgte, konnte die Enzymspezifität dieser Reaktion weder bestätigt noch ausgeschlossen werden. Es gab keine Anzeichen dafür, dass die NirK andere Stickstoff-Substrate (NO, HNO, NH_4^+) oxidiert.

Da das untersuchte Enzym von einer Metagenom-Bibliothek (Contig 54d9) stammte und es für weitere Studien von Vorteil wäre, die NirK von *Ca.* N. viennensis zur

Verfügung zu haben, wurde ihre Expression in *E. coli* angestrebt. Das Gen wurde in den Expressionsvektor pET28a ligiert, doch nach der Sequenzierung der Klone stellte sich heraus, dass die amplifizierte DNA von dem ebenfalls im Labor verfügbaren Schwesternstamm EN123 stammte.

Zusätzlich wurde versucht, die NirK in verschiedenen Proteinfraktionen von *Ca.* N. viennensis nachzuweisen, um festzustellen ob die in Transkriptomstudien gefundene Expression auch im Proteom nachvollziehbar ist. Jedoch konnte keines der durch MALDI-TOF identifizierten Peptide der gesuchten Nitritreduktase zugeordnet werden.

Um biochemische Experimente mit Rohextrakten durchführen zu können, musste aufgrund des langsamen Wachstums und der geringen Zelldichte von *Ca.* N. viennensis die Ausbeute an Zellen mittels Vergrößerung der Kultur auf mehrere Liter erhöht werden. Der Prozess der Ammoniumoxidation war im Zellextrakt nicht nachweisbar. HAO Aktivität wurde nur indirekt durch die Reduktion des Elektronenakzeptors festgestellt, jedoch abermals ohne die Bildung von Nitrit. Weiters wurden keine Hinweise auf NO Aktivität gefunden.

Interessanterweise konnte sowohl im Zellextrakt als auch in der löslichen und unlöslichen Fraktion des Zellextrakts Nitritreduktaseaktivtät nachgewiesen werden. Dies ist ein Indiz für die Relevanz dieser Reaktion in dem Organismus. Ob diese Aktivität auf die NirK zurückzuführen ist, bleibt noch ungeklärt.

Ein weiteres Experiment um Indizien für NO als mögliches Zwischenprodukt in der archaealen Ammoniumoxidation zu erhalten, war die Kultivierung von *Ca.* N. viennensis in Gegenwart eines spezifischen NO-Fängers (PTIO, Abkürzung für 2-phenyl-4,4,5,5-tetramethylimidazolineoxyl-1-oxyl-3-oxide). Nitrosospira multiformis (AOB) und *E. coli* Kulturen fungierten als Kontrollen. In vergleichbaren Konzentrationen wurde das Wachstum von *Ca.* N. viennensis am stärksten von PTIO inhibiert. Somit könnte NO ein wichtiges (Zwischen-) Produkt in der Ammoniumoxidation sein. Weiters deuten diese Ergebnisse darauf hin, dass der Mechanismus der Ammoniumoxidation oder zumindest der enzymatische Apparat der AOAs anders ist als der von AOB.

In dieser Studie konnte die physiologisch relevante Aktivität des NirK Homologs nicht eindeutig bestimmt werden. In Zellextrakten wurde jedoch Nitritreduktaseaktivität nachgewiesen. Als mögliches (Zwischen-)Produkt wurden nur Hinweise auf NO gefunden. Aufgrund der Komplexität des Prozesses scheint es nicht einfach, die Ammoniumoxidation *in vitro* nachzuvollziehen. Komplexe Elektronentransferprozesse, eine Vielzahl von involvierten Enzymen und reaktive N-Spezies erschweren ihre Aufklärung. Weitere biochemische Verfahren müssen hinzugezogen werden, um diesen Mechanismus aufzuklären.

Curriculum vitae

Personal data

First name:	Christine Elisabeth
Last name:	Bauer
Date of birth:	03.08.1984
Citizenship:	Austrian

Education:

Since 07. 2011	Diploma Thesis: „Biochemical and physiological studies on the energy metabolism of ammonia oxidizing archaea" Department of Genetics in Ecology, Prof. Schleper
Since 10. 2007	Studies in Microbiology and Genetics (diploma)
10. 2003 – 6. 2007	Studies in Biology (diploma)
10. 2003 – 6. 2005	Studies in Law (diploma)
1997 – 06. 2003	Bundesrealgymnasium Kurzwiese, Eisenstadt, Austria
1995 – 1997	AHS Kurzwiese, Eisenstadt, Austria
1994 – 1995	Theresianum Eisenstadt, Austria
1990 – 1994	Volksschule Eisenstadt, Austria

Further qualifications:

Foreign languages:	Fluent in English
Computer skills:	Basic Knowledge of Word & Excel

Scientific activities:

Positions: Studienassistentin SS 2011

Workshops: Early Career Scientist Workshop $ICoN_2$/ENC
                            Nijmegen, The Netherlands (07/2011)

Conferences: 16th European N-cycle meeting/Second International
                            Conference on Nitrification ($ICoN_2$)
                            Nijmegen, The Netherlands (07/2011)

Posters: **M. Stieglmeier**, **C. Bauer**, **J.** Schweichhart, M. Tourna, T. Urich, C.
            Schleper.
            Nitrososphaera viennensis, an ammonia oxidizing archaeon from soil.
            Nijmegen, The Netherlands, 2011 (Co-presentation of poster)